Kotzebue Harbor Feasibility Study

Navigation Improvements at Cape Blossom

Kotzebue, Alaska

Appendix C: Hydraulics and Hydrology

US Army Corps
of Engineers
Alaska District

Hydraulic Appendix

TABLE OF CONTENTS

FIGURES

TABLES

1.0 INTRODUCTION

This hydraulic design appendix describes the technical aspects of the Kotzebue navigation improvements. It provides the background for determining the Federal interest in construction of a navigation improvement project. To determine the feasibility of a project, model studies were conducted of the waves, currents, and sediment movement at the site.

1.1 Background

Fuel and goods shipped to Kotzebue supply the city and outlying communities. There is a navigation inefficiency associated with the shipping due to a long (12-15 mile) shallow draft channel that must be transited to reach the dock at Kotzebue. A lack of sufficient draft for the ocean going barges delivering fuel and goods results in the barges anchoring offshore in deep water, and smaller barges lightering the fuel and goods into Kotzebue.

1.2 Description of Project Area

Kotzebue is approximately 550 miles northwest of Anchorage and 26 miles above the Arctic Circle (Figure 1). It is the regional hub for the northwest Arctic Borough (Figure 2). The city is located on the north tip of the 3-mile long Baldwin Peninsula which is bounded on the north and west by Kotzebue Sound and on the east by Hotham Inlet, known locally as Kobuk Lake (Figure 3).

The population of Kotzebue is 3,200 according to the 2010 Census. The region lacks road access. Kotzebue serves as a hub as it is near the discharges of the Kobuk, Noatak, and Selawick Rivers. Kotzebue and the surrounding villages are accessible via water and air in the summer and air and snow machine or dogsled in the winter.

Currently, ocean going barges anchor 12 -15 miles offshore and lighter fuel and goods to shore. Once goods arrive in Kotzebue, smaller river going barges load the fuel and goods for delivery to the surrounding villages. The purpose of this project is to determine the feasibility of constructing improvements that would increase the navigation efficiency for delivery of fuel and goods to Kotzebue.

Figure 1 State of Alaska

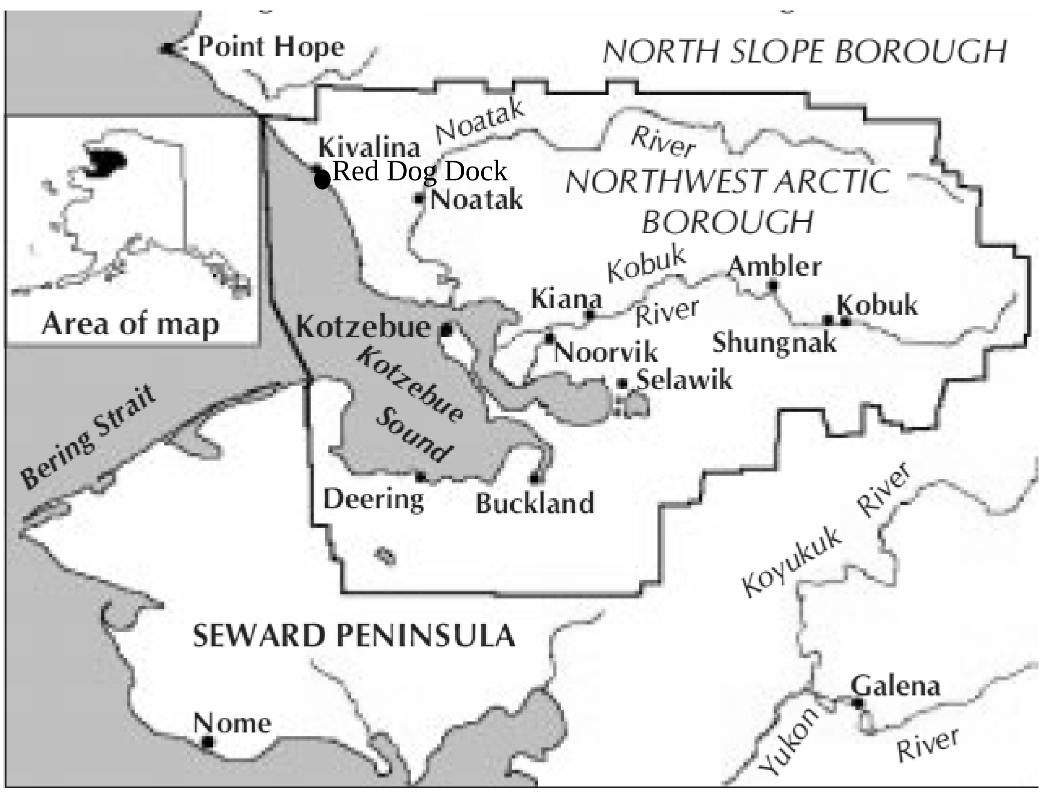

Figure 2 Northwest Arctic Borough

Figure 3 Kotzebue, Hotham Inlet, and the Kobuk River

2.0 NEEDS AND OPPORTUNITIES

Identification of the opportunities, problems, needs, and concerns in the study area provided the major issues and direction of the study effort. The main navigation problem at Kotzebue is inefficiency related to the ability of ocean-going barges to land at Kotzebue. A combination of lack of modern facilities and lack of sufficient draft combine to require barges to anchor offshore and lighter goods 12-15 miles to Kotzebue. Some goods are consumed within the community while others are trans-loaded onto riverine barges and shipped to outlying communities. All goods brought into Kotzebue are consumed within the region.

A secondary problem is that riverine barges are currently forced to wait for ice to go out of Hotham Inlet prior to attempting deliveries up the Kobuk River. The Kobuk River opens well in advance of Hotham Inlet but the barges are not able to load until ice has cleared from the inlet. By this time, water levels may not be sufficient for barges to transit the river to far upstream communities. This requires goods to be delivered by air, greatly increasing final prices.

Opportunities exist to increase the efficiency of delivery of goods to Kotzebue and the villages which rely on shipments from Kotzebue. If sufficient draft existed for ocean-going barges to access shore side facilities, the efficiency of these operations could be increased.

3.0 STUDY CONSTRAINTS

Constraints identified for the project design include:

1) The channel location needs to align with the location of the planned State of Alaska road

2) Beach access must be maintained to enable subsistence activities

3) Near shore fish movement must be unimpeded.

4.0 CLIMATOLOGY, METEOROLOGY, HYDROLOGY

4.1 Temperature and Precipitation

Kotzebue falls within the arctic climate zone, characterized by seasonal extremes in temperature (Table 1). Winters are long and harsh, and summers are short but warm. Kotzebue Sound is ice-free from early July until early October. (Alaska Department of Community and Economic Development-Kotzebue)

Table 1 Temperature and Precipitation

	Jan	*Feb*	*Mar*	*Apr*	*May*	*Jun*	*Jul*	*Aug*	*Sep*	*Oct*	*Nov*	*Dec*
Mean Min Temperature [F]	-9.5	-7.8	-6.7	5.4	26.0	39.9	49.7	47.3	37.9	20.1	4.0	-4.1
Mean Temperature [F]	-2.8	-0.8	1.1	13.3	31.9	45.7	54.6	51.7	42.3	24.3	9.1	2.3
Mean Max Temperature [F]	3.9	6.3	8.8	21.2	37.8	51.5	59.5	56.1	46.7	28.5	14.2	8.7
Mean Precipitation [Inch]	0.6	0.7	0.4	0.54	0.4	0.6	1.5	2.2	1.6	1.0	0.8	0.8
Snowfall [Inch]	9.1	9.6	5.9	5.1	1.2	0.0	0.0	0.0	0.8	6.1	10.5	11.5

4.2 Ice Conditions

Ice generally begins accumulating in the south Chukchi Sea in October. It begins forming along the northeast coast of Russia and proceeds down the Chukchi Peninsula to Cape Dezhnev (Figure 4). Generally, by the time ice has reached Cape Dezhnev, ice is also forming along the western Alaska coast. Ice along the Russian coast generally grows faster than the ice along the Alaska coast. Ice on both coasts continues to grow until access to the Chukchi Sea is cut off by ice in the Bering Strait. Shortly after the Bering Strait is iced up the Chukchi Sea ices over.

The characteristics of the sea ice at Kotzebue are not typical of sea ice in the Chukchi Sea. Due to water depths of less than four feet offshore, the ice becomes grounded and does not move until breakup in June. Because of the lack of movement, the ice does not build up on shore or form pressure ridges close to shore. Ice can be pushed onshore during breakup if the wind is from the west.

At Cape Blossom, little information is available on ice characteristics. Local reports indicate that the ice is similar to ice at Kotzebue with very little riding up on shore. (Tetra Tech and Wright Forssen Associates, 1983)

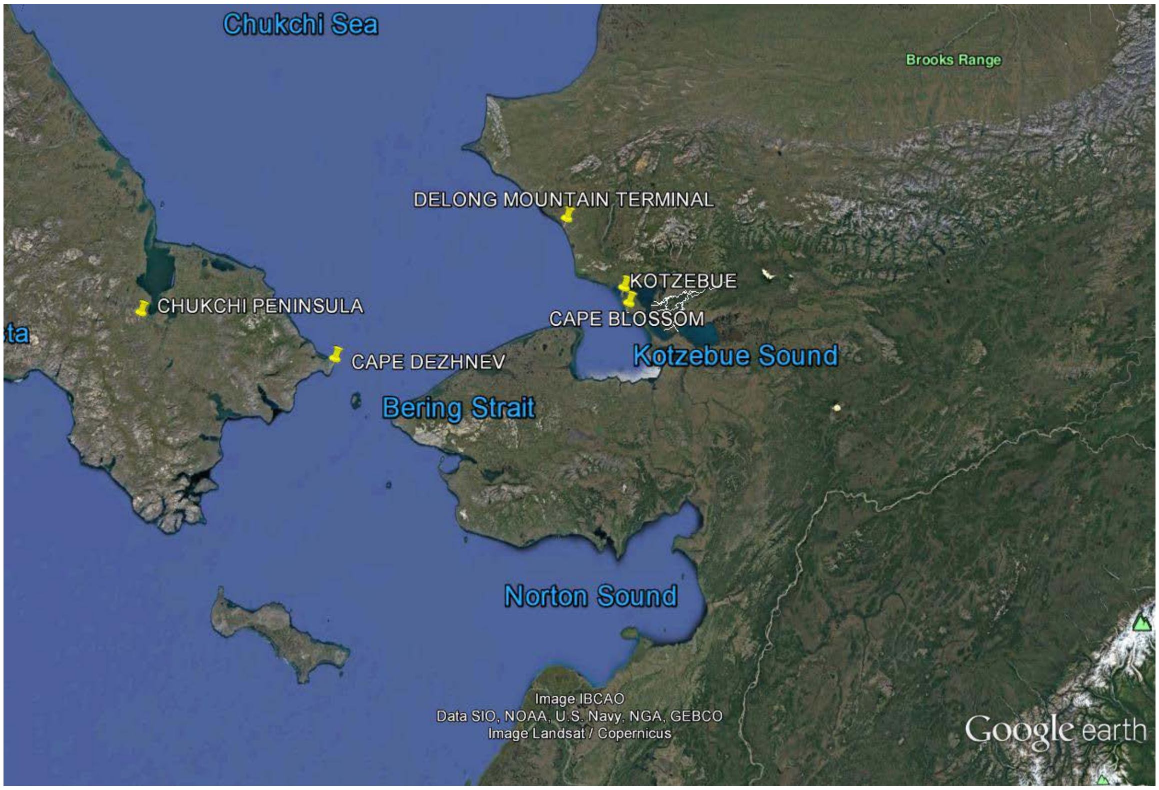

Figure 4 Location of Chukchi Peninsula, Cape Dezhnev, and Kotzebue

4.2.1 Ice Thickness

Ice thickness measurements were made offshore of Kotzebue on Kotzebue Sound. This may or may not be representative of the ice thickness at Cape Blossom, but it is the closest location of thickness measurements and provides ice thicknesses that may be experienced at Cape Blossom (Table 2)

Table 2 Maximum ice thickness for each measurement year (Bilello & Bates, 1966) (Bilello & Bates, 1971) (Bilello & Bates, 1972) (Bilello & Bates, 1991)

Date	Ice Thickness [in.]	Measurement Location
May 4/May 11, 1963	49	Offshore of Kotzebue 1½ miles NE of Weather Bureau Air Station
May 16, 1964	53	Offshore of Kotzebue 1½ miles NNE of Weather Bureau Air Station
April 29, 1967	44.5	Offshore of Kotzebue ½ miles NNE of Weather Bureau Air Station
April 27, 1968	42	Offshore of Kotzebue 1½ miles NNE of Weather Bureau Air Station
April 19, 1969	58	100 yards offshore of Kotzebue on Kotzebue Sound
April 25/May 2, 1970	47.5	Offshore from Kotzebue on Kotzebue Sound
May 5, 1973	48	Inner Kotzebue Sound
April 13, 1974	61	50 feet out from shore on Kotzebue Sound

4.2.2 Open Water Season

Weekly historical ice conditions were evaluated for the Navigation Improvements Study at the Delong Mountain Terminal (approximately 80 miles NNW of Kotzebue) (United States Army Corps of Engineers Alaska District, 2005). The ice conditions were extracted from the United States Ice Center's Sea Ice Grid (SIGRID) database from 1972 to 2001. Table 3 and Table 4 show the earliest and latest open water season dates.

Table 3 Open water season dates 1972 to 2001

Ice Cover				
	0 Tenths Ice Cover		**5 Tenths Ice Cover**	
	Ice Out	Ice In	Ice Out	Ice In
Earliest Date	9 June	4 October	7 June	9 October
Mean Date	6 July	29 October	27 June	4 November
Latest Date	28 July	19 November	18 July	23 November

Table 4 Open water season length [days] 1972 to 2001

Ice Cover		
	0 Tenths Ice Cover	5 Tenths
Minimum Season	78	108
Mean Season	115	131
Maximum Season	148	160

4.3 Tides

Kotzebue is in an area of small semi-diurnal tides with two high waters and two low waters each lunar day. The tidal parameters in Table 5 are based on Kotzebue control station 9490424 as determined by NOAA.

Table 5 Tidal Parameters - Kotzebue (9490424)

Parameter	Elevation (feet MLLW)
Mean Higher High Water (MHHW)	0.71
Mean High Water (MHW)	0.64
Mean Tide Level (MTL)**	0.39
Mean Sea Level (MSL)*	0.34
Mean Low Water (MLW)	0.13
Mean Lower Low Water (MLLW)	0.00

*****MSL The arithmetic mean of hourly heights observed over the National Tidal Datum Epoch. Shorter series are specified in the name; e.g. monthly mean sea level and yearly mean sea level.
******MTL The arithmetic mean of mean high water and mean low water.

4.4 Wind

Wind measurements at the project site were not available; however, wind information for hindcast points near the project site (Figure 5) was available through the Wave Information Study (WIS). The wind hindcast for these points was performed for the years 1985-2014 by Oceanweather Inc. (OWI) under contract to Coastal Hydraulics Laboratory (CHL) of the United States Army Corps of Engineers' (USACE) Engineering Research and Development Center (ERDC). Information from the wind hindcast was used as a forcing mechanism for the wave, current, and water level modeling that was performed for the sediment transport study. The wind hindcast was supplemented with selected storms from the early 1950's through 1984 to produce an extreme analysis of the deep water waves.

The Interactive Optimum Kinematic Analysis (IOKA) System (Cox et al. 1995) was used to construct the wind fields. All wind field estimates were restricted to a target domain that encompassed Kotzebue. Five critical elements are required for the IOKA system:

- Background wind fields
- Point source measurements (airport anemometer records, buoy data)
- Ship records (archived wind speed and direction)
- Scatterometer estimates of the wind speed
- Kinematic control points (KCPs).

These data sets (excluding the KCPs) must be adjusted for stability and brought to a common reference level. Stability accounts for the changes in the boundary layer due to differences between air and water temperatures. Considerations to the differences in boundary layer effects over the pack ice were neglected.

Background wind fields were derived from the National Center for Environmental Prediction/National Center for Atmospheric Research (NCEP/NCAR) Reanalysis Project. These wind fields were spatially interpolated to a fixed spherical grid.

Point source measurements such as buoy data and airport records reflect wind speeds and directions based on short time burst averaging. These are temporally interpolated to hourly data. Land based wind measurements were also adjusted for boundary layer effects.

Scatterometer wind fields derived from satellites are not true wind speed measurements. They are derived from inversion techniques and are extremely useful because of the spatial coverage obtained during one satellite pass. The repeat cycle is 35 days (on a 12 hour orbit); therefore, temporally continuous data are not available as in the case of point source measurements. In addition, data from all satellite-based scatterometers do not span the entire hindcast period, or any of the pre-1982 extreme storms that were considered in the study. Including these data may produce a series of discontinuities in the development of the wind field climatology; however, use of these data adds considerable value to the final wind products, and outweighs concerns regarding the consistency of the climatological wind products.

Once all data sets were transformed to equivalently neutral, stable 33.3 feet (10 meter) winds, the IOKA system is used. Each input wind data product carries a specified weight which can be overridden by an OWI analyst at any time. Background wind fields are ingested into OWI's Graphical Wind Work Station, displaying all the available data sets (point source measurements, scatterometer data). The NCEP/NCAR Reanalysis wind fields are at a 6-hour time step, so all 1-hour point source wind measurements are repositioned via "moving centers relocation". This assures continuity between successive wind fields.

The use of KCPs in the IOKA system allows the analyst to input and define ultra-fine scale features such as frontal passages, maintain jet streaks, and control orographic effects near coastal boundaries. The analyst can use the KCPs to define data sparse areas using continuity analysis, satellite interpretation, climatology of developing systems, and other analysis tools. The IOKA system contains a looping mechanism that will continually update the new wind field based on revisions performed by the analyst.

The final step in the construction of the OWI regional wind fields was to spatially interpolate the winds to a target domain and resolution. The final wind fields were spatially interpolated to the target domain at a longitudinal resolution of 0.50°, a latitudinal resolution of 0.25° at a time step of 6-hours. This was done because the NCEP/NCAR Reanalysis wind fields are resolved at 6-hour time steps.

The location of the wind field save point (82072) is shown in Figure 5. The wind roses associated with the typical open water season are shown in Figure 6 - Figure 10

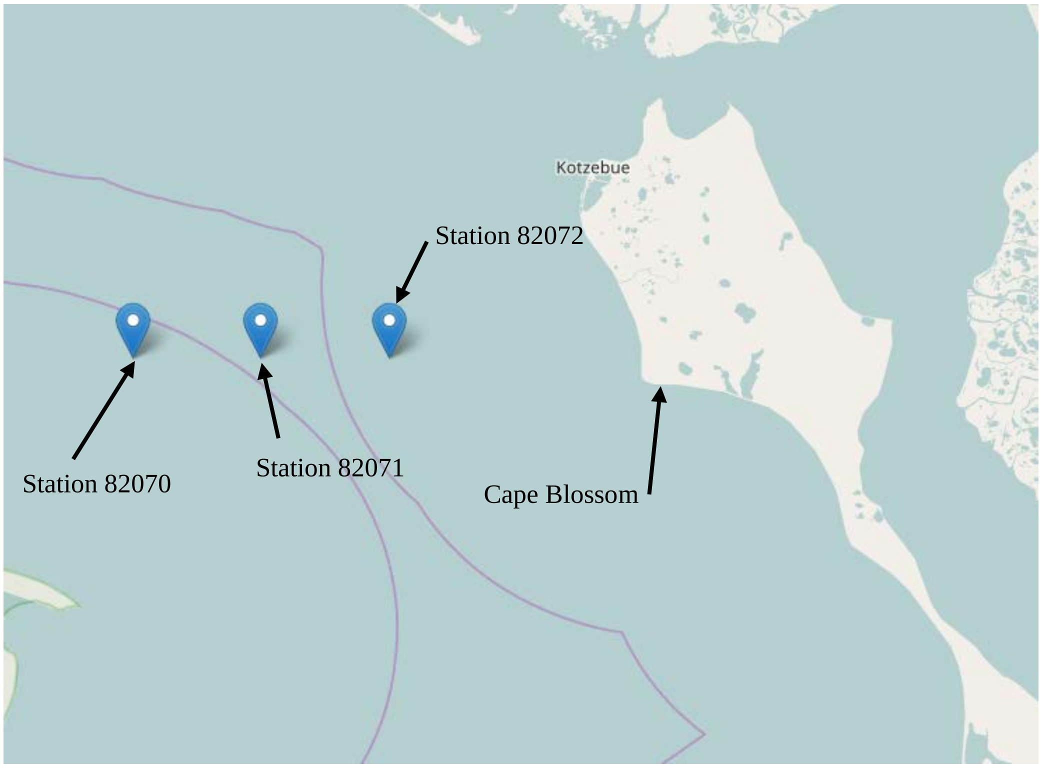

Figure 5 Location of wind save point for study

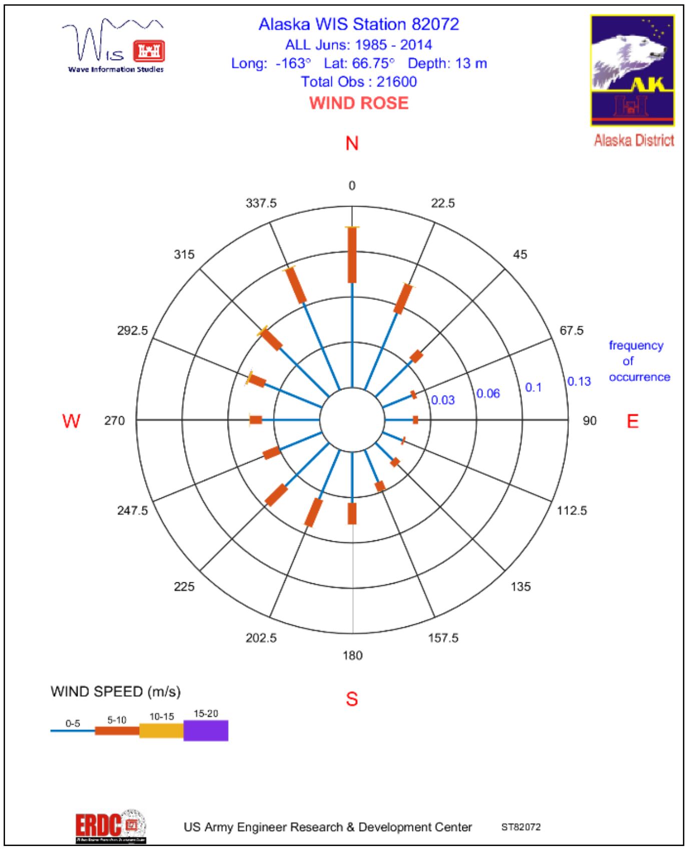

Figure 6 Wind Rose June 1985-2014

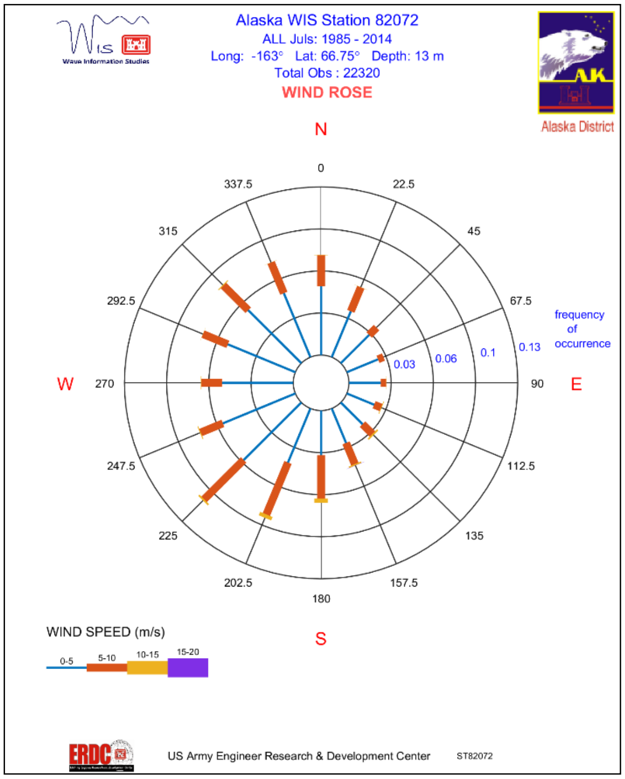

Figure 7 Wind Rose July 1985-2014

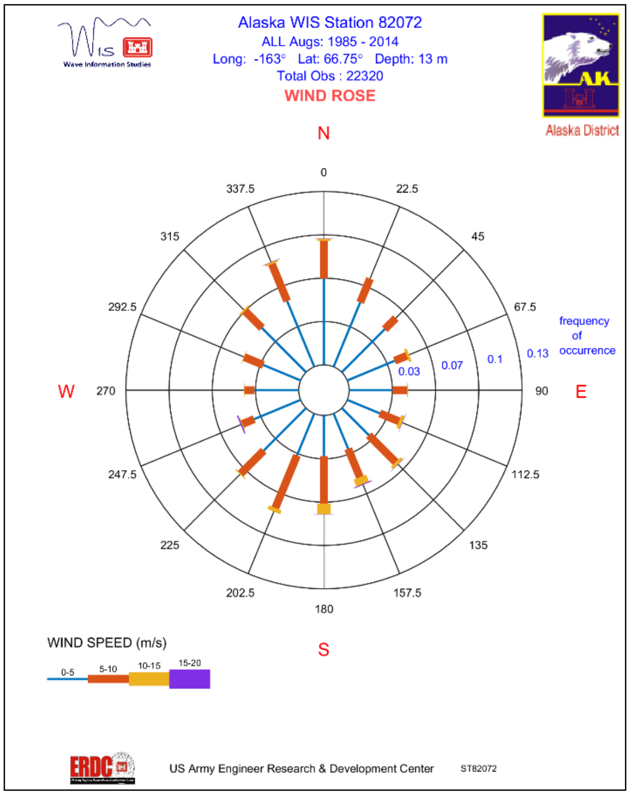

Figure 8 Wind Rose 1985 - 2014 August

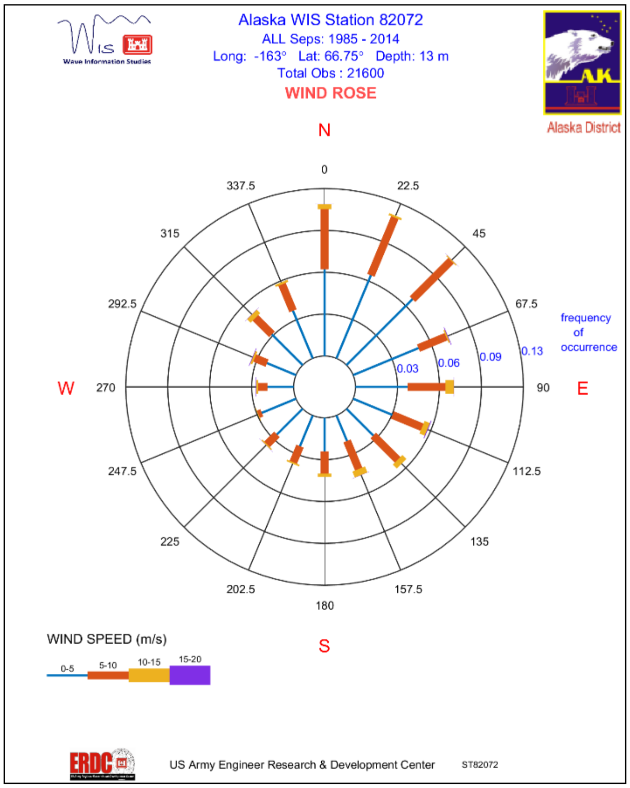

Figure 9 Wind Rose 1985 - 2014 September

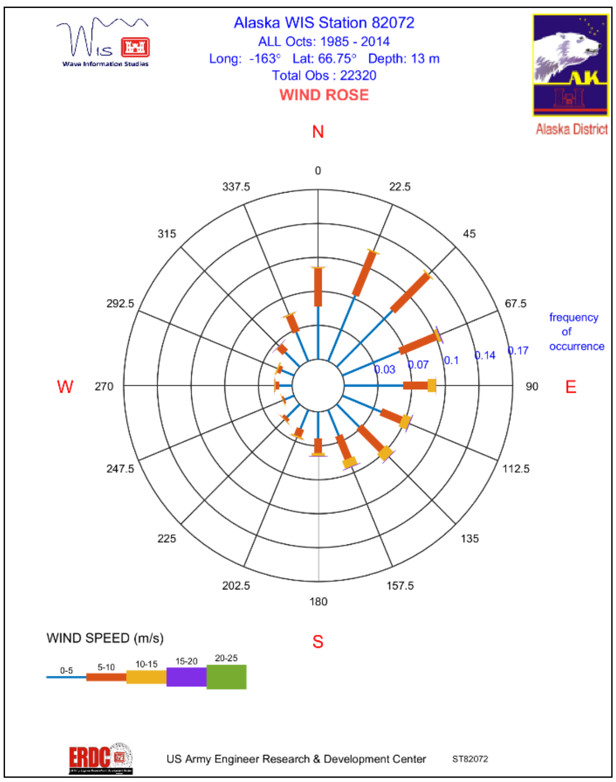

Figure 10 Wind Rose 1985 - 2014 October

5.0 GEOLOGY AND SOILS

The Baldwin Peninsula presents a gently rolling, sometimes flat topography, the surface of which is marked by polygonal ground thaw lakes. Broad morainal ridges rising up to 150 feet above the general surface form the topographic backbone of the peninsula. This rolling topography is typically bordered at the coast by bluffs 20 to 100 feet high. (Tetra Tech and Wright Forssen Associates, 1983)

The beach at the foot of the highest bluffs is usually less than 50 feet wide. The active erosion of the bluffs bordering the western edge of the peninsula is evidence of a retrograding shoreline. The lakes which dot the surface of the peninsula, and the surrounding lowlands appear to be thaw lakes that have originated due to the thawing permafrost. These lakes are typically shallow and freeze to the bottom in winter although some larger, deeper lakes may be potential sources of water on a year-round basis. In general, the soils on Baldwin Peninsula are poorly drained. The active layer, which may thaw to a depth of about two feet during the summer is typically saturated. The combination of fine grained and organic soils, gentle to flat slopes, and permafrost at the base of a shallow active layer all contribute to poor drainage conditions. (Tetra Tech and Wright Forssen Associates, 1983)

Silt, organic silt, and peat are the predominant soil types at Cape Blossom. Brown organic silt and peat occur from the surface to depths typically between 10 and 20 feet. The thickness of these surficial soils, as exposed in the coastal bluffs range from less than 5 feet to greater than 20 feet. Massive ice is a common constituent of these soils. Gray silts, typically devoid of organics underlie the surficial soils. (Tetra Tech and Wright Forssen Associates, 1983)

Actively eroding slopes are common to the bluffs that border the coast. In places the bluffs are completely bare of vegetation, quite steep and cut by steep walled gullies. Mud flows, debris slides, and block slumping are common along the front of the bluffs. (Tetra Tech and Wright Forssen Associates, 1983)

Bedrock does not outcrop on the Baldwin Peninsula. Bedrock was reported to have been intercepted at a depth of 82 feet in a hole drilled 1,000 feet west of the airport. (State of Alaska Department of Transportation & Public Facilities Northern RegionMaterial Section, 2009)

6.0 CIRCULATION AND WATER LEVELS

Information on circulation and water levels at the site was needed to evaluate ship navigation, and determine the potential for currents to erode, transport, and deposit sediment into the proposed navigation channel and turning basin. Existing information on the currents and water level at the site was sparse. Data available consisted of information found during a literature search of the area and measured data collected from deployment of an Acoustic Wave and Current profiler (AWAC) in 2016. Numerical modeling was used to characterize circulation and water levels.

Historic water-surface elevations and currents for storm events were computed by the CHL using the two-dimensional numerical models within CSTORM modeling system: the Advanced CIRCulation (ADCIRC) model (Luettich, 1992) (Kolar, 1992), and the Steady-state spectral Wave (STWAVE) model (Smith, 2001) (Massey, 2011). The CSTORM coupling framework controls the two-way passing of data between the ADCIRC and STWAVE models. Specifically, ADCIRC passes updated depth-integrated currents and water surface elevations along with wind forcing to STWAVE, and in turn, STWAVE provides ADCIRC wave radiation stress gradient forcing. The ADCIRC and STWAVE boundary are shown in Figure 11.

The CSTORM output was then used in a Multi-Block Geophysical Scale Hydrodynamic and Sediment Transport Modeling System (GSBM) to provide channel infilling estimates using the sediment transport model SEDZLJ.

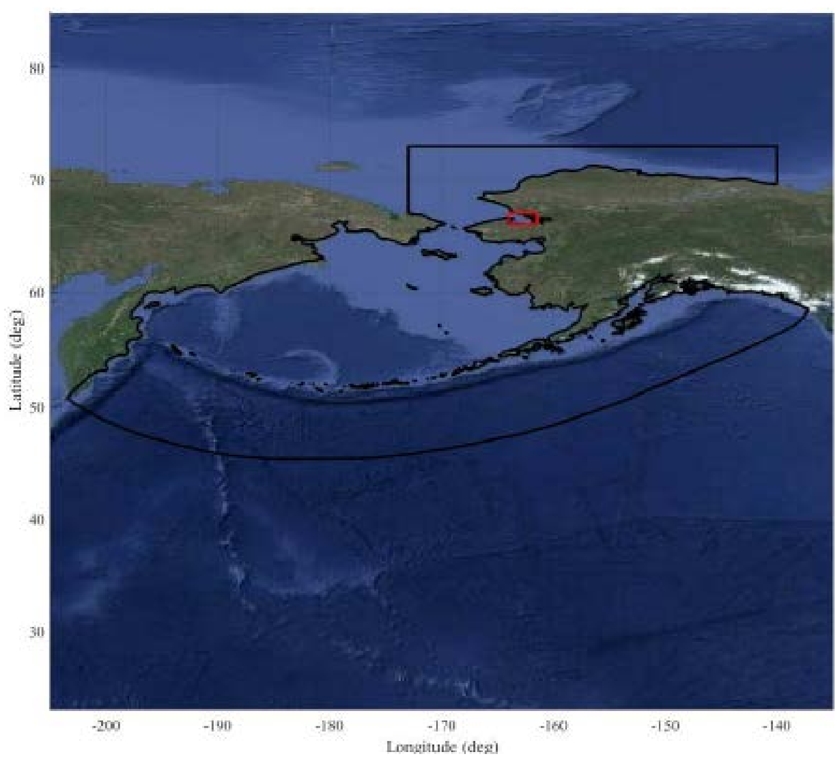

Figure 11 Map showing the ADCIRC model boundary as black lines and the STWAVE boundary as red lines.

The ADCIRC model is an unstructured-grid, finite-element, long-wave model developed under the USACE Dredging Research Program (DRP, Griffis et al. 1995). The model was developed as a family of two- and three-dimensional codes with the capability of:

a. Simulating tidal circulation and storm surge propagation over large computational domains, while simultaneously providing high resolution in areas of complex shoreline and bathymetry. The targeted areas of interest include continental shelves, nearshore areas, and estuaries.

b. Representing all pertinent physics of the three-dimensional equations of motion. These include tidal potential, Coriolis, and all nonlinear terms of the governing equations.

c. Providing accurate and efficient computations over periods ranging from months to years.

The ADCIRC model solves its governing equations with a finite element algorithm over arbitrary bathymetry encompassed by irregular sea and shore boundaries. This algorithm allows for flexible spatial resolution over the entire computational domain and has demonstrated robust stability characteristics. The advantage of this flexibility in developing a computational grid is that larger elements can be specified in the open ocean regions where less resolution is needed, whereas smaller elements can be applied in the nearshore areas where finer resolution is required to resolve hydrodynamic details. The bathymetry and boundaries for the computational grid are shown in Figure 12. The ADCIRC grid resolution near the project site is shown in Figure 13 and the grid resolution of the channel is shown in Figure 14.

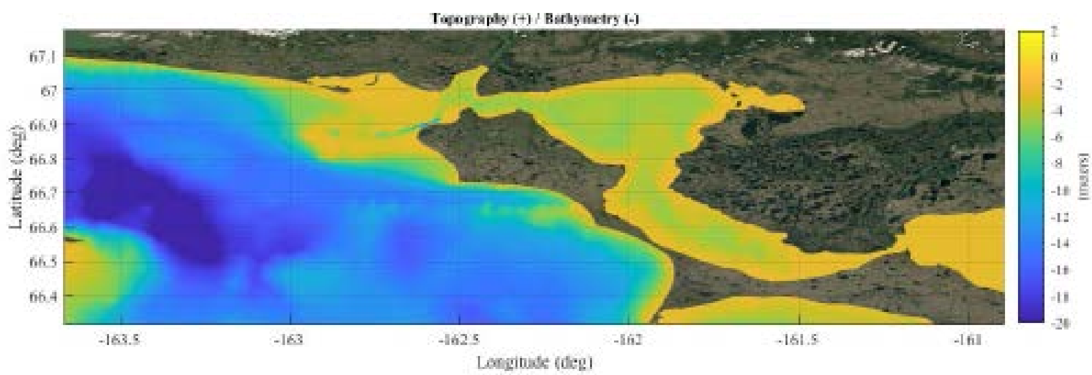

Figure 12 Map showing a portion of Kotzebue Sound with the ADCIRC bathymetric values.

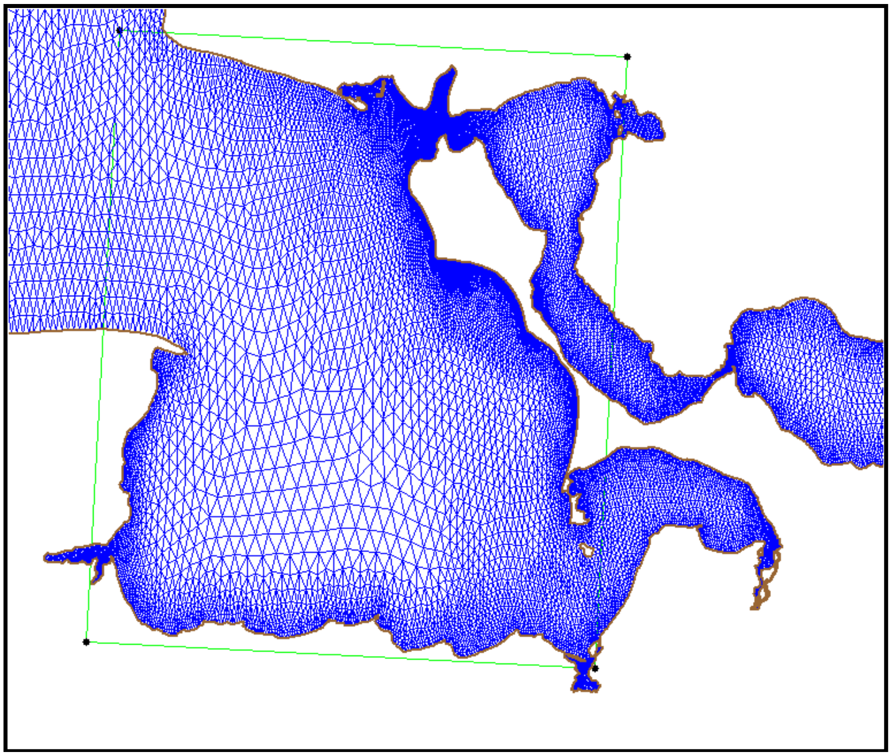

Figure 13 Grid resolution near the project site.

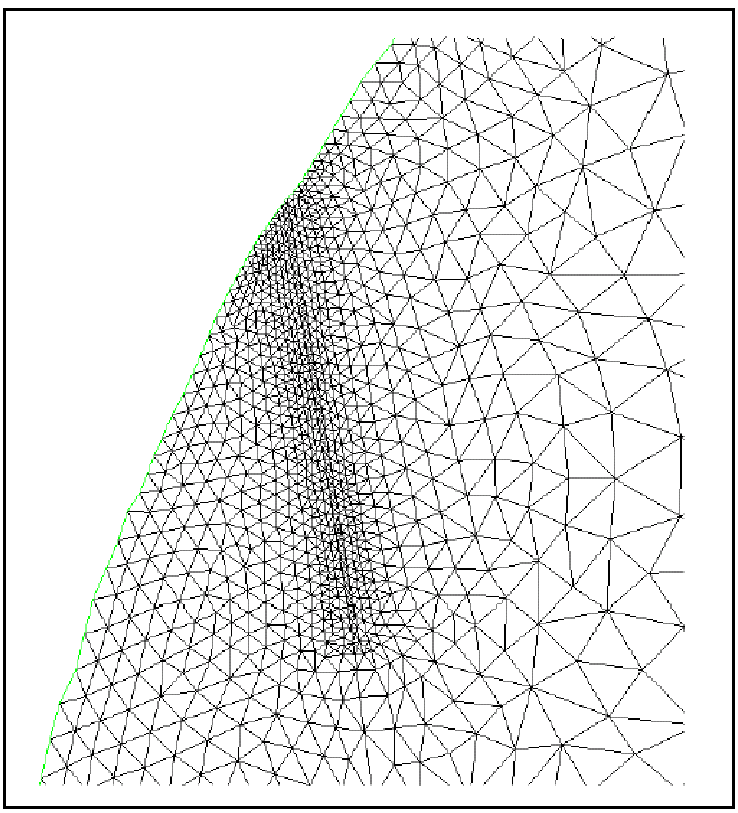

Figure 14 Grid resolution of the proposed channel.

The STWAVE model is a steady state finite difference model based on the wave action balance equation. It simulates depth-induced wave refraction and shoaling, current-induced refraction and shoaling, depth- and steepness-induced wave breaking, wind-wave growth, and wave-wave interaction and white capping that redistribute and dissipate energy in a growing wave field. It transformed the deep-water waves from the WIS points to nearshore. A map showing the ADCIRC mesh and the STWAVE grid are shown in Figure 15.

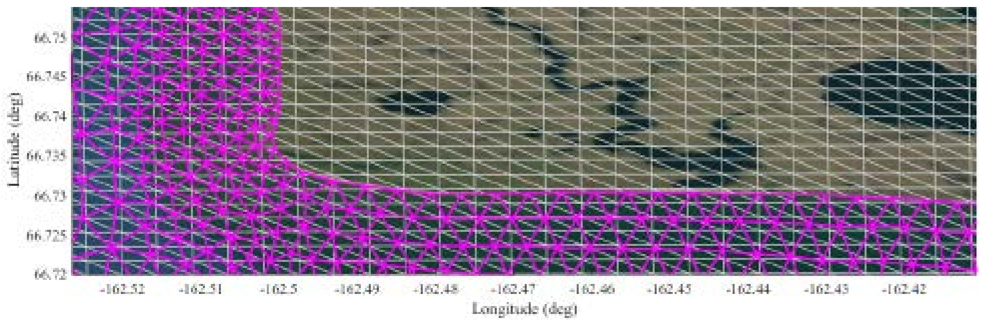

Figure 15 Map showing the ADCIRC mesh (magenta) and the STWAVE grid (gray) near Cape Blossom

The GSBM uses the CSTORM output to feed into the regional scale hydrodynamic and sediment transport models CH3D-WES and SEDZLJ respectively. The GSMB hydrodynamic and sediment modules utilize a non-orthogonal, boundary-fitted grid, which allows for the representation of deep navigation channels with irregular shoreline configurations. The GSMB model domain is shown in Figure 16

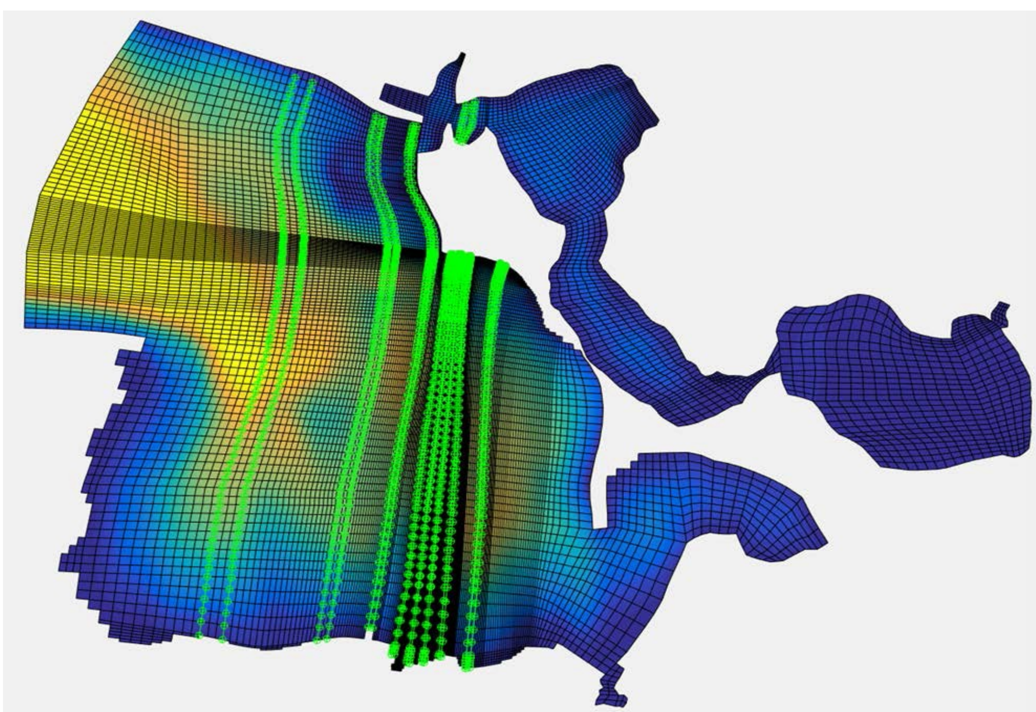

Figure 16 GSMB model domain

6.1 Model Verification

Work on the water level and circulation modeling began with model verification to demonstrate that grid resolution, bathymetry, and boundary conditions are adequately described to reproduce known or observed hydrodynamic conditions.

ADCIRC generated water levels were checked against tide stations at Kotzebue and Red Dog Dock (aka Delong Mountain Terminal). A sample of the ADCIRC water surface elevation time series data is shown in Figure 17 and Figure 18 along with the measured water surface elevations and predicted tide elevations. ADCIRC represents the measured water surface elevations well up until about September 11, 2011 where ADCIRC under predicts the water surface elevations by between 0.7 and 2.0 feet. The overall trends match well and suggest that the wind values in the area are likely low for that portion of the simulation. The station at Kotzebue did not have measured data after September 15, 2011.
A sample of the OWI generated pressure and wind fields for this project were compared with measured values at the Ralph Wien Memorial Airport at Kotzebue. The OWI pressure and wind fields matched well and are shown in Figure 19 - Figure 20.

Next the CH3D portion of the GSMB model was evaluated with respect to NOAA water surface elevations that were available for Cape Krusenstern (approximately 33 miles northwest of Cape Blossom), Deering, and Kotzebue. The comparison of the GSBM value and the NOAA value matched well and is shown in Figure 22 to Figure 24

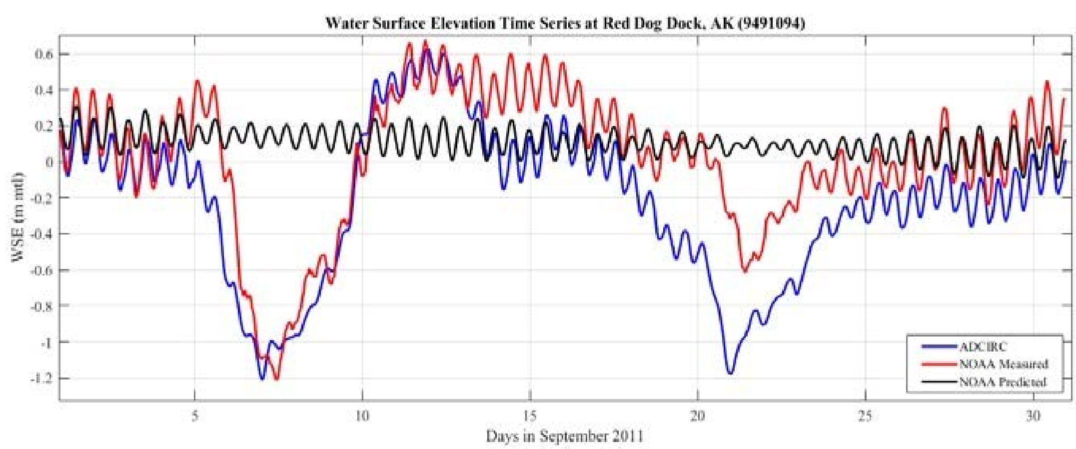

Figure 17 Time series comparison of water surface elevations at Red Dog Dock (aka Delong Mountain Terminal) for September 2011

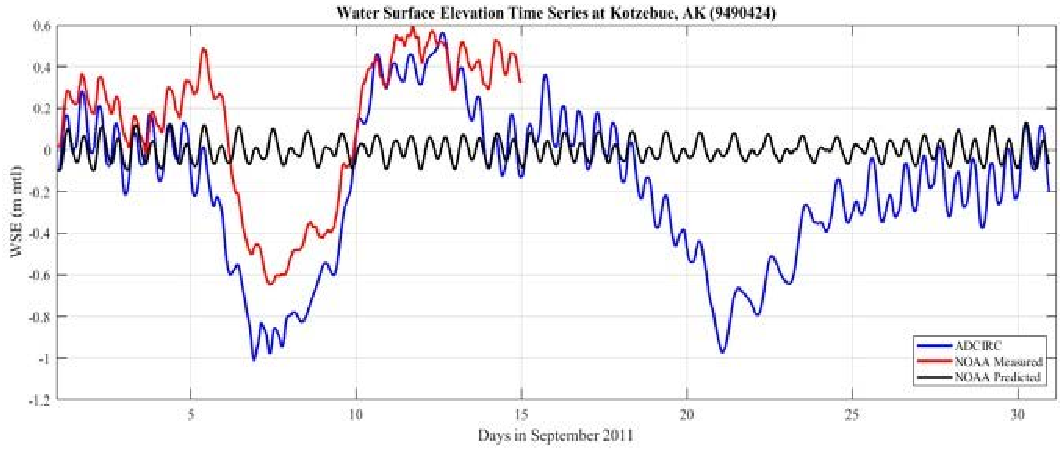

Figure 18 Time series comparison of water surface elevations at Kotzebue for September 2011

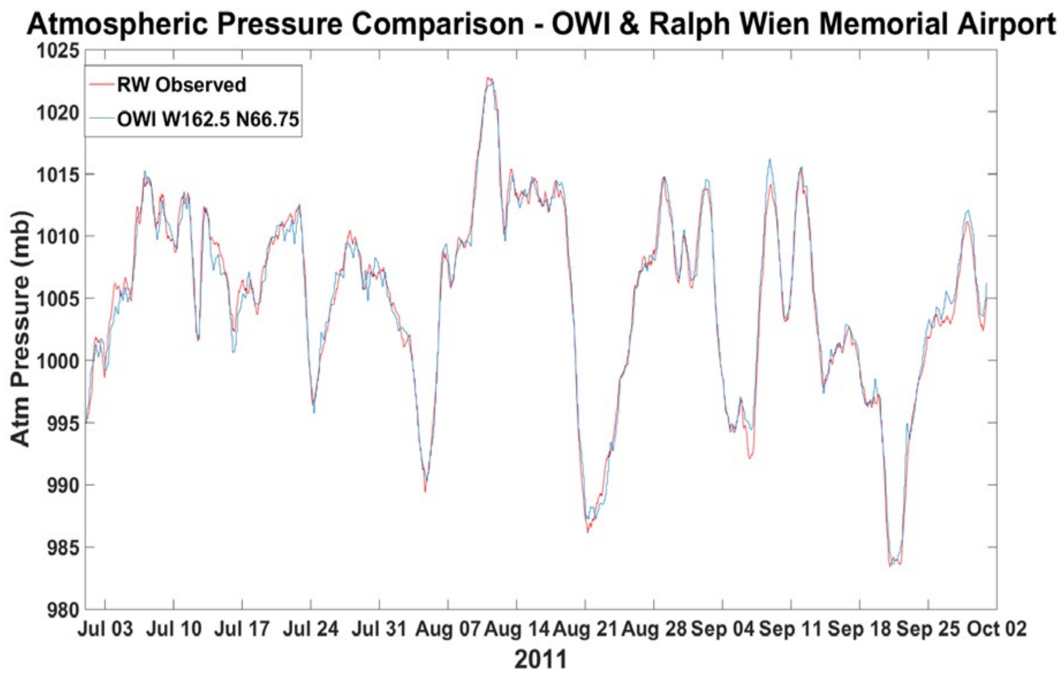

Figure 19 Comparison of Observed and OWI Atmospheric Pressure

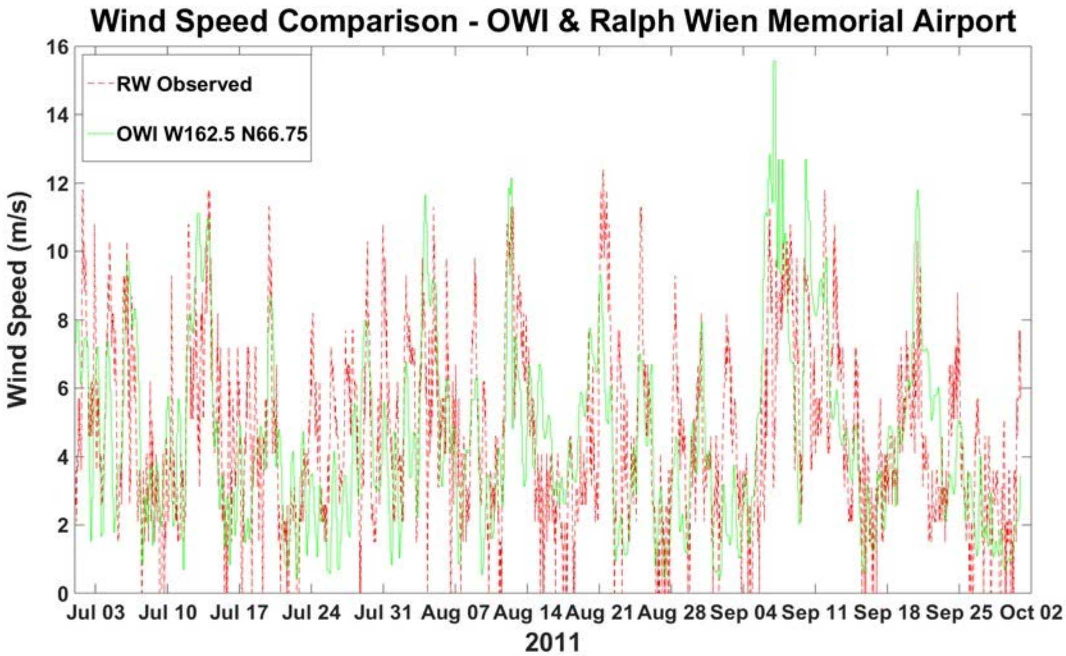

Figure 20 Comparison of observed and OWI wind speed

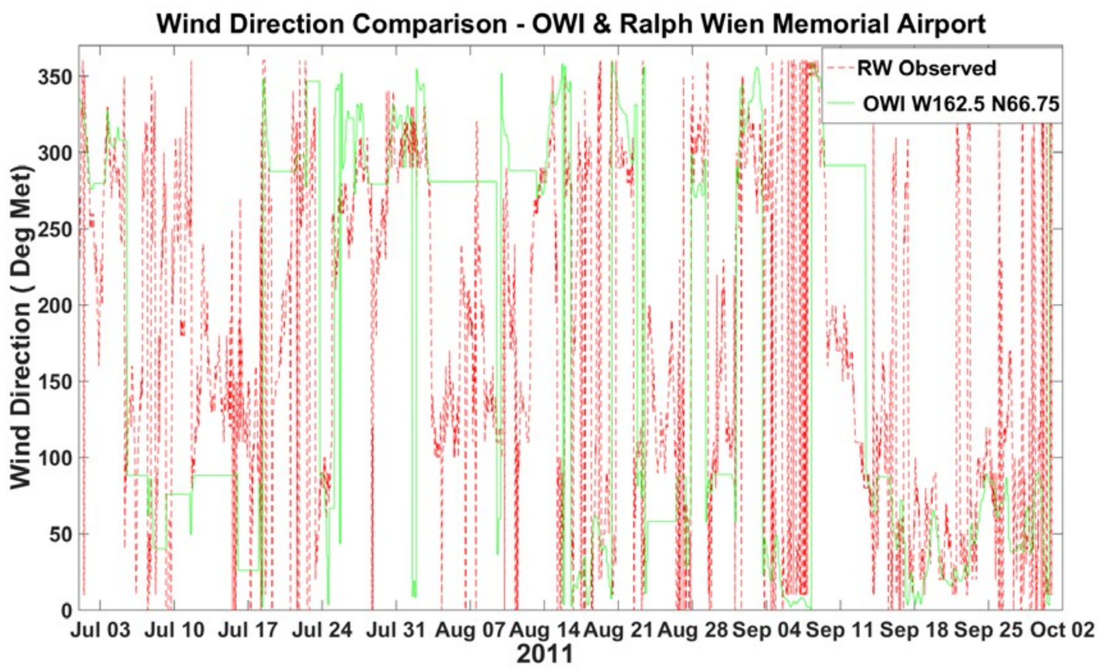

Figure 21 Comparison of observed and OWI wind direction

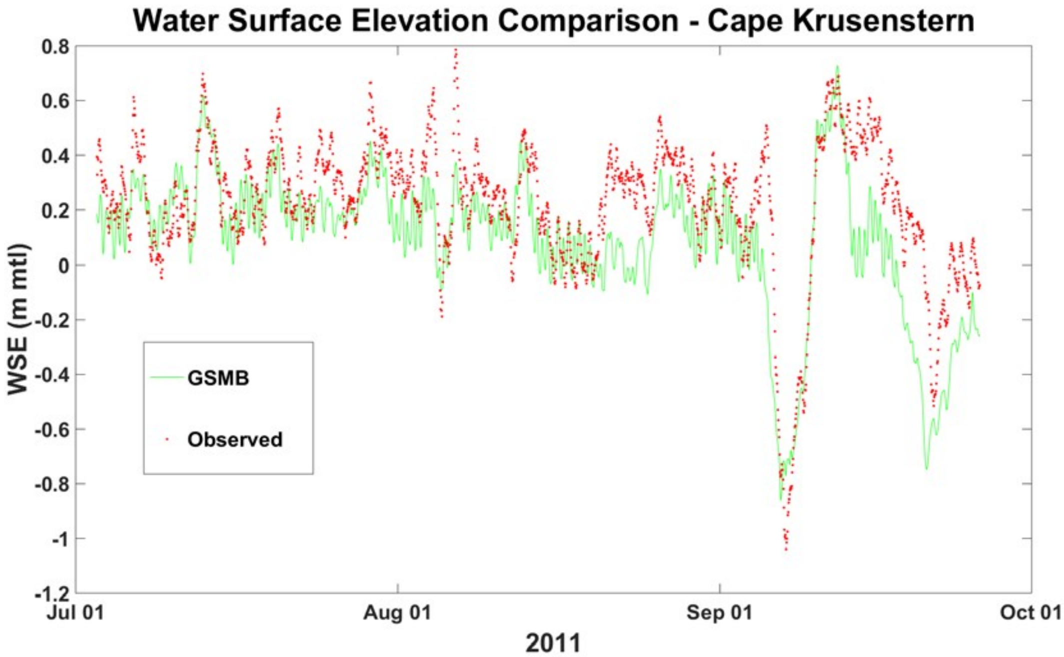

Figure 22 Cape Krusenstern water surface elevation model

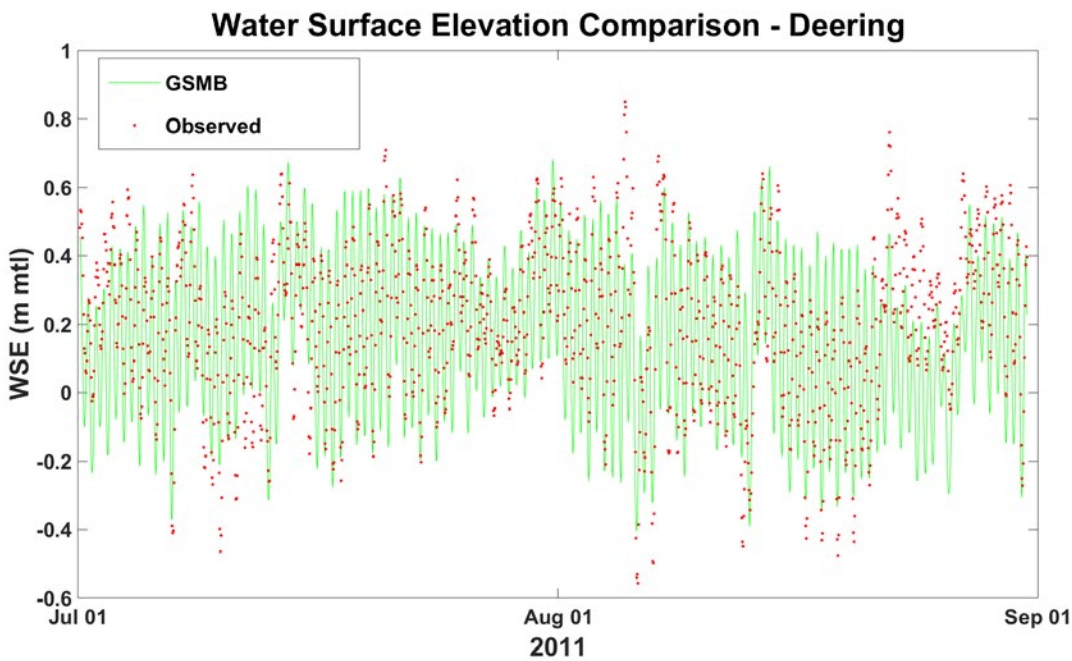

Figure 23 Deering water surface elevation comparison

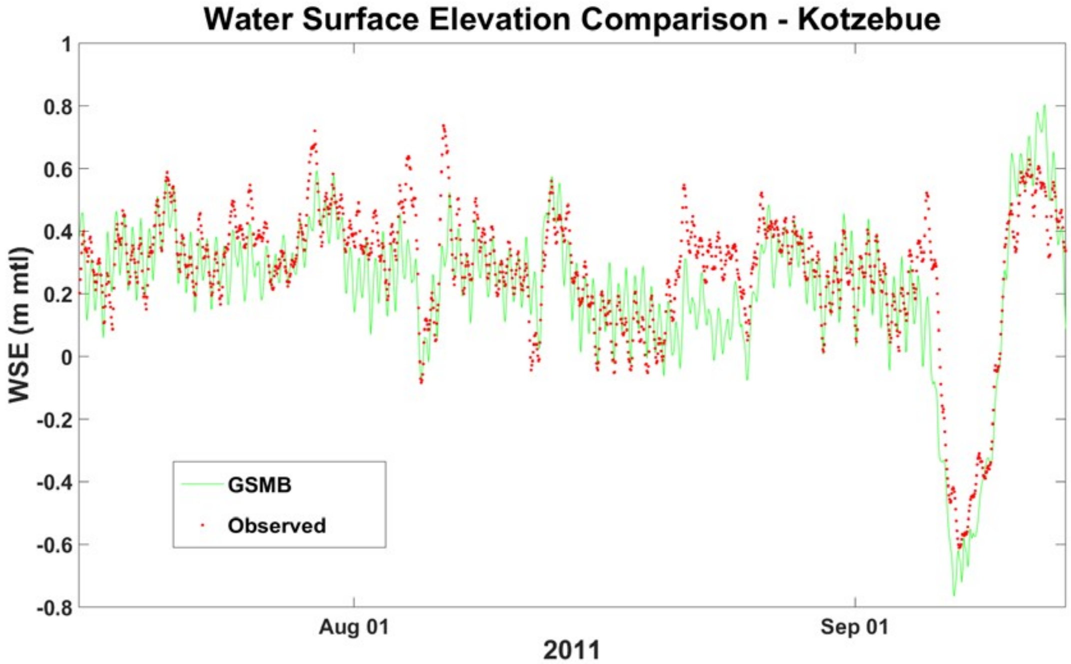

Figure 24 Kotzebue water surface elevation comparison

6.2 Circulation

6.2.1 Literature Search

Information on the circulation in Kotzebue Sound was available in from a study of the Cape Thompson area in support of the Project Chariot Plowshare Program and studies on the flow of water through the Bering Straits.

Water from the Bering Sea flows predominantly north through the Bering Strait. North of the Bering Strait the sea broadens and there is a large embayment to the east leading to Kotzebue Sound. The north flowing current that passes through the Bering Strait and enters the embayment decelerates, broadens, and turns eastward towards Kotzebue Sound tending to follow the bottom contours. (Coachman & Tripp, 1970) (Creager & McManus, 1966) (Flemming & Heggarty, 1966)

6.2.2 Current Measurement

During the summer of 2016 the Field Data Collection and Analysis Branch of the Engineering Research and Development Center's (ERDC) Waterways Experiment Station (WES) traveled to Cape Blossom From September 14, 2016 to October 20, 2016 an Acoustic Wave and Current profiler (AWAC) was deployed at Cape Blossom to acquire data on the local current climate, including the vertical structure of the currents. The profiler was deployed near the proposed channel location at a depth of approximately -30 feet (Figure 25).

Figure 25 AWAC profiler location

During the AWAC deployment period, the airport at Kotzebue recorded wind with velocities of 25 miles per hour or greater and gusts up to 37 miles per hour. The wind direction during this time generally shifted between east and west.

Measured current velocities and direction from the first bin of the water column above the instrument (approximately 5 feet above the bed) are shown in Figure 26. Figure 27 is a plot of a shorter time span. The lower panel in these figures shows current speed in meters per second (m/sec) and direction in degrees relative to true north. A direction of zero degrees indicates current flowing to the north; 180 degrees indicates current flowing to the south. The local shoreline azimuth at the study site is about 270 degrees. Currents with a direction of 270 degrees are moving along the coast to the west; currents with directions of 90 degrees are moving along the coast to the east. For the measurement period, the current direction fluctuated between east and west.

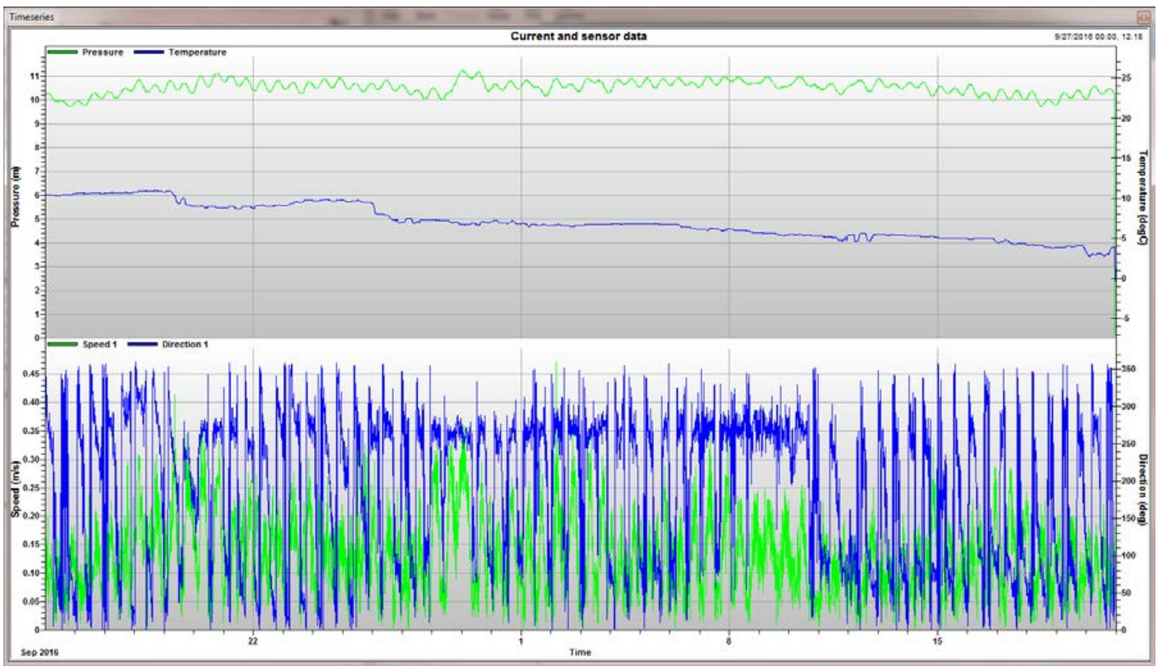

Figure 26 Current speed and direction time series for the 2016 deployment

Figure 27 Current speed and direction for September 24-30, 2016

6.2.3 Circulation

Currents at the Cape Blossom site were modeled using tidal forcing from the CSTORM simulation as applied at the western open boundary along with OWI wind and atmospheric pressure inputs. A list of the top current events from the model results are shown in Table 6.

Table 6 Top model predicted current events at Cape Blossom

Cape Blossom Project Site Currents	
Date	**Max Current Speed (m/s)**
Nov 1985	0.97
Nov 1970	0.95
Oct 1989	0.94
Nov 1966	0.90
Nov 1978	0.89
Apr 1998	0.89
Nov 2009	0.87
Nov 1978	0.87
Nov 1989	0.87
Nov 1965	0.86

6.3 Water Level

Water level increase is typically a result of wave setup, storm surge, and tide. Water level decrease is typically a result of wave set-down, wind set-down, and tide. Relative sea level rise is a longer term change in water level and its effects on a project is an additional factor that needs to be considered.

6.3.1 Wave Setup/Set-down

Wave setup is the water level rise at the coast caused by breaking waves. Conversely, wave set-down is a water level decrease at the coast before the waves break. This navigation project is beyond the coast line affected by breaking waves, so the water level change due to the effects of wave set-up or set-down was not evaluated.

6.3.2 Surge/Wind Set-Down

Surge and wind set-down are caused by wind driven transport of seawater over relatively shallow and large unobstructed waters, and are characterized by a change in water level beyond the normal tidal variations. Surge is an increase in water elevation and wind set-down is a decrease in the water elevation. Friction at the air-sea interface is increased when the air is colder than the water, which causes more wind-driven transport. Low pressure events can add to the increased water levels associated with surge, and high pressure events can reduce, even further, the water levels associated with wind set-down. Kotzebue Sound is relatively shallow and experiences wind and pressures that create surge and set-down conditions.

Surge

A study of water levels was performed the CHL using CSTORM and CH3D. Results of the Empirical Simulation Technique (EST) analysis used to generate stage –frequency relationships for Kotzebue and the top ten surge events used to develop the frequency of occurrence relationship is shown in Table 7 and Table 8.

Table 7 Stage Frequency Analysis for Kotzebue

Return Period [years]	Kotzebue Surge Level [ft MLLW]	Cape Blossom Surge Level [ft MTL]
5	4.0	4.1
10	5.1	5.6
50	8.1	8.7
100	9.6	10

Table 8 Top 10 surge events for Kotzebue and Cape Blossom

	Date	Kotzebue Maximum Water Level [ft MLLW]		Date	Cape Blossom Maximum Water Level [ft MTL]
1	Nov 1970	9.6		Nov 1970	9.2
2	Nov 1966	6.9		Nov 1966	6.9
3	Nov 1974	6.6		Aug 1962	6.6
4	Oct 1996	6.2		Nov 1974	6.2
5	Nov 2011	5.8		Oct 1996	5.9
6	Aug 1962	6.8		Nov 2011	5.6
7	Dec 2004	5.7		Dec 2004	5.6
8	Apr 2002	5.3		Nov 1965	5.2
9	Nov 1965	5.2		Apr 2002	4.9
10	Nov 1978	4.9		Sep 2005	4.3

Wind Set-Down

More important to channel navigation is the occurrence of wind set-down. Wind set-down events can affect ability of a fully loaded barge to transit the channel and maintain a safe under-keel clearance. The ADCIRC model used for the Delong Mountain Terminal Navigation Study (Figure 28) predicted water surface elevations for a hypothetical season which included analysis of the occurrence of set-down events. The frequency of occurrence for water level set-down for the hypothetical year is shown in Figure 29. The information for the analysis was based on a very limited data set and was very dependent on the water surface differential that was imposed on the north and south boundaries of the ADCIRC model domain.

For the July through November season, set-down exceeded –4.9 feet less than 2 percent of the time; –3.3 feet about 3 percent of the time; and –1.6 feet 14 percent of the time. Typically, when set-down occurred, it was less than –1.2 feet (Figure 29 – note departures (wind set-down) shown are in meters). The maximum set-down increased as the open water season moved into fall with a maximum value of –7.6 feet. For the purpose of this study, it was assumed that ships trying to deliver during set-down events will wait offshore until conditions permit channel transit.

Figure 28 Location of Delong Mountain Terminal and Cape Blossom

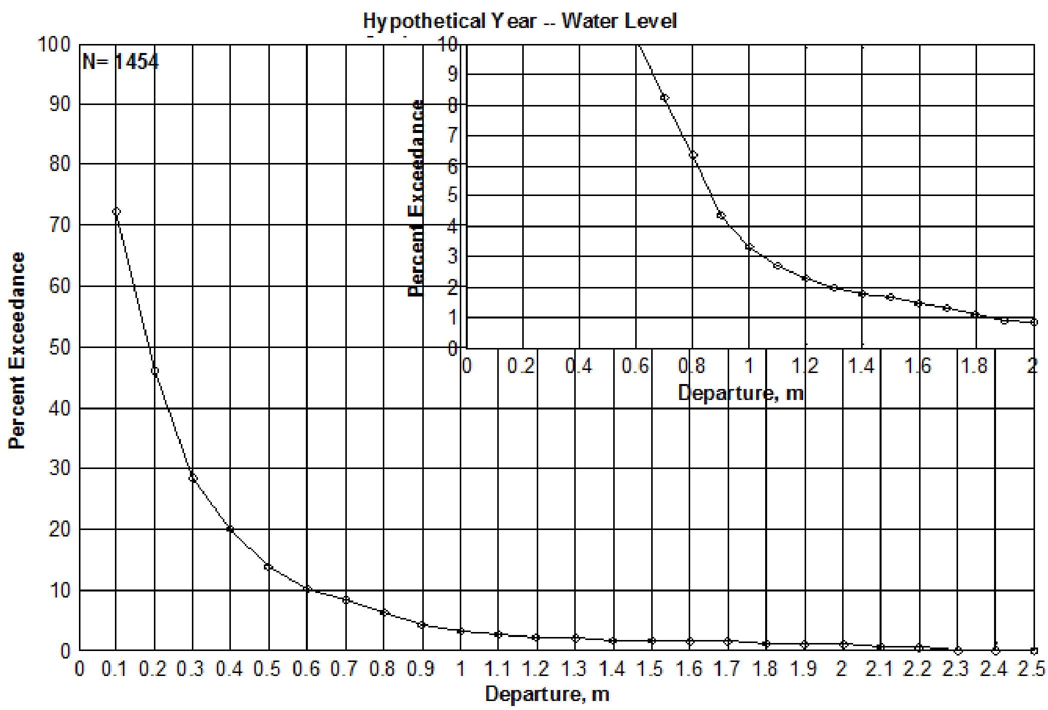

Figure 29 Frequency-of-occurrence for water level set-down hypothetical open-water season at the Delong Mountain Terminal. Note departure shown is in meters.

6.3.3 Tide

Tidal forcing from the CSTORM simulations was applied at the western open boundary. The CSTORM simulations used seven harmonic constituents (M_2, S_2, N_2, K_1, O_1, Q_1, and K_2) to produce the tidal boundary, with M_2 being the primary with an amplitude of about 0.3 feet. The influence of the Solar Semiannual and Solar Annual constituents on the tide variation observed at Red Dog Dock (aka Delong Mountain Terminal) is greater than the spring tide range and could not be dismissed. To account for the unresolved tidal constituent forcing, the NOAA predicted tide signal at Red Dog Dock was filtered to remove the tidal and atmospherically forced response. The resulting filtered signal, which was added to the offshore water surface elevation boundary forcing is shown in Figure 30.

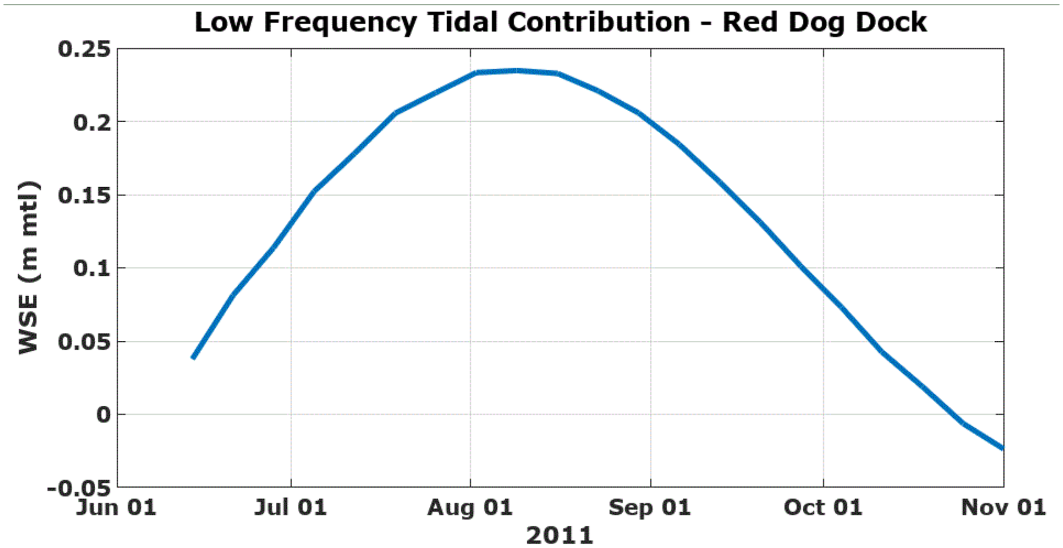

Figure 30 Low frequency tidal contribution.

6.3.4 Sea Level Rise

Evidence suggests that the arctic environment is experiencing a warming trend. The magnitude, duration, and effect of a warming trend is not known; however a shrinking polar ice pack could result in an extended open water season and an increase in frequency of the large storms that could impact a proposed navigation channel.

The Corps of Engineers requires that planning studies and engineering designs over the project life cycle, for both existing and proposed projects consider alternatives that are formulated and evaluated for the entire range of possible future rates of sea-level change (SLC), represented by three scenarios of “low,” “intermediate,” and “high” sea-level change. According to USACE guidance in ER 1100-2-8162 and ETL 1100-2-1, SLC “low” rate is the historic SLC. The “intermediate” and “high” rates are computed using the following:

Estimate the “intermediate” rate of local mean sea-level change using the modified NRC Curve I and the NRC equations. Add those to the local historic rate of vertical land movement.

Estimate the “high” rate of local mean sea-level change using the modified NRC Curve III and NRC equations. Add those to the local rate of vertical land movement. This “high” rate exceeds the upper bounds of IPCC estimates from both 2001 and 2007 to accommodate potential rapid loss of ice from Antarctica and Greenland.

NRC Equations

The 1987 NRC described these three scenarios using the following equation:

$$E(t) = 0.0012t + bt^2$$

in which t represents years, starting in 1986, b is a constant, and $E(t)$ is the eustatic sea-level change, in meters, as a function of t. The NRC committee recommended “projections be updated approximately every decade to incorporate additional data.” At the time the NRC report was prepared, the estimate of global mean sea-level change was approximately 1.2 mm/year. Using the current estimate of 1.7 mm/year for GMSL change, as presented by the IPCC (IPCC 2007), results in this equation being modified to be:

$$E(t) = 0.0017t + bt^2$$

The three scenarios proposed by the NRC result in global eustatic sea-level rise values, by the year 2100, of 0.5 meters, 1.0 meters, and 1.5 meters. Adjusting the equation to include the historic GMSL change rate of 1.7 mm/year and the start date of 1992 (which corresponds to the midpoint of the current National Tidal Datum Epoch of 1983-2001), results in updated values for the variable b being equal to 2.71E-5 for modified NRC Curve I, 7.00E-5 for modified NRC Curve II, and 1.13E-4 for modified NRC Curve III. The three GMSL rise scenarios are depicted in Figure 31.

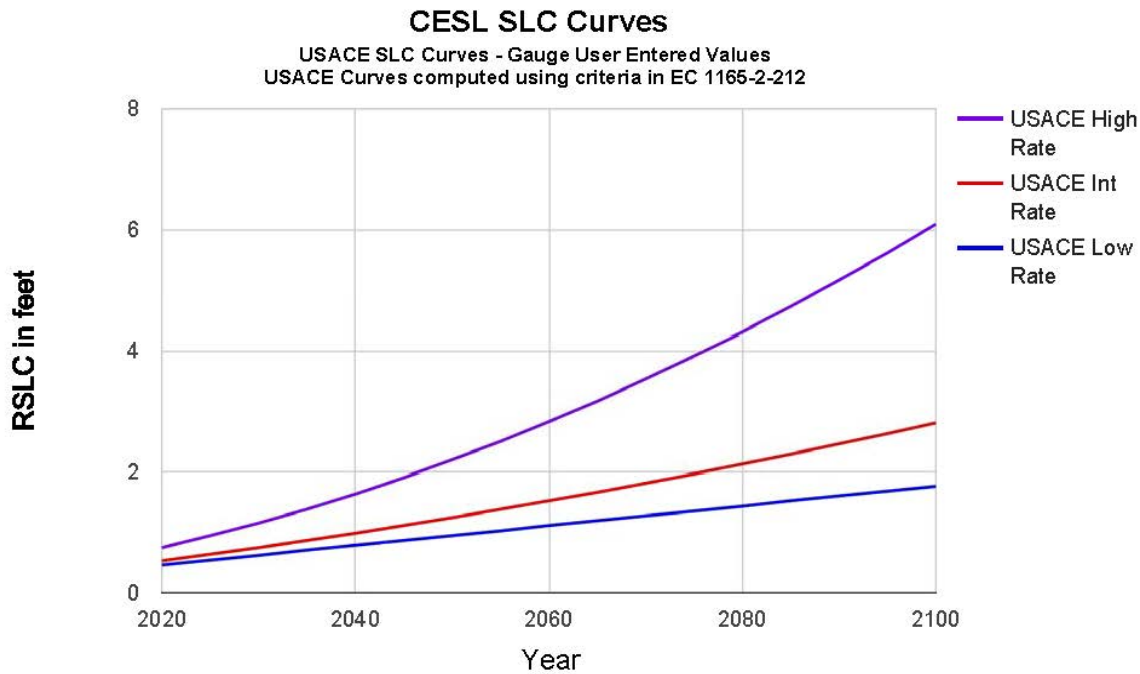

Figure 31 Scenarios for GMSL Rise (based on updates to NRC 1987 equation).

Manipulating the equation to account for the fact that it was developed for eustatic sea level rise starting in 1992, while projects will actually be constructed at some date after 1992, results in the following equation:

$$E(t_2) - E(t_1) = 0.0017(t_2 - t_1) + b(t_2^2 - t_1^2)$$

where t_1 is the time between the project's construction date and 1992 and t_2 is the time between a future date at which one wants an estimate for sea-level change and 1992 (or $t_2 = t_1$ + number of years after construction) .

The USACE SLC scenarios were developed using the guidance in ER 1100-2-8162 and ETL 1100-2-1. Assuming a eustatic SLC rate of 1.7 mm/year and start date of 1992 (mid-year of the NOAA National Tidal Datum Epoch (NTDE) of 1983-2001), the updated values for the variable b in the 1987 NRC report are equal to 2.71E-5 for the modified NRC Curve I (USACE Intermediate Scenario), and 1.13E-4 for modified NRC Curve III (USACE High Rate Scenario). The USACE Low Rate Scenario extrapolates the historic rate of sea level change.

There is no sea level trend data for Kotzebue or the area around Kotzebue. The Permanent Service for Mean Sea Level (PSMSL) has sea level trends published for Providenia, Russia, which is the closest station to Kotzebue with a long term record. The record length for Providenia is 32 years which is less than the recommended two tidal epoch duration of about 40 years, but it is the longest record near Kotzebue. The published sea level trend for Providenia is +0.1299 inches/year. This value was used with the equations in ER 1100-2-8162 to determine the possible sea level rise at the end of the project life.

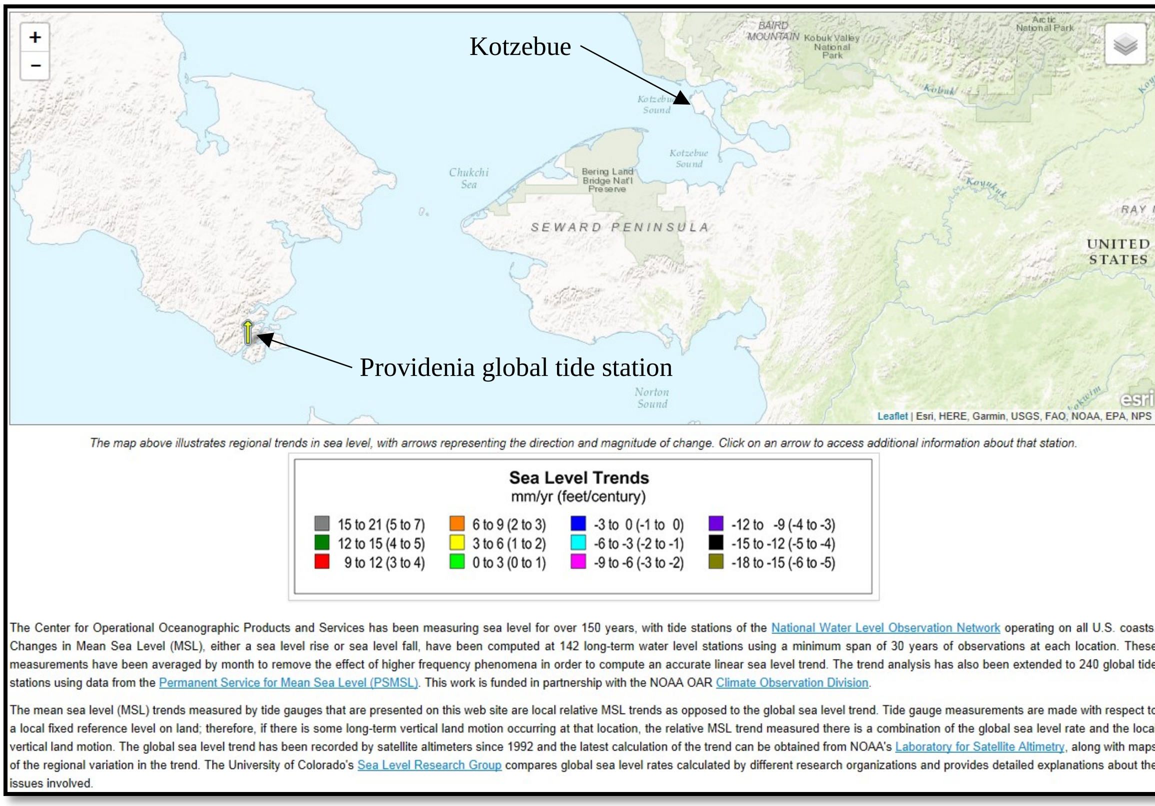

Figure 32 Location of Providenia, Russia

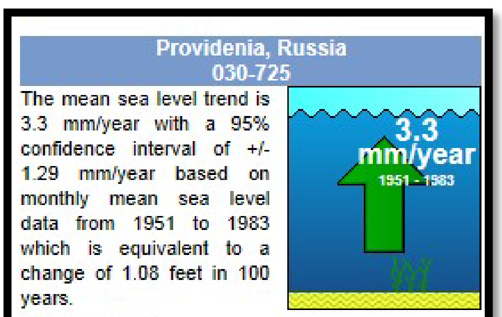

Figure 33 Sea level trend in Providenia, Russia

In addition to looking at the SLC based on Providenia, Russia, the SLC was evaluated using the GMSL change (1.7 mm/year or 0.0669 inches/year) added to the vertical land movement (VLM) at Kotzebue as measured by the Jet Propulsion Laboratory (JPL), California Institute of Technology under contract with the National Aeronautics and Space Administration (NASA) (Figure 34). The VLM reported by JPL is -0.0659 inches/year (Figure 35). This was subtracted from the GMSL change and resulted in a SLC of 0.133 inches/year (rising sea level).

Figure 34 Location of JPL's vertical land movement data site at Kotzebue

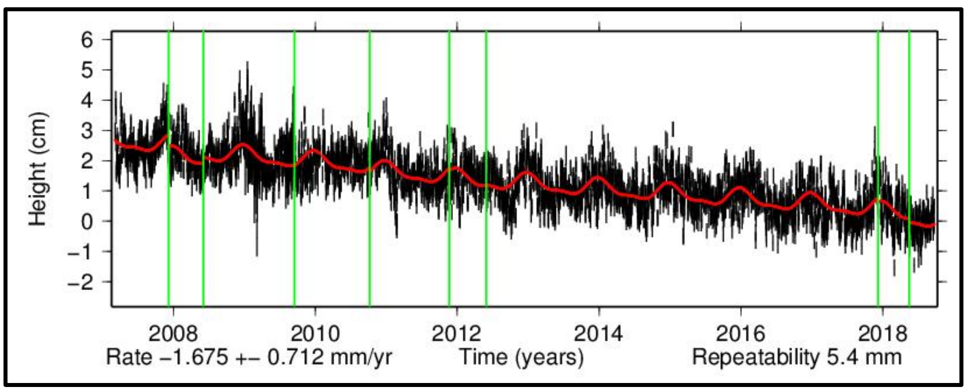

Figure 35 Vertical land movement data for Kotzebue

For a fifty year project life, a project in the Kotzebue area could see sea level rise as much as 2.52 feet (Table 9). A navigation channel will not be adversely affected by sea level rise. Maintenance dredging depth requirements could be re-evaluated in the event that the sea level rises to a level where the under-keel clearance is greater needed for the function of the facility. While sea level rise may not adversely affect the dredge channel, it is an important consideration for the shore side facilities and the structures built to connect to the channel. The local sponsor will need to consider the effects of sea level change during their design to ensure that they remain functional in the future.

Table 9 Sea level rise prediction for a 50 year project life

	Low	Intermediate	High
Using Providenia Russia Mean Sea Level Trend	0.54 feet	1.01 feet	2.51 feet
Using GMSL and VLM at Kotzebue	0.55 feet	1.02 feet	2.52 feet

7.0 WAVE CLIMATE

The CHL performed a deep-water wave hindcast for the west coast of Alaska. The hindcast was driven by the wind data described in Section 4.4 Wind and was coupled with weekly ice field data to quantify the open water capable of wind-wave growth. The west coast hindcast includes 469 special output locations. Three of the special output locations (shown in Figure 36) are at the entrance to Kotzebue Sound. These locations provide percent occurrence statistics (wave height, period, and direction) and extreme storm analysis.

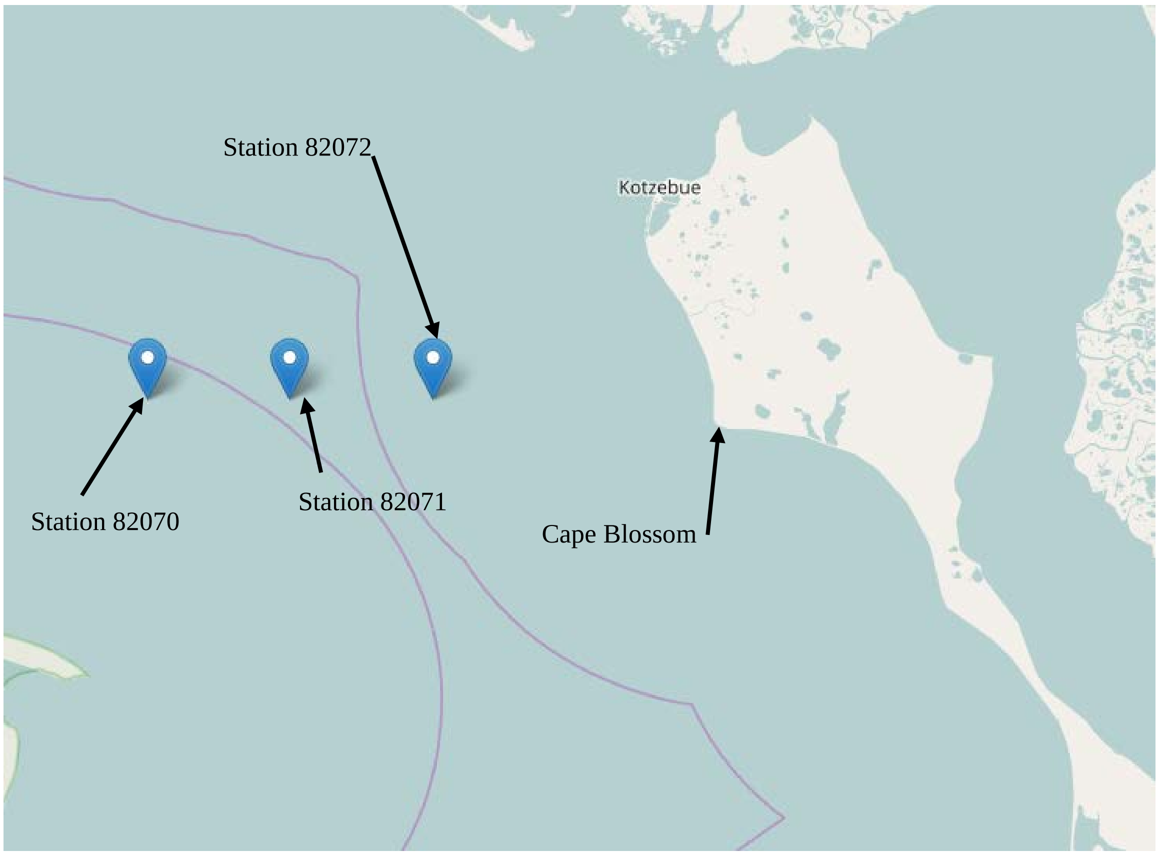

Figure 36 Wind and deep water wave special output locations

7.1 Ice Field Specification

A predetermined concentration level of the ice field must be set to either open water or land. An area of ice concentration of 70-percent or greater was used to switch the water point to land. This concentration was chosen based on previous wave hindcast experience at the Delong Mountain Terminal. Examples of sea ice differences are shown in Figure 37 and are derived from NOAA's Observers Guide to Sea Ice (prepared by Dr. O. Smith, University of Alaska, Anchorage, http://response.restoration.noaa.gov/sites/default/files/Sea_Ice_Guide.pdf).

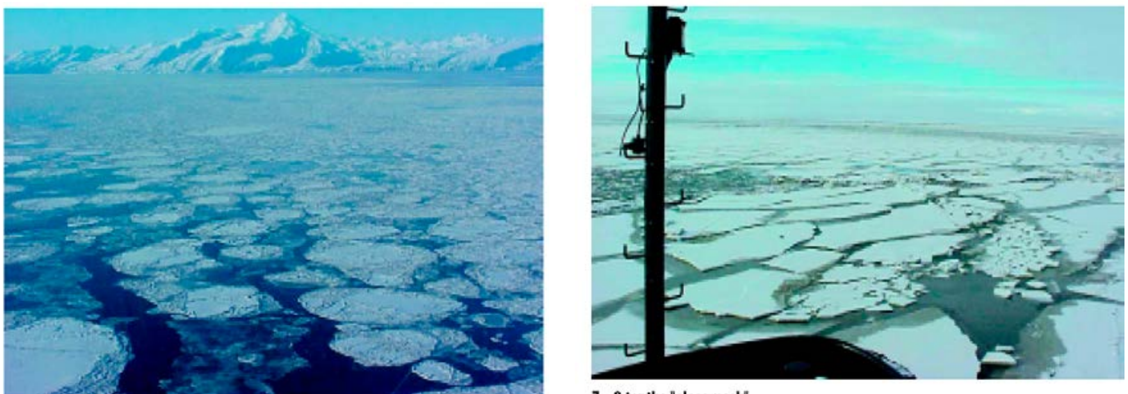

5 - 6 tenths "open drift" 7 - 8 tenths "close pack"

Left 50 to 60 percent, right panel 70 to 80 percent concentration.

Figure 37 Examples of sea ice concentration.

Mean weekly ice maps were used for the western Alaska hindcast modeling effort. An example of the final digital ice map for week 31 (30 July through 5 August) in 1998 is presented in Figure 38. Digital ice field maps are derived from remote sensing techniques using visible and infrared imagery from polar orbiting satellites. Algorithms are then used to estimate the sea ice concentration. These images are then translated to gridded information, and archived at the National Oceanic and Atmospheric Administration (NOAA), National Environmental Satellite Data Information Services (NESDIS). Ice maps for selected storm events prior to the 1972 digital database were constructed by Oceanweather, Inc.

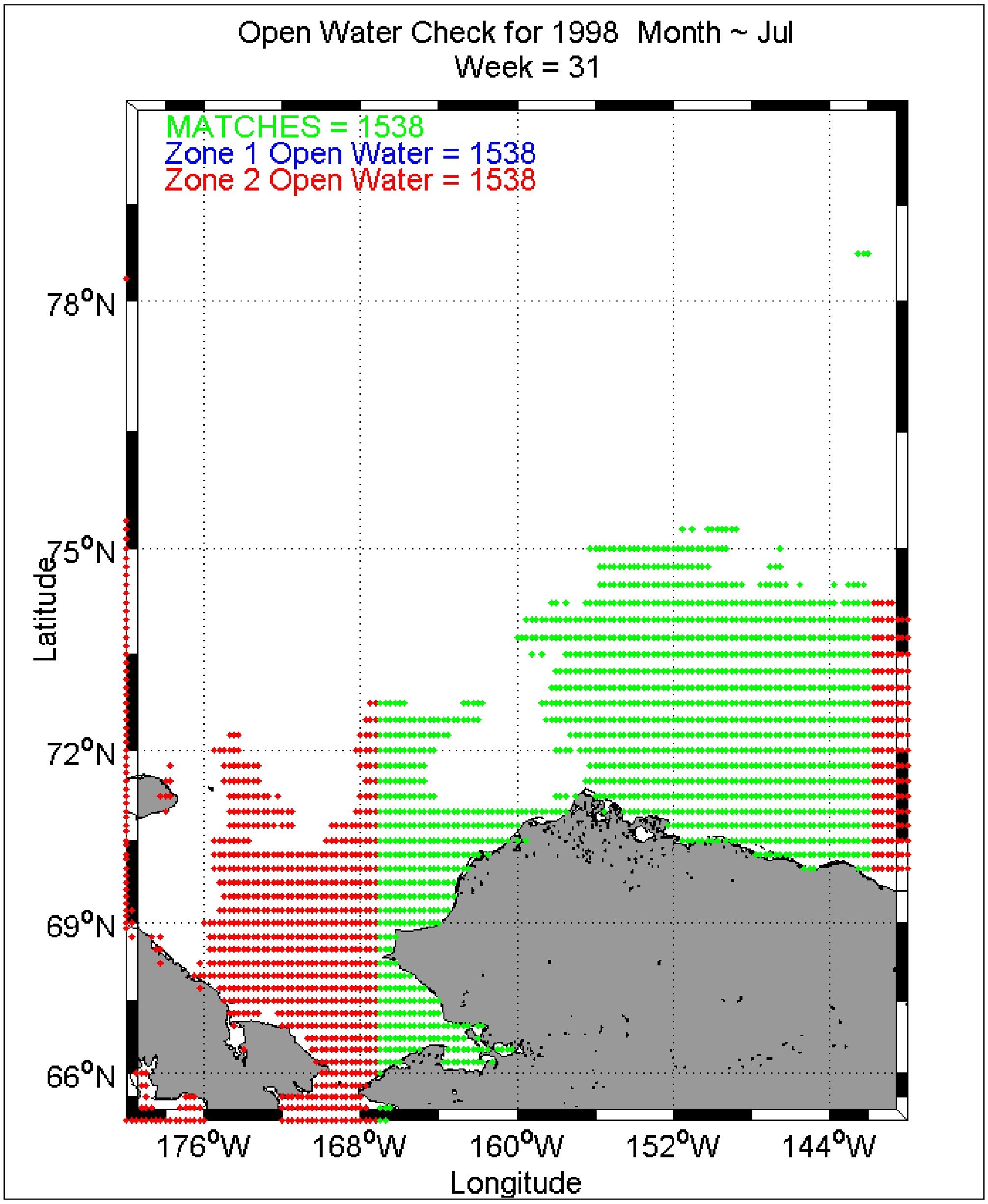

Figure 38. Example of the final ice mask used in wave model simulation.

Note the symbols identify the open water area. The zones refer to the level of grid refinement.

7.2 Deep Water Wave Hindcast

The deep water waves for the hindcast save points were analyzed using the **WA**ve prediction **M**odel (WAM). WAM is a third generation wave model which predicts directional spectra as well as wave properties such as significant wave height, mean wave direction and frequency, swell wave height and mean direction. All source terms (wind input, wave-wave interaction, white-capping, wave bottom effects, and wave breaking) are specified with the same degree of freedom in WAM with which the resulting directional wave spectra are specified. There is no a priori assumption governing the shape of the frequency or directional wave spectrum. WAM has been used extensively at weather prediction centers with the option to include ice coverage. The development and verification of the WAM model for the western Alaska hindcast are detailed in the USACE Navigation Improvements Draft Interim Feasibility Report, Delong Mountain Terminal (United States Army Corps of Engineers Alaska District, 2005) and an unpublished USACE CHL report *Offshore Wind and Wave Climate* performed for the USACE Barrow Storm Damage Reduction Project (Jensen, 2009).

Model Assumptions for WAM are:

- Time dependent wave action balance equation.
- Wave growth based on sea surface roughness and wind characteristics.
- Nonlinear wave and wave interaction by Discrete Interaction Approximation (DIA).
- Free form of spectral shape.
- High dissipation rate to short waves.

7.3 Extreme and Average Wave Climate

7.3.1 Extreme Storms

Selected severe historic storms dating back to 1954 were included in the hindcast to provide higher confidence in the extreme wave estimates (those representing 50-year return-period events). The largest wave of record in the extremal wave analysis for save point 82072 (Figure 36) occurred in August 1962. The peak significant deep-water wave height was 14.4 feet with a 10.18-second period. A plot of the deep-water significant wave height and the return period for 82072 is shown in Figure 39 and significant wave heights for the top 10 storms from 1954 to 2009 are shown below the plot along with their ranking.

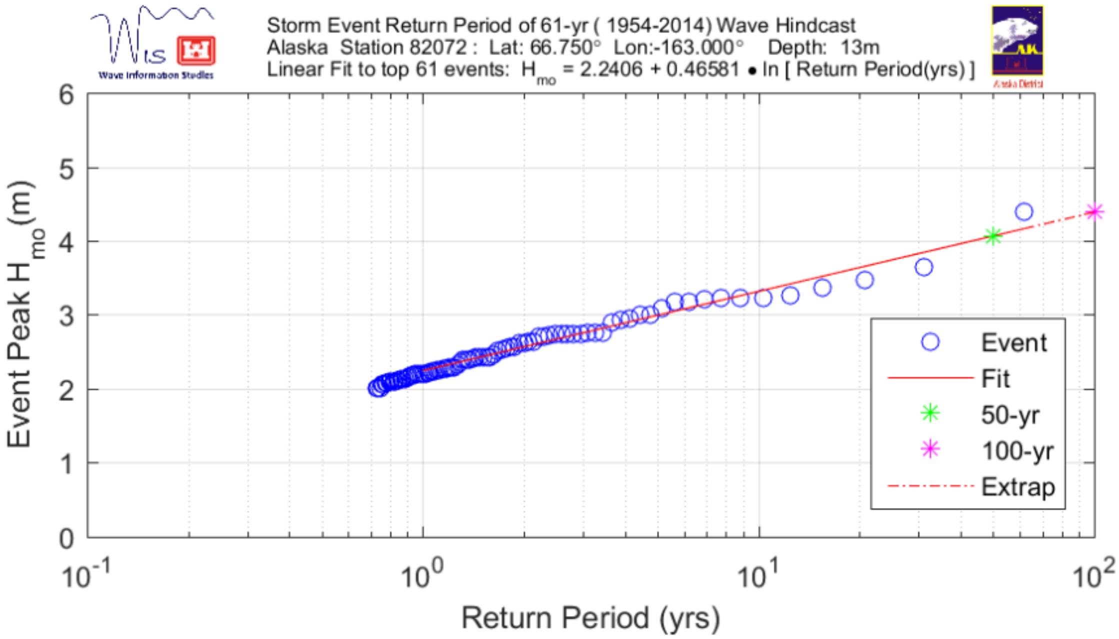

Top 10 events based on Peak H_{mo}

Event	Date/Time(UTC)	H_{mo}	T_p	θ_{mean}	Event	Date/Time(UTC)	H_{mo}	T_p	θ_{mean}
1	1962/08/30 21:00	4.39	10.18	287.0	6	1973/10/02 19:00	3.23	11.12	308.0
2	1997/10/04 01:00	3.65	7.43	271.0	7	1960/09/26 20:00	3.23	7.01	183.0
3	1996/11/09 13:00	3.46	7.09	144.0	8	1990/08/27 07:00	3.22	7.55	253.0
4	1990/11/05 07:00	3.37	7.90	264.0	9	2011/11/09 13:00	3.20	6.90	125.0
5	1992/10/06 13:00	3.26	7.15	159.0	10	1993/11/17 07:00	3.18	11.63	293.0

An event is defined as any period when H_{mo} > 2.00m θ_{mean} is direction that waves are arriving from

ERDC US Army Engineer Research & Development Center   ST82072

Figure 39 Deep water wave height return period for save point nearest the project site.

7.3.2 Average Deep-Water Wave Climate

The average deep-water wave climate in the project area is dominated by waves from the north-west as shown in wave roses shown in Figure 40 to Figure 45. The wave rose for all months (Figure 40) shows the same north-west tendency as the wave roses for June through October (Figure 41 through Figure 45). Wave heights between 0 to 3.25 feet dominate the wave climate from June through October. Wave heights of 3.3 and greater occur less than 10% of the time. Table 10 illustrates the percentage of occurrence of waves during the open water season.

While the deep water wave climate at the entrance to Kotzebue Sound is dominated by waves from the northwest, the record of the top ten storms indicates that significant waves from the southeast are also possible.

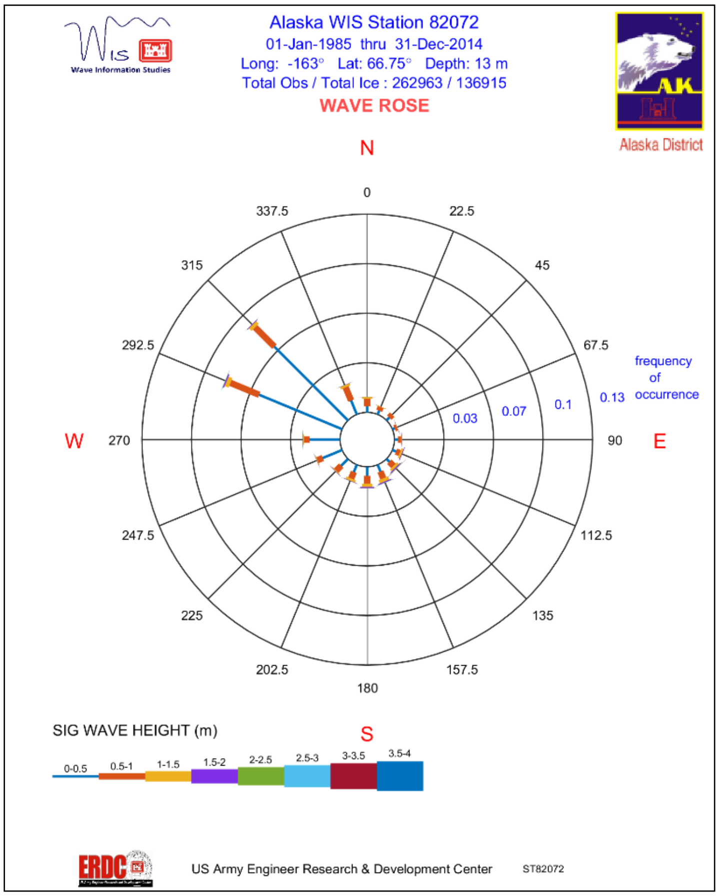

Figure 40 Wave rose for all hindcast years, January through December

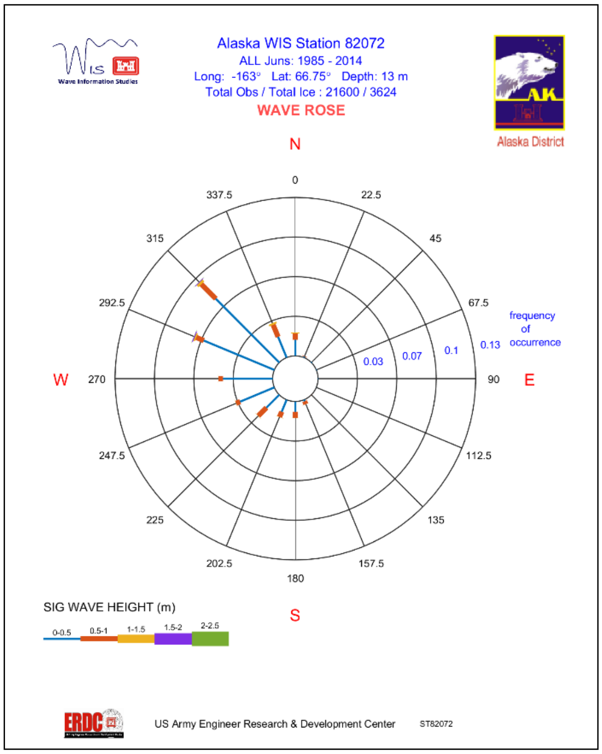

Figure 41 Wave rose for all hindcast years, June

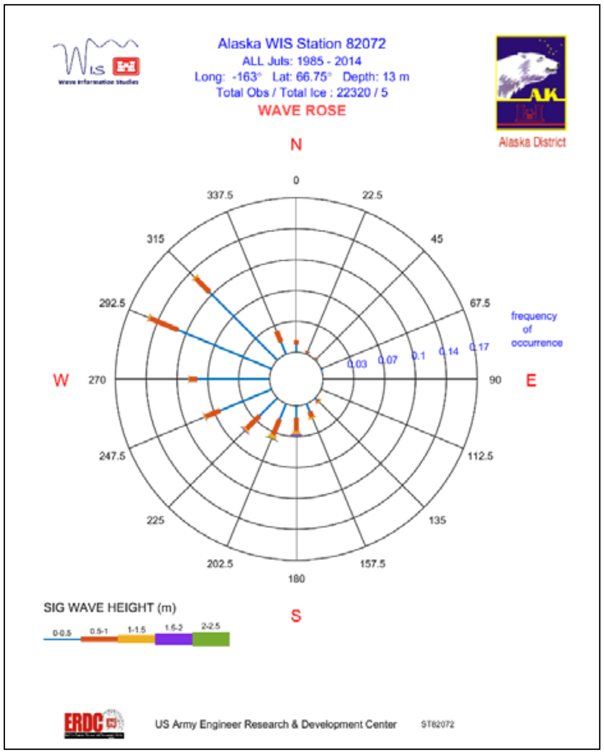

Figure 42 Wave rose for all hindcast years, July

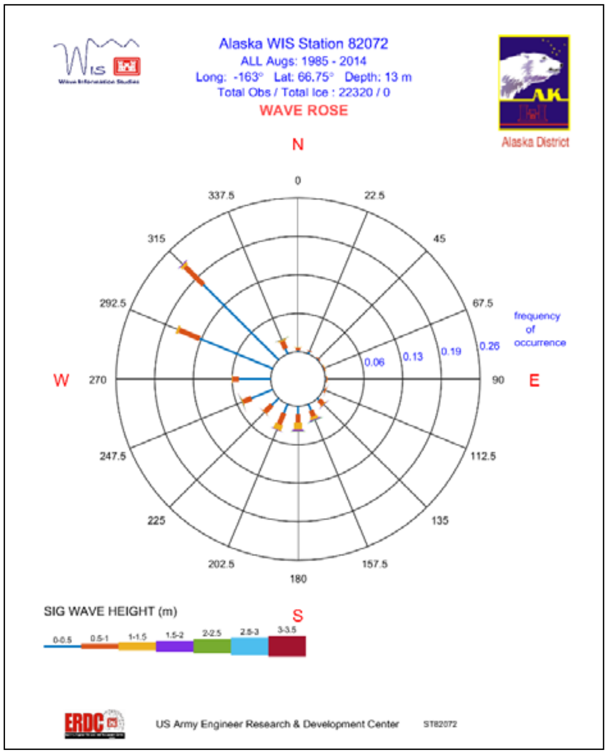

Figure 43 Wave rose for all hindcast years, August

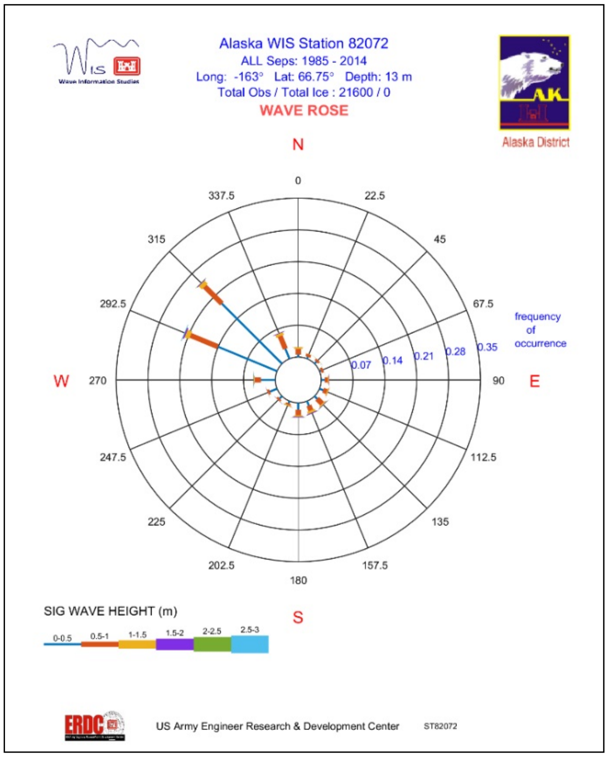

Figure 44 Wave rose for all hindcast years, September

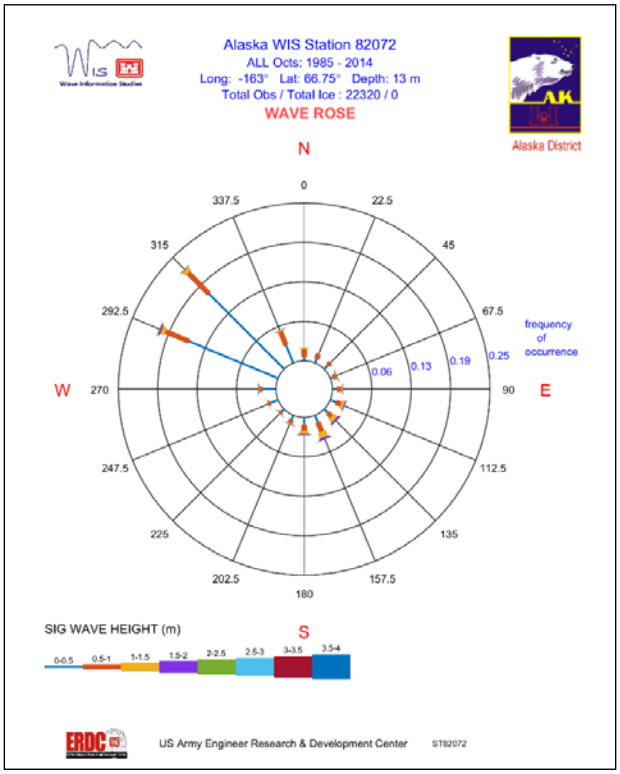

Figure 45 Wave rose for all hindcast years, October

Table 10 Percent of occurrence of wave heights for all directions (save point 82072)

Wave Height

	Calms 0-0.3 feet	0.3-1.6 feet	1.6-3.3 feet	3.3+ feet
June*	46.1	29.0	7.3	0.9
July	33.1	47.3	17.2	2.4
August	24.3	48.9	20.7	6.0
September	17.6	48.9	26.2	7.4
October	21.1	49.1	21.8	8.0
***includes periods of ice cover**				

7.4 Shallow Water Wave

An Acoustic Wave and Current Profiler (AWAC) was deployed from September 15, 2016 to October 20, 2016 to measure the wave and current climate at the site. The instrument was deployed in approximately 30 feet of water at the location shown in Figure 25. A plot of the measured wave data is shown in Figure 46. The largest wave height measured during the deployment was 6.6 feet (2 meters). Records from the Kotzebue Airport indicate that wind speeds reached 29 miles per hour during the time that the wave height reached 6.6 feet.

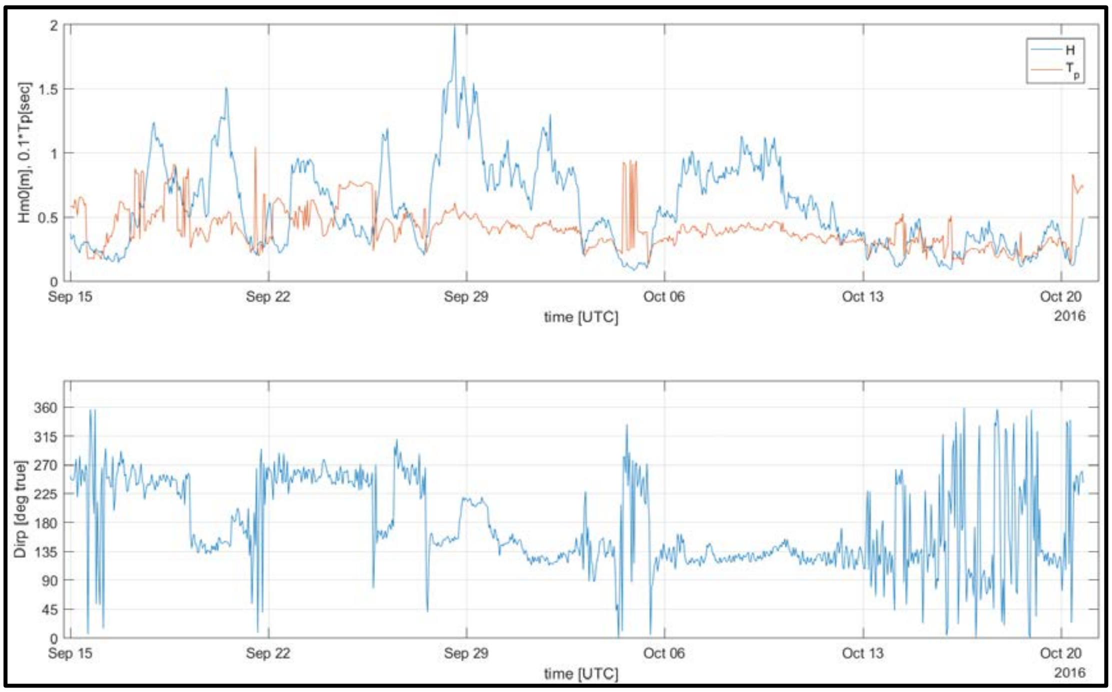

Note: Note: Wave period data is multiplied by 0.1

Figure 46 Wave data from AWAC 2016 deployment.

In addition to the measured wave data, the shallow water wave was analyzed using the Steady-State Spectral Wave (STWAVE) model. STWAVE was used to look at the deep-water wave transformation into the proposed project site and development of a locally generated wind wave to help characterize the near shore wave. It was also used to determine the operational wave climate that could be experienced by a vessel transiting the channel during the open water season.

STWAVE is a steady state finite difference model based on the wave action balance equation. It simulates depth-induced wave refraction and shoaling, current-induced refraction and shoaling, depth- and steepness-induced wave breaking, wind-wave growth, and wave-wave interaction and white capping that redistribute and dissipate energy in a growing wave field.

7.4.1 Bathymetry

Figure 47 shows a contour plot of the bathymetry for Cape Blossom generated by STWAVE. The grid incorporates digital bathymetry from a 2011 NOAA survey and hand input bathymetry from NOAA bathymetric charts for the area.

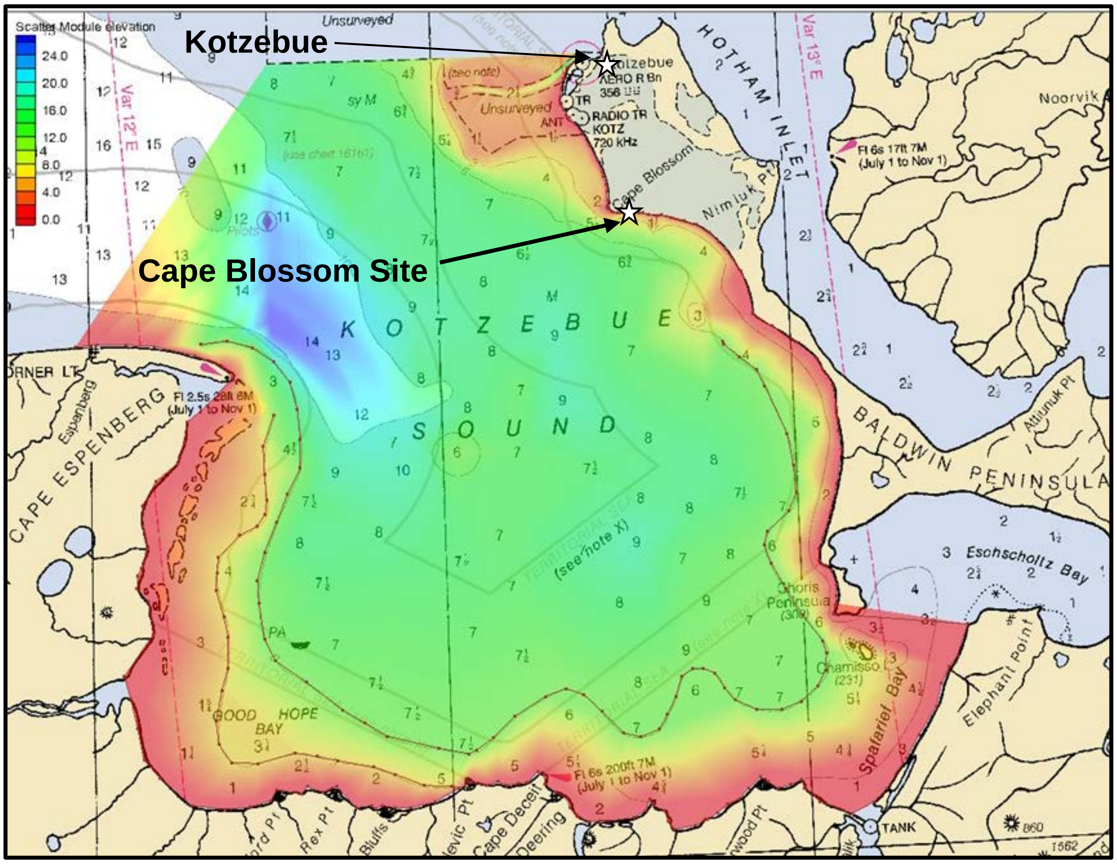

Figure 47 STWAVE bathymetry for Cape Blossom, AK (depths in meters).

Sample output

Figure 48 through Figure 51 show examples of output from STWAVE. Figure 48 and Figure 49 show a transformed deep-water wave. The incident wave for this condition is from the northwest with a wave height of 3.3 feet and a period of 10 seconds. As shown by the vector arrows, the incident wave refracts and starts to turn shoreward as it enters Kotzebue Sound. Figure 50 and Figure 51 show a wind grown wave with wind from the south-southeast at 13 m/s.

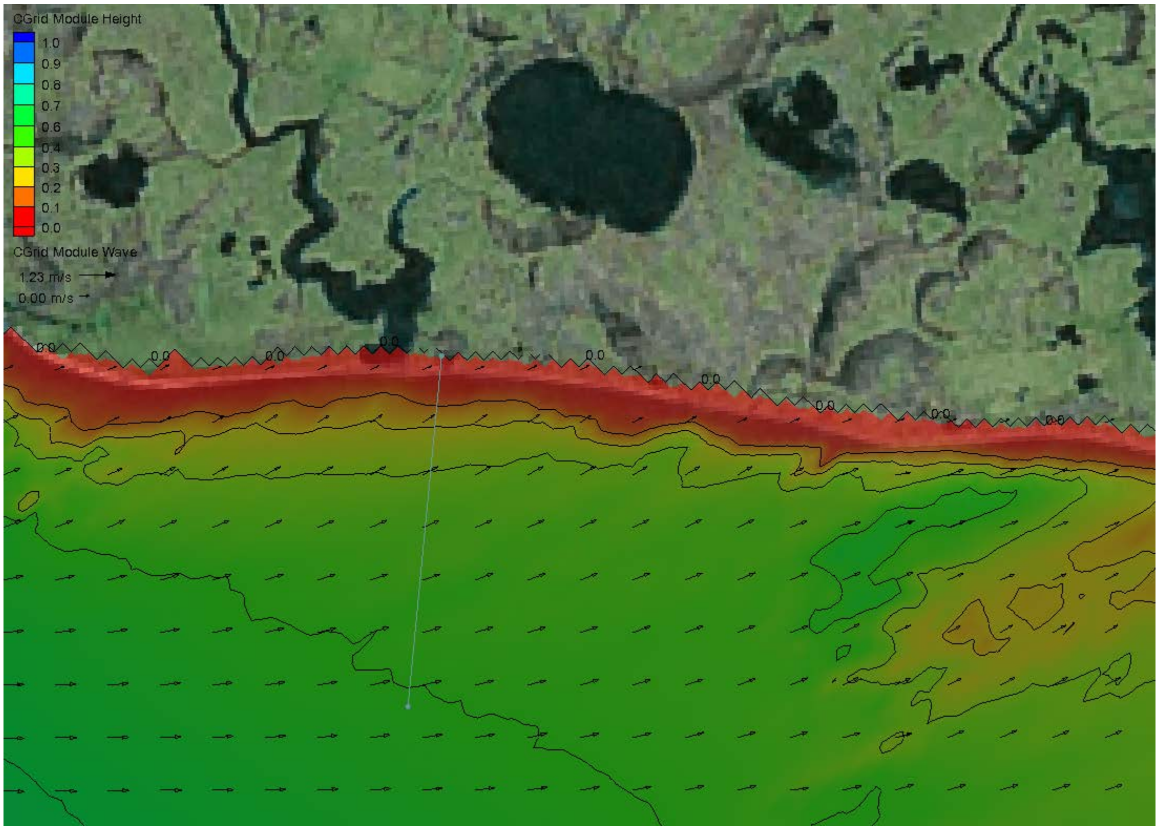

Figure 48 Sample STWAVE transformed wave height. Note legend is in meters (Boundary wave height = 3.3 feet (1 meter)).

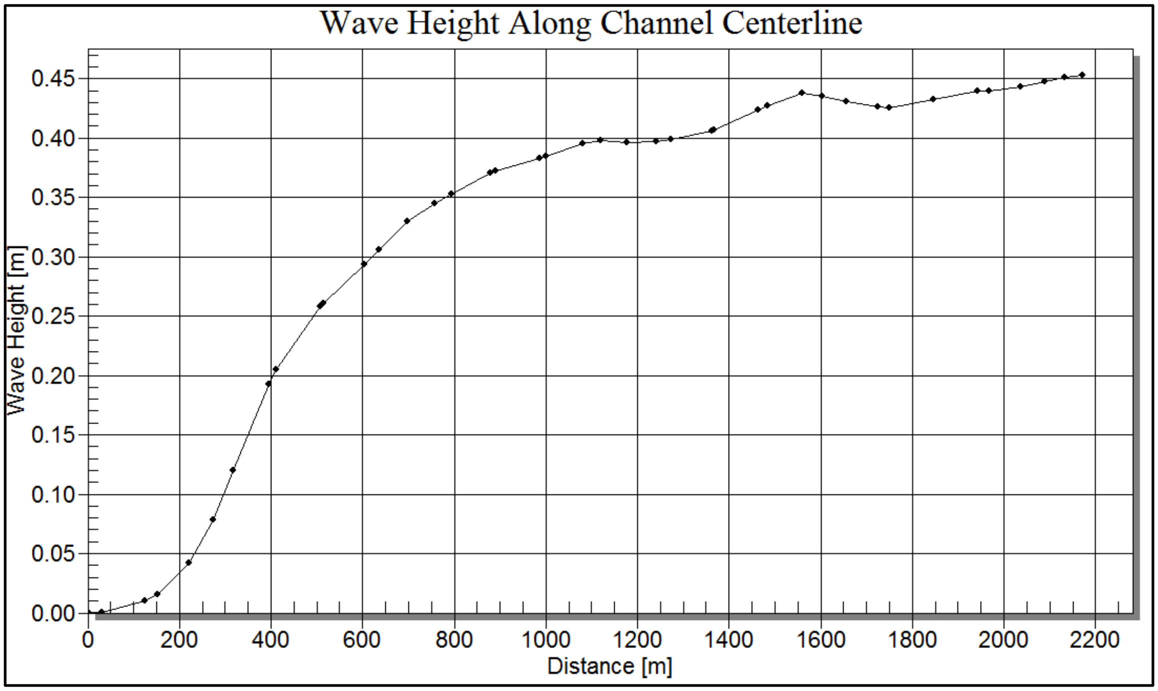

Figure 49 Transformed wave heights along channel centerline for northwest wave. Note plot shown is in meters (Boundary wave height = 3.3 feet (1 meter))

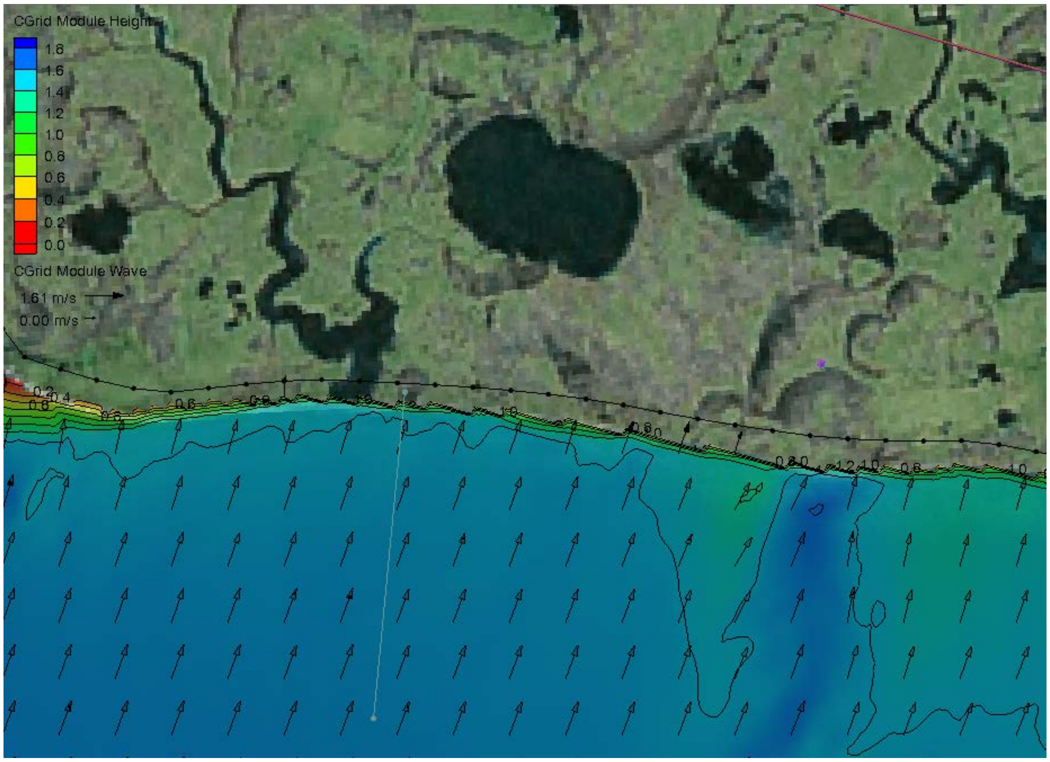

Figure 50 Wind grown wave from south southwest (Wind = 13 m/s)

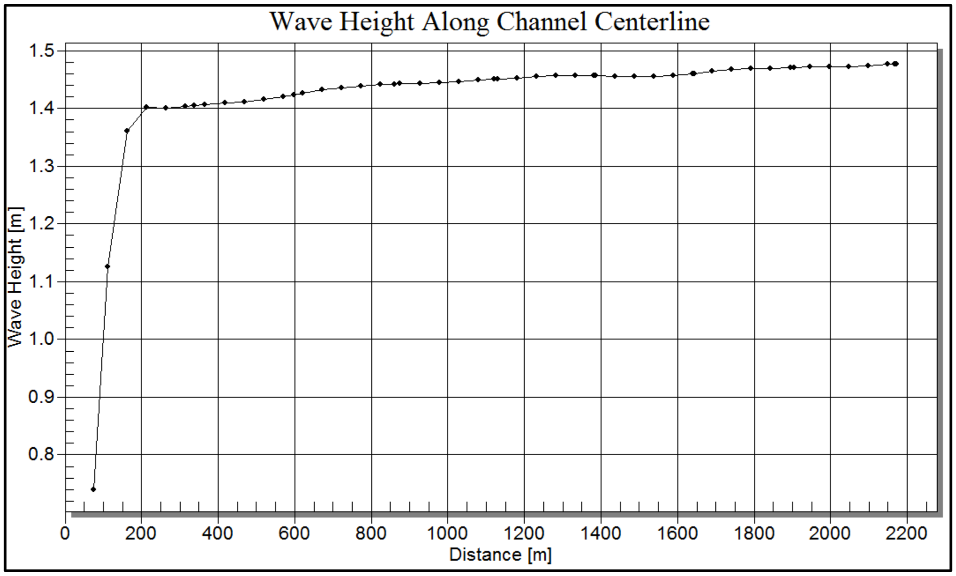

Figure 51 Wind grown wave height along channel centerline (Boundary wind speed = 13 m/s)

7.4.2 Summary of Results

The STWAVE modeling simulations indicate that wind speeds of 19.5 miles per hour can generate waves 3.3 feet or greater at the seaward end of the entrance channel. They also indicate that a one 3.3 foot deep-water wave is reduced by 25 to 55 percent as it reaches the channel (Table 11).

Table 11 Wave transformation during the shipping season

Wind developed wave at the seaward end of the channel		
Wind Direction (from which)	Wind Speed (mph)	Resulting wave at the seaward end of the channel (feet)
East (local wind generated wave)	25.0	1.3
	19.5	0.7
	14.0	0.2
Southeast (local wind generated wave)	30.6	3.9
	25.0	3.3
	19.5	2.3
South (local wind generated wave)	30.6	5.2
	25.0	4.1
	19.5	3.3
Southwest (local wind generated wave)	25.0	4.5
	19.5	3.3
	14.0	2.3
Transformed wave at the seaward end of the channel from deep water wave		
Wave Direction (from which)	Deep water wave height (feet)	Resulting wave at channel entrance (feet)
West (transformed deep water wave)	3.3	2.5
Northwest (transformed deep water wave)	3.3	1.5

The frequency of the events that can generate waves greater than 3.3 feet and require a delay in channel transit is minor as shown in Table 12 .

Table 12 Percent occurrence of waves greater than 3.3 feet at the channel during shipping season

Wind Generated Waves		Percent Occurrence During Shipping Season		
Wind speed needed for waves $\geq$ 3.3 feet	Wind Direction (degrees)	July	August	September
$\geq$25 mph	East (78.75-101.25)	0.01	0.08	0.66
$\geq$25 mph	Southeast (101.25-168.75)	0.33	1.25	1.55
$\geq$19.5 mph	South (168.75-191.25)	1.46	2.08	0.86
$\geq$19.5 mph	Southwest (191.25-258.75)	2.27	2.67	0.88
Deep Water Waves		Percent Occurrence During Shipping Season		
Deep water wave height (feet)	Wave Direction	July	August	September
3.3 or greater	West (258.75 – 281.25)	0.09	0.15	0.30
3.3 or greater	Northwest (281.25-303.75)	0.21	0.44	1.54

8.0 SEDIMENT MOVEMENT

Estimates of sediment transport rely on the combined wave and current conditions and sediment properties at the site. The sediment properties along the length of the channel were determined from core sampling and on-site erosion rate tests using the USACE High Shear Stress flume (SEDflume). This information was then used in a sediment transport model (SEDZLJ) to determine channel infilling volumes and the stability of the dredged material placement.

8.1 Nearshore Sediment

The beach at Cape Blossom is primarily composed of sand and gravel. Behind the beach is a thick organic mat with exposed melting permafrost (Figure 52 and Figure 53).

Figure 52 Beach and organic mat in the area of the proposed navigation improvement.

Figure 53 Exposed permafrost in the organic mat.

8.2 Offshore Sediment

8.2.1 Surface Grab Samples

During the 2016 field effort to measure currents, the Field Data Collection and Analysis Branch of the ERDC's WES also collected six surface samples grab samples in water depths ranging from 5 to 30 feet in the area of navigation feature alignment (Figure 54). The samples consisted primarily of fine, organic silt. A few samples contained fine to very fine sand. It was assumed that the organic material noted in the samples was from the eroding bluffs that were observed along the coastline.

Figure 54 Location of grab samples during the 2016 season

8.2.2 Core Samples

In the summer of 2017 the team returned to Cape Blossom to collect core samples for an erosion study using SEDFLUME to address the site-specific mobility of the sediments along the proposed navigation feature. Five shallow (up to 9 inches deep) core samples were collected at intervals along the proposed navigation channel. The core locations of are shown in Figure 55. The cores were comprised primarily of silt and sand, with a small fraction of clay.

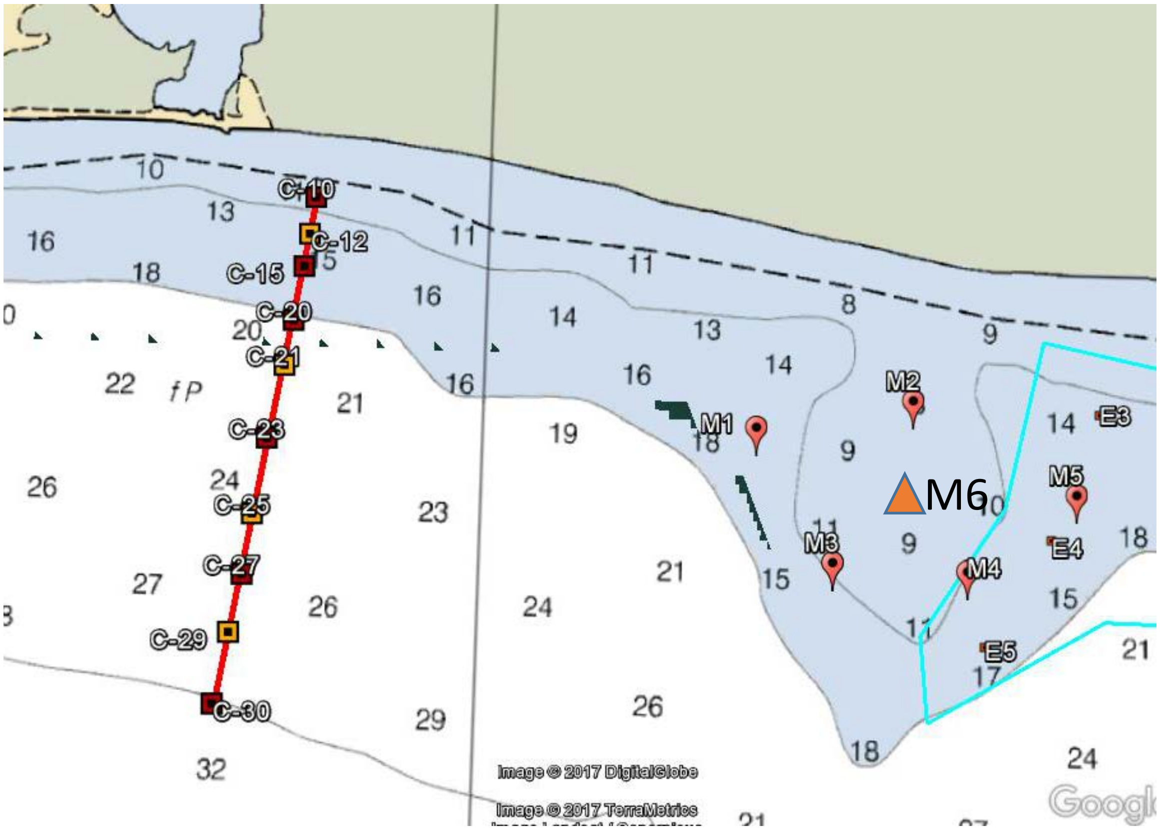

Figure 55 Map of sample locations

The core samples collected in the summer of 2017 were analyzed using SEDflume. SEDflume is a straight, closed conduit rectangular cross-section flume in which detailed measurements of critical shear stress of erosion and erosion rate as a function of sediment depth are made using relatively undisturbed sediment cores collected at the site to be modeled. The resulting data provides more accurate sediment erosion rates that can be used as input to SEDZLJ. For this study, it was used to estimate the stability of the native material surrounding the dredged channel.

Core C10

The upper 6-8cm was silty sand, and exhibited slightly cohesive erosion behavior. The layer beneath was mostly clean sand with some silt. This sediment eroded with little cohesive influence. The top 8cm is grouped together for erosion behavior and has a critical stress of 0.50Pa and a stress exponent of 3.6. This core behaved significantly different than C15-25, which had higher fines content.

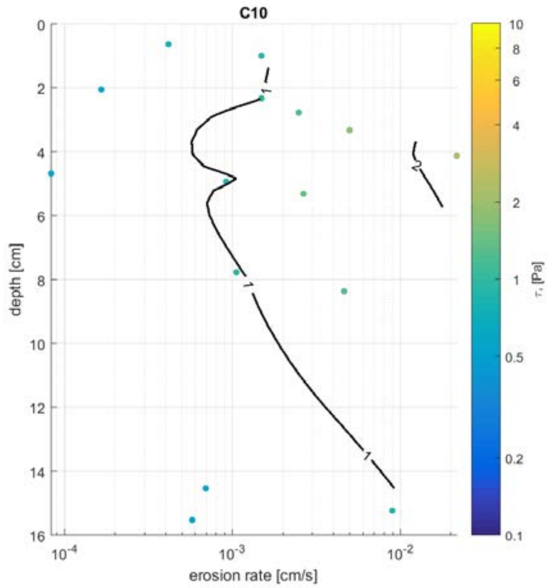

Figure 56 Core C10 erosion versus depth. Symbols indicate data points and symbol color indicates the applied shear stress. Contours indicate the variation of erosion at a given shear stress with depth.

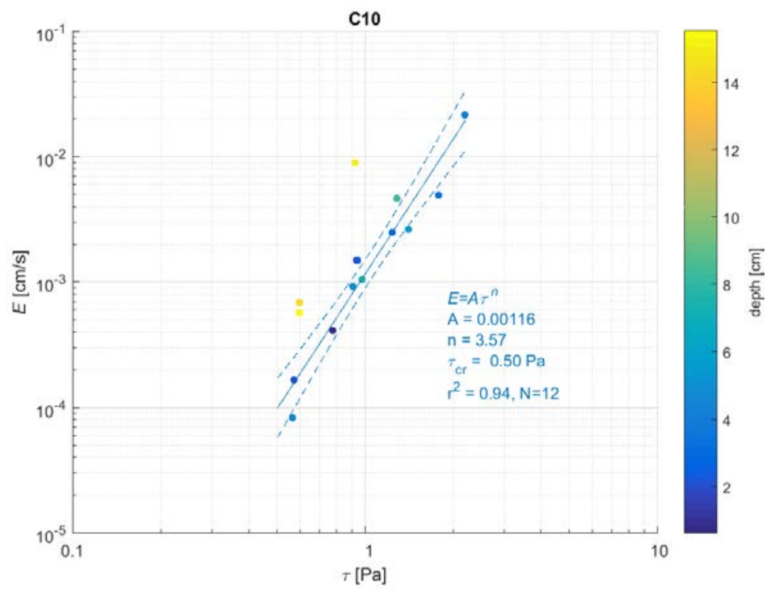

Figure 57 Core C10 erosion versus shear stress. Symbol color indicates depth of sample below the initial sediment-water interface.

Table 13 Core C10 Physical Sample Analysis

Sample	Depth [cm]	Bulk density [g/cm3]	Clay	Silt	Sand	D10 [um]	D50 [um]	D90 [um]
C10-1	1.3	1.70	2.1%	57.4%	40.5%	11.4	48.8	188.5
C10-2	6.0	2.07	0.7%	11.6%	87.8%	53.4	124.6	214.8
C10-3	12.2	2.01	0.0%	4.0%	96.0%	76.9	124.6	195.0
C10-4	15.8	2.10	0.0%	4.9%	95.1%	74.8	123.8	195.5

Core C15

Worm tubes and varying fractions of sand and gravel were noted during the erosion testing. In the upper 5cm of the core, worm tubes and particulate organic matter were noted to erode. Between 5 -10 cm, the presence of worm tubes and organic matter decreased and erosion rates reduced. At approximately 10cm, the presence of gravel and sand was noted in the core and the erosion rates correspondingly increased. Despite the variations in erosion with depth, the erosion data follow a fairly consistent trend versus shear stress. The variations associated with organic matter and gravel or sand-enriched layers contribute to increased spread around the trend line, but none-the-less a reasonable single trend line and expression for erosion versus shear stress is possible.

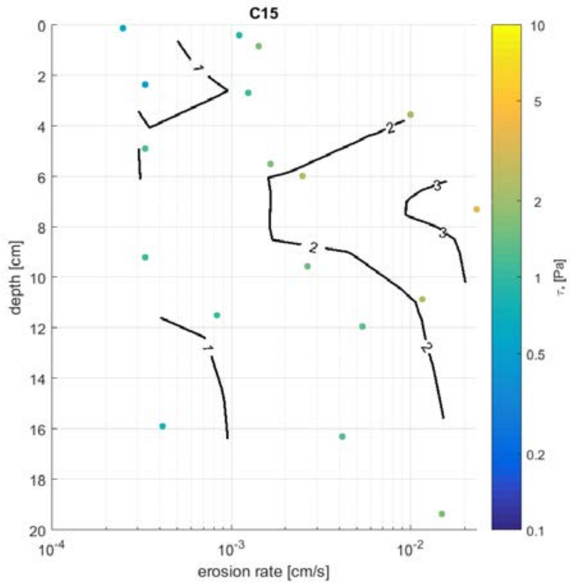

Figure 58 Core C15 erosion versus depth. Symbols indicate data points and symbol color indicates the applied shear stress. Contours indicate the variation of erosion at a given shear stress with depth.

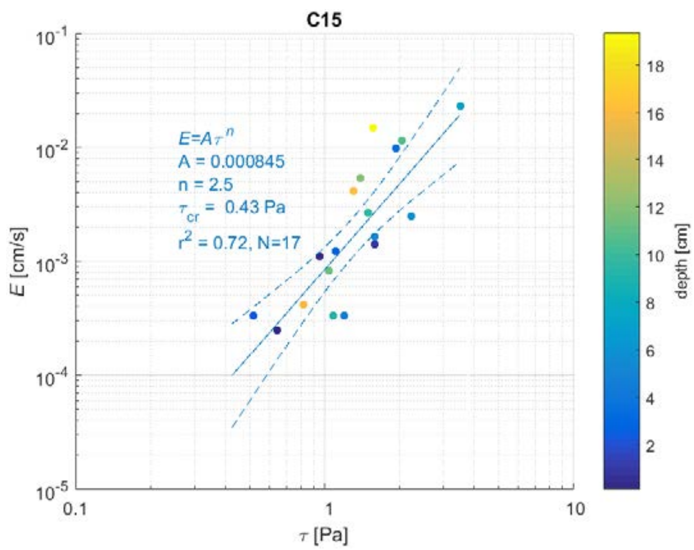

Figure 59 Core C15 erosion versus shear stress. Symbol color indicates depth of sample below the initial sediment-water interface

Table 14 Core C15 Physical Sample Analysis

Sample	Depth [cm]	Bulk density [g/cm3]	Clay	Silt	Sand	D10 [um]	D50 [um]	D90 [um]
C15-1	1.2	1.95	2.0%	43.8%	54.2%	10.8	70.3	187.3
C15-2	8.2	2.07	0.9%	26.1%	73.0%	28.6	100.1	241.3
C15-3	12.3	2.06	1.0%	44.3%	54.6%	26.1	67.8	144.2
C15-4	20.2	1.91	1.0%	35.5%	63.5%	26.8	80.6	203.3

Core C20

Core C20 was overfilled during collection. The core was collected in rough seas with waves on the beam, creating marginally safe working conditions. When the plunger was inserted, the top 2-3 cm of the core was pushed past the top of the core tube and discarded. This was considered acceptable, given the conditions and the marine forecast, which was for deteriorating conditions over the day. Upper 6 cm of the core was described as light grayish brown and sandy in appearance. The core was characterized during erosion as having alternating silt with sand and gravel to mostly silt or sandy silt. During erosion, layers with higher silt content eroded slower than those with more sand and gravel. This situation is reflected in the erosion data (E vs. Depth and E vs. Tau), which have two populations, poorly distinguished given the wide variability associated with the layering of sand and silt. This case could be represented as two populations, as given in the 2-layer model or as a single layer with bulk properties (GSD) composited from the cores samples.

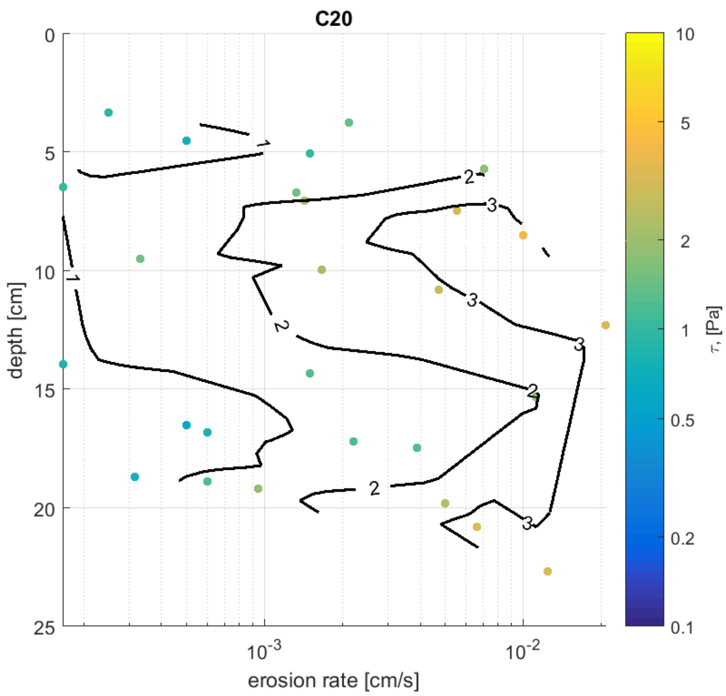

Figure 60 Core C20 erosion versus depth. Symbols indicate data points and symbol color indicates the applied shear stress. Contours indicate the variation of erosion at a given shear stress with depth

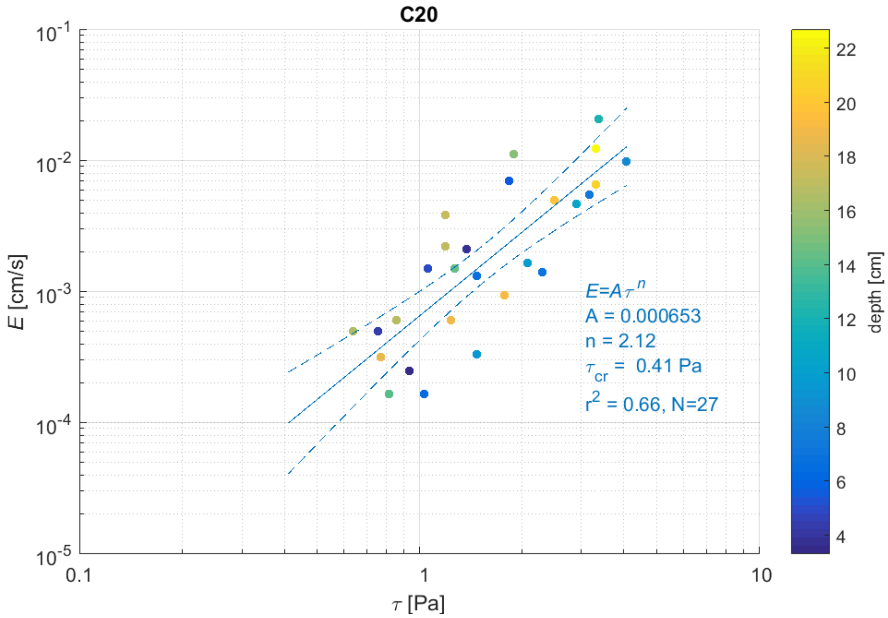

Figure 61 Core C20 erosion versus shear stress (single layer model). Symbol color indicates depth of sample below the initial sediment-water interface.

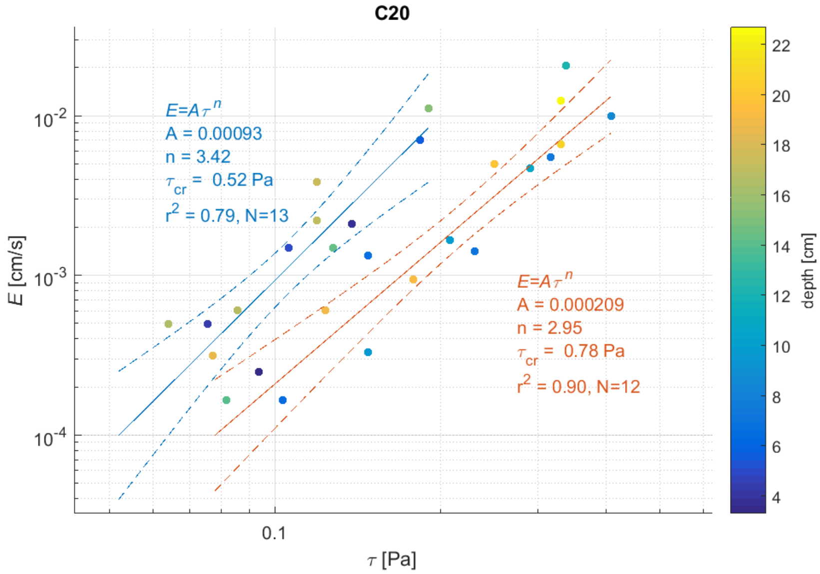

Figure 62 Core C20 erosion versus shear stress (two layer model. Symbol color indicates depth of sample below the initial sediment-water interface.

Table 15 Core C20 Physical Sample Analysis

Sample	Depth [cm]	Bulk density [g/cm3]	Clay	Silt	Sand	D10 [um]	D50 [um]	D90 [um]
C20-1	4.1	2.01	1.4%	26.4%	72.2%	18.3	144.0	600.6
C20-2	9.0	2.10	2.4%	41.3%	56.3%	10.6	76.4	305.1
C20-3	13.1	2.04	1.7%	41.6%	56.7%	16.0	72.1	188.7
C20-4	17.9	1.99	1.2%	26.4%	72.5%	22.8	178.1	583.0
C20-5	23.1	1.90	2.4%	67.2%	30.4%	9.9	39.8	122.5

Core C25

The erosion was well behaved with little evident lamination. The upper layer (top 10 cm) contained worm tubes. The top 4 cm eroded in a consistent manner with a tau_cr of 0.36 Pa. The deeper layer (5-14cm) maintained a similar slope with shear stress, but had a higher tau_cr, 0.88 Pa. The deeper layer was firmly compacted compared to the upper layer. The deepest erosion data (~14-17 cm) could have been influenced by a fracture created in the core during collection. The fracture was located at 17cm depth.

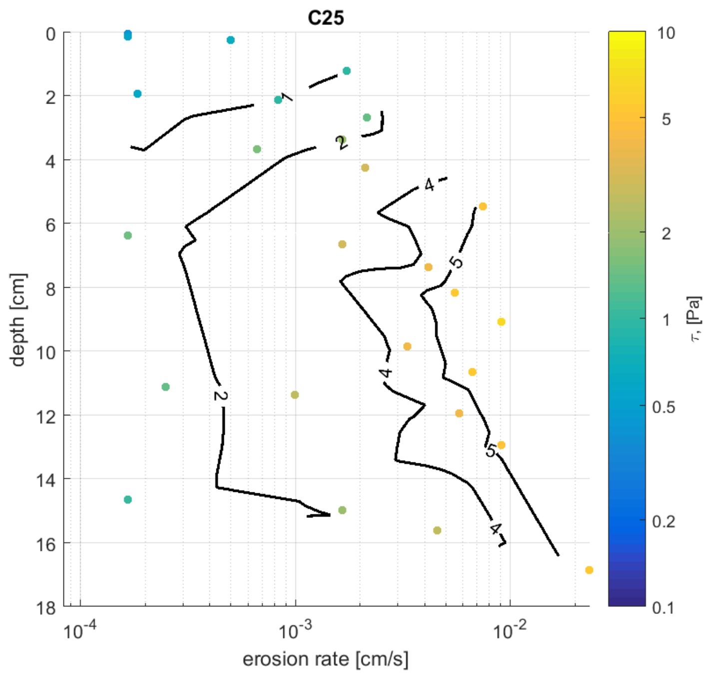

Figure 63. Core C25 erosion versus depth. Symbols indicate data points and symbol color indicates the applied shear stress. Contours indicate the variation of erosion at a given shear stress with depth

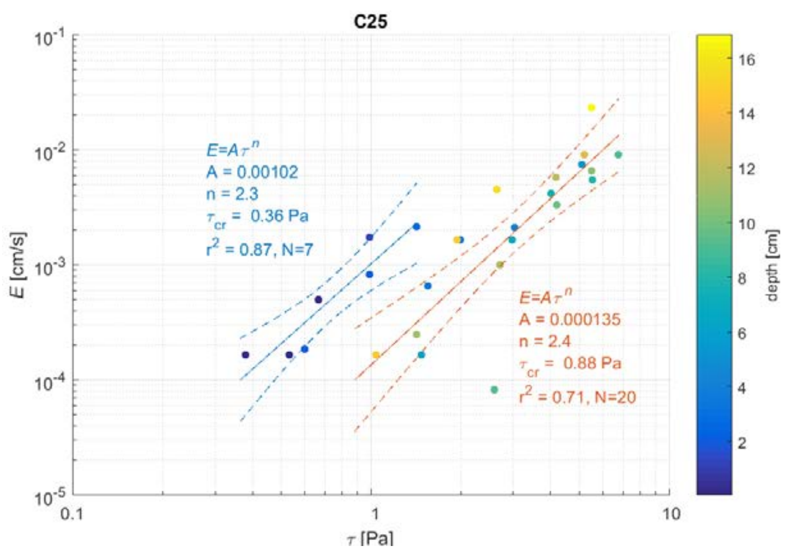

Figure 64 Core C25 erosion versus shear stress. Symbol color indicates depth of sample below the initial sediment-water interface.

Table 16 Physical Sample Analysis

Sample	Depth [cm]	Bulk density [g/cm3]	Clay	Silt	Sand	D10 [um]	D50 [um]	D90 [um]
C25-1	1.4	1.98	3.0%	33.8%	63.2%	9.3	105.5	254.2
C25-2	6.0	1.92	2.7%	41.8%	55.5%	9.5	76.9	221.8
C25-3	11.0	1.92	4.2%	65.9%	29.9%	6.5	33.2	136.6
C25-4	17.2	2.04	4.2%	46.2%	49.6%	6.9	62.1	167.0

Core C30

The surface layer of C30, 0-0.8cm, was composed of loose, unconsolidated sediment. The erosion was described as fluffy with light flocs being eroded. The critical shear stress of the surface layer was 0.43Pa, similar to the surface layer for the shallower cores along the channel. The surface was also rough, with worm tubes, which may have accentuated surface erosion at higher flows. The layer beneath the surface fluff (1.4-3.2cm) was slightly more erosion resistant with a critical shear stress of 0.59Pa. This intermediate layer appears to be a transition layer to the densely packed silt of the lower layer. The lower layer was markedly more erosion resistant than the upper layers with a critical shear stress of 2.7Pa. This lower layer was very consistent in erosion behavior with depth.

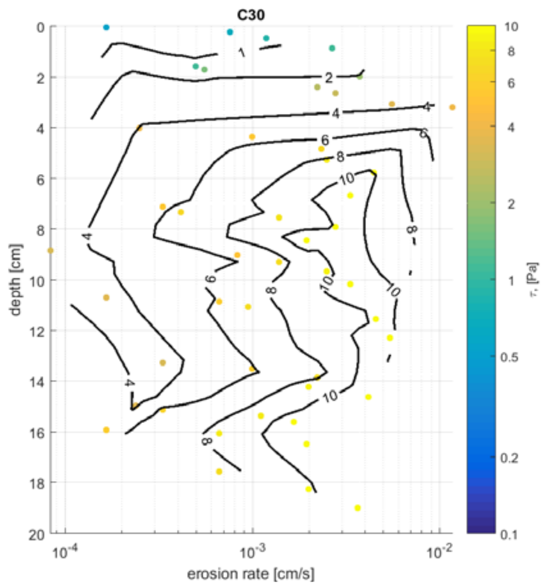

Figure 65 Core C30 erosion versus depth. Symbols indicate data points and symbol color indicates the applied shear stress. Contours indicate the variation of erosion at a given shear stress with depth

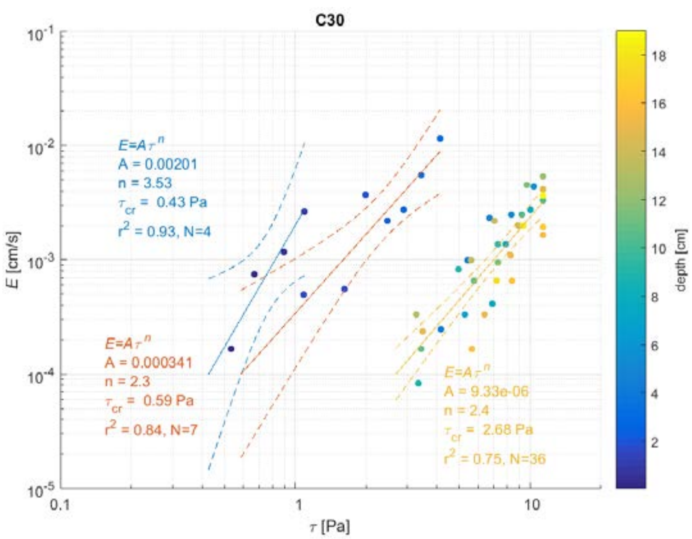

Figure 66 Core C30 erosion versus shear stress. Symbol color indicates depth of sample below the initial sediment-water interface.

Table 17 Physical Sample Analysis

Sample	Depth [cm]	Bulk density [g/cm3]	Clay	Silt	Sand	D10 [um]	D50 [um]	D90 [um]
C30-1	1.0	1.84	3.3%	50.1%	46.6%	8.0	55.0	294.2
C30-2	3.5	1.86	3.9%	66.2%	29.9%	6.8	35.3	150.1
C30-3	8.7	1.81	4.8%	71.4%	23.9%	6.1	30.5	111.6
C30-4	12.7	1.83	5.3%	77.6%	17.1%	5.7	24.3	86.7
C30-5	16.8	1.98	5.0%	68.4%	26.6%	6.0	31.8	118.3
C30-6	19.3	1.98	5.7%	72.8%	21.5%	5.4	26.0	101.9

Core M6

The surface layer, 0-4cm, was primarily granular silty and sandy pebbles, a mixture of large pebbles and cobbles, mixed with some sand and silt. Photos were taken for size analysis from these layers (two samples). Between 4 -18 cm, the core was composed of layers of gravelly silt, with interspersed thin peaty lenses. The peaty lenses exhibited more erosion resistance, but all-in-all, the layer was well characterized by the erosion data. The critical shear stress for the underlying cohesive material was 0.27Pa, less than that of the surrounding bed, and the shear stress exponent was comparable to the surface layers of the adjacent shelf (the C** samples).

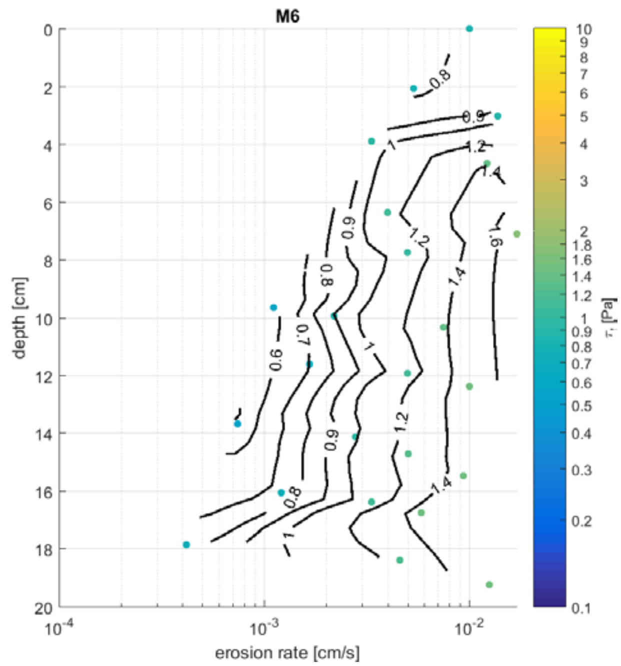

Figure 67 Core M6 erosion versus depth. Symbols indicate data points and symbol color indicates the applied shear stress. Contours indicate the variation of erosion at a given shear stress with depth

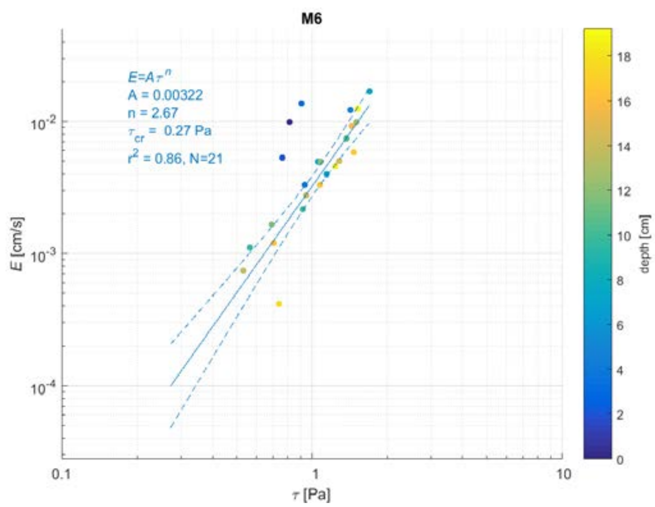

Figure 68 Core M6 erosion versus shear stress. Symbol color indicates depth of sample below the initial sediment-water interface.

Table 18 Physical Sample Analysis

Sample	Depth [cm]	Bulk density [g/cm3]	Clay	Silt	Sand	D10 [um]	D50 [um]	D90 [um]
M6-1	8.2	1.73	1.9%	51.9%	46.2%	12.4	56.2	387.3
M6-2	13.0	1.94	1.9%	66.7%	31.4%	18.2	47.1	98.3
M6-3	17.1	1.89	1.7%	61.3%	37.0%	15.0	49.3	128.8
M6-4	19.7	1.87	2.1%	71.4%	26.5%	12.1	38.7	105.5

8.2.3 Summary of SEDflume Results

The trendlines from the SEDflume tests and associated parameters for all cores and layers are presented in Figure 69. This presentation of data suggests similar groupings of cores and layers by similar erosion behavior. These groupings of similarly eroding sediment layers are:

1. Sediment groups C10, C20-1, C30-1, and M6 have similar erosion thresholds near 0.5 Pa and similar shear stress exponents (approximately n = 3.5). These groups were surface sediments that were high in sand content and had rough surfaces with either gravel or worm tubes that could have generated increased local stresses to mobilize sediment.
2. Sediment groups C15, C20-2, C25-1, and C30-2 behave similarly with critical stresses between 0.4 and 0.6 Pa and shear stress exponents generally around 2.3-2.5. These groups represent moderately consolidated mixed sand and silt beds.
3. With further compaction of the mixed silt-sand beds comes higher erosion resistance. Layers C25-2 and C30-3 show behavior departing from that of the previously described sediments. These layers have critical shear stresses greater than 0.75 Pa and has high as 2.7 Pa. For Core C-30, clay content and relatively high bulk density (1.9-2.0 g/cm3) increased slightly with depth, likely contributing to the increased erosion resistance. Similarly, C25-2 had modest increases in clay content coupled with high bed density between 1.9 and 2.0 g/cm3. Comparing the differences between the physical properties of C25-2 and C30-3 to the other eroded cores suggests that sediment with clay content higher than 2-3% and sand content less than 60% contribute to significantly increased erosion resistance.

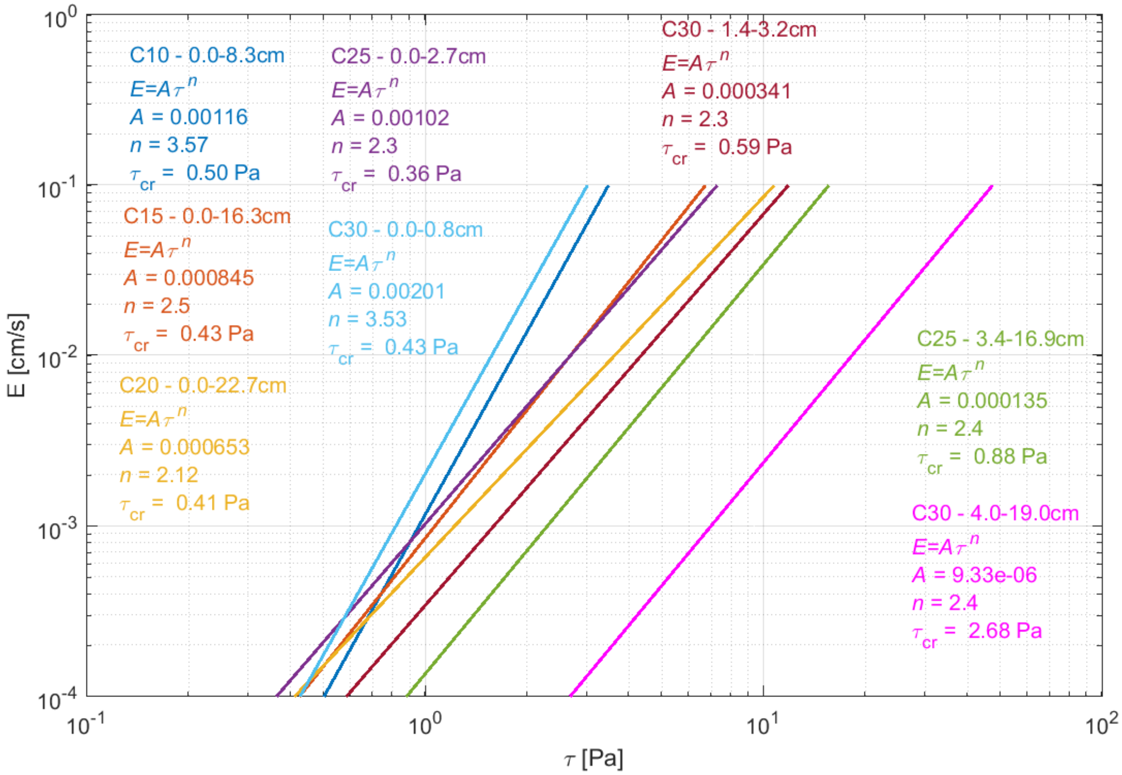

Figure 69 Best fit lines and associated parameters for all cores and layers from the study

8.3 Sediment Transport Model

The SEDZLJ sediment bed model developed by Jones and Lick (2000, 2001) was used to characterize the sediment transport at the site. SEDZLJ represents the dynamic process of erosion, bedload transport, bed sorting, armoring, consolidation of fine-grain sediment dominated sediment beds, settling of flocculated cohesive sediment, settling of individual non cohesive sediment particles and deposition. An active layer formation is used to describe the sediment bed interactions during erosion and deposition. The active layer facilitates coarsening during the bed armoring process.

8.4 Channel Infilling

The period of record 1954-2014 was evaluated for worst case storm event for sediment transport. The driving mechanisms for sediment movement and channel infilling during the storms were identified as water level, wave height, or currents. No single storm event was found that coincided with the top events for all three drivers.

Because of the limited data at the site, storms for the period of record, that had the highest potential for sediment transport were selected for analysis. The ERDC numeric modelers for this study were highly experienced with modeling the fast moving arctic storms having performed this function for several other projects for the Alaska District. Their engineering judgement coupled with the Alaska District’s regional knowledge and experience was used to select the storms used to evaluate the channel infilling potential.

The storms selected for sediment transport evaluation had top events for at least one of the driving mechanisms for sediment transport. Individual storms were evaluated along with an entire open water season each being selected based on the potential for sediment transport into the channel. The storms generally occurred between September and November with the majority of the energetic storms occurring in November. The CSTORM model was used to simulate six selected storms and one 6-month open water season (Table 19).

Table 19 Selected storms to evaluate infilling

Month Year	Major Driver for Storm Selection
November 1970	**Water level/Currents**
November 1974	**Water level**
October 1989	**Currents**
November 1989	**Currents**
September 1990	**Waves**
November 1990	**Wave/Currents**
June-November 2011	**Water Level/Waves**

Wave heights and direction vectors at the peak of each storm are shown in Figure 70 though Figure 83 along with the infilling experienced at the end of each month of the storm occurrence. Infilling appears to be greatest with storms from the southeast. Storms from the southwest are associated with minimal to no infilling and possible scour.

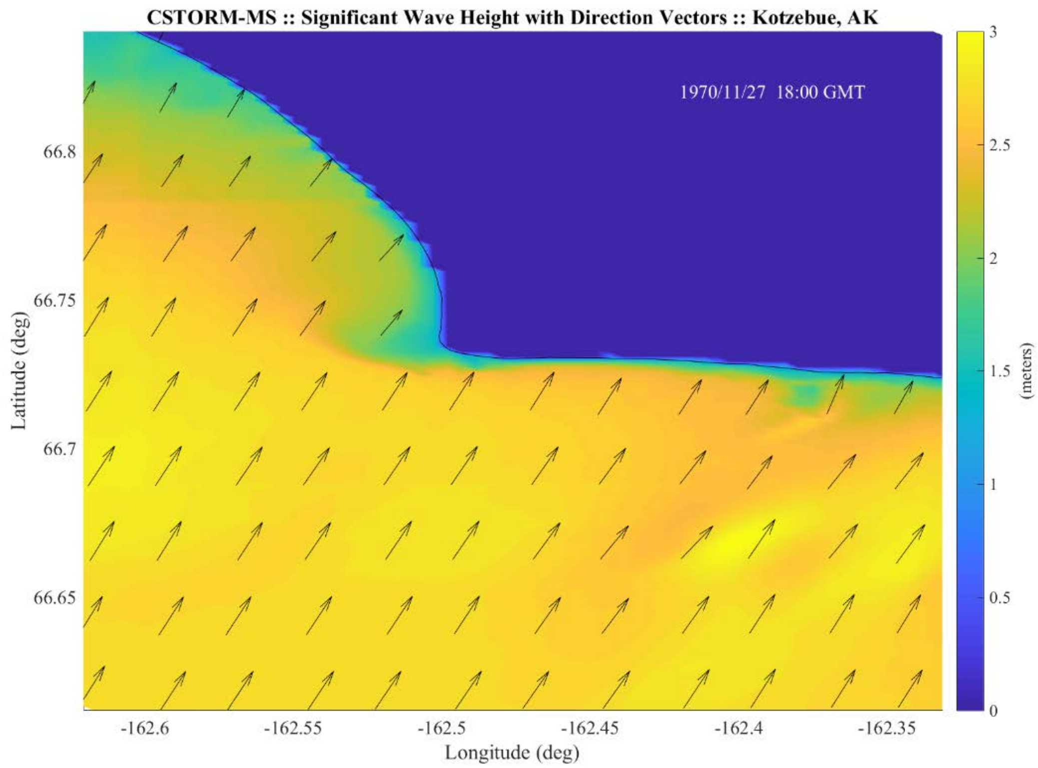

Figure 70 Significant wave height and direction for November 1970 storm

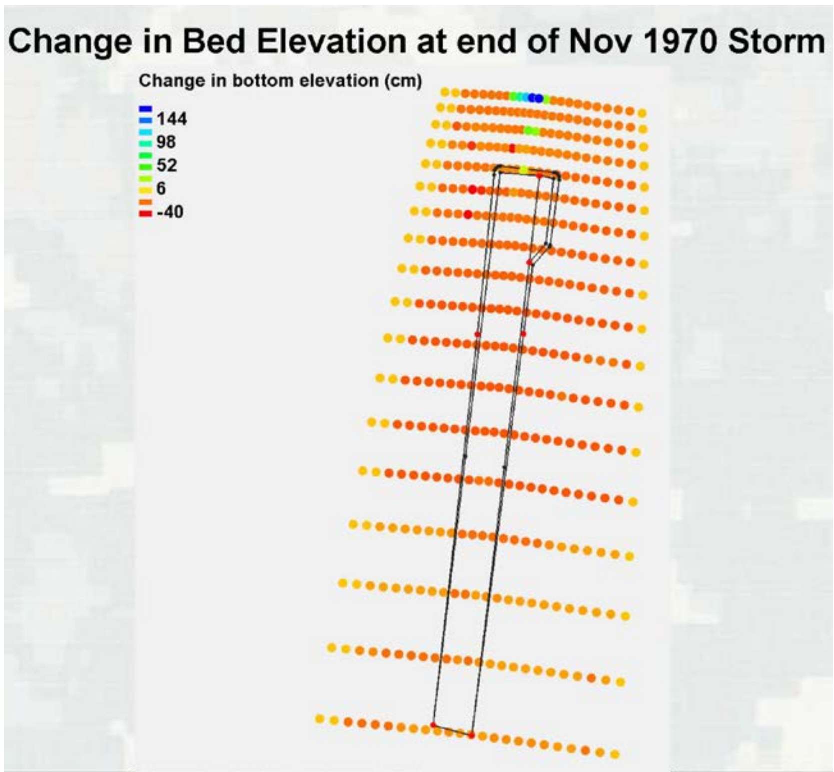

Figure 71 Change in sea bed elevation at the end of November 1970

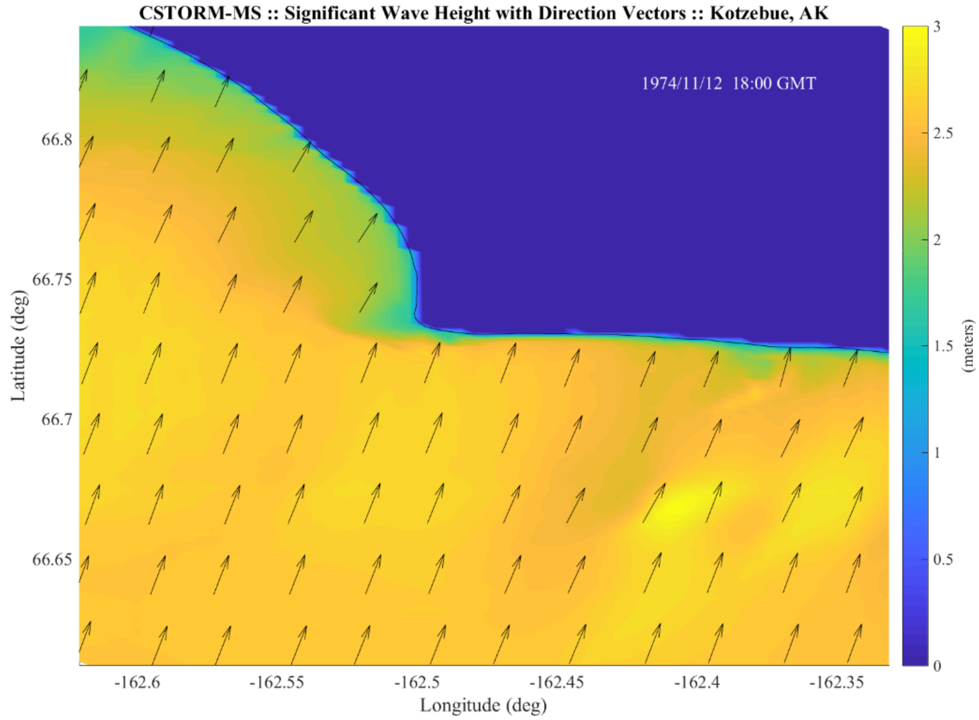

Figure 72 Significant wave height and direction for November 1974 storm

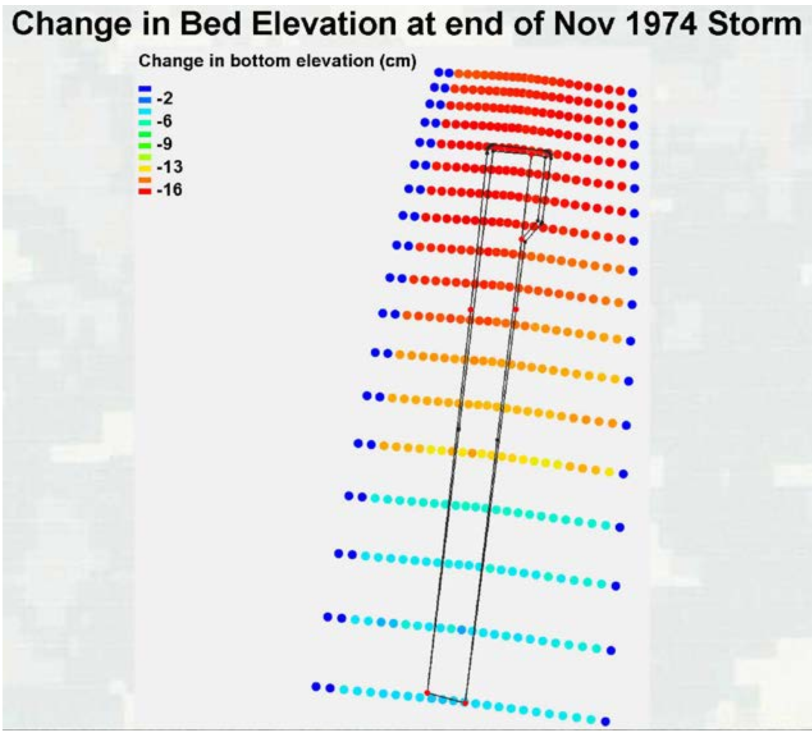

Figure 73 Change in sea bed elevation at the end of November 1974

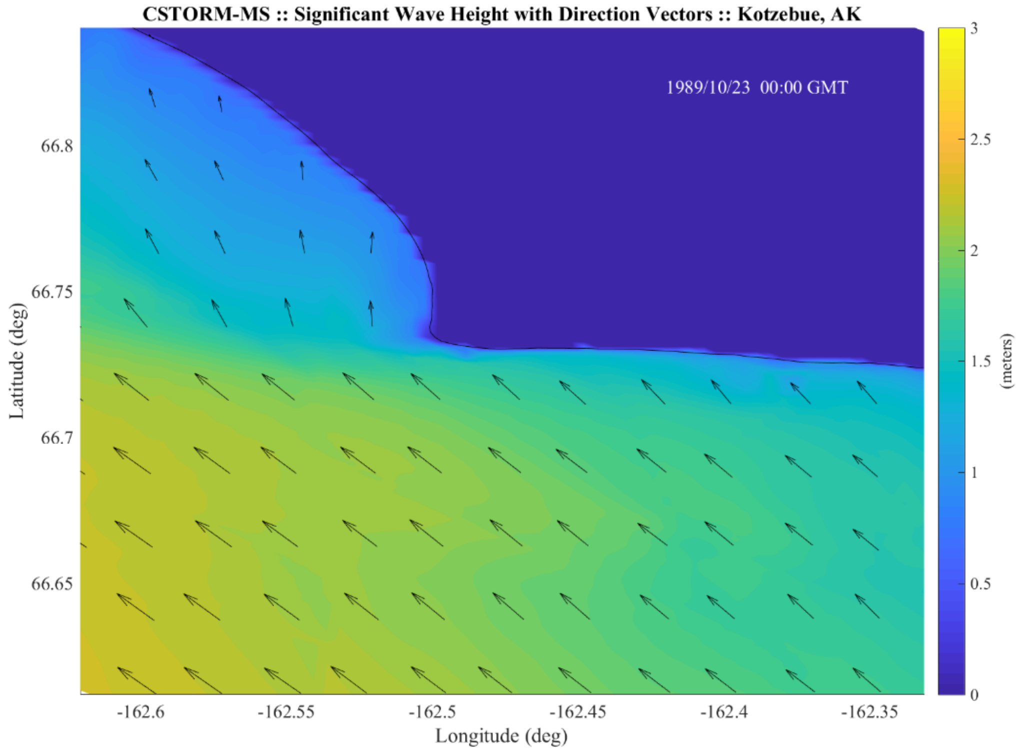

Figure 74 Significant wave height and direction for October 1989 storm

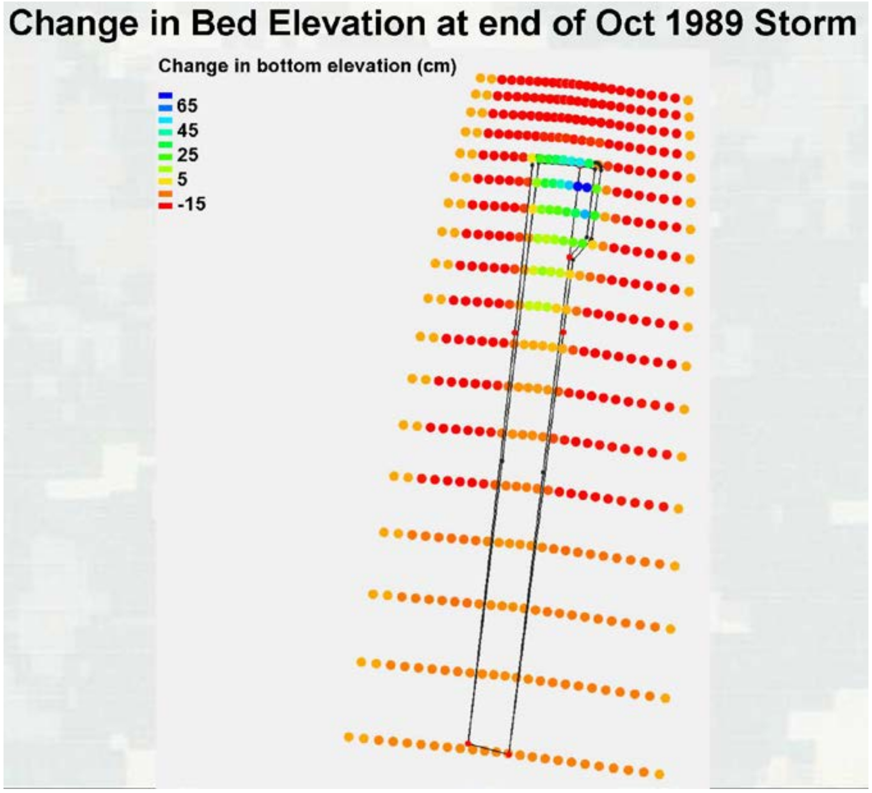

Figure 75 Change in sea bed elevation at the end of October 1989

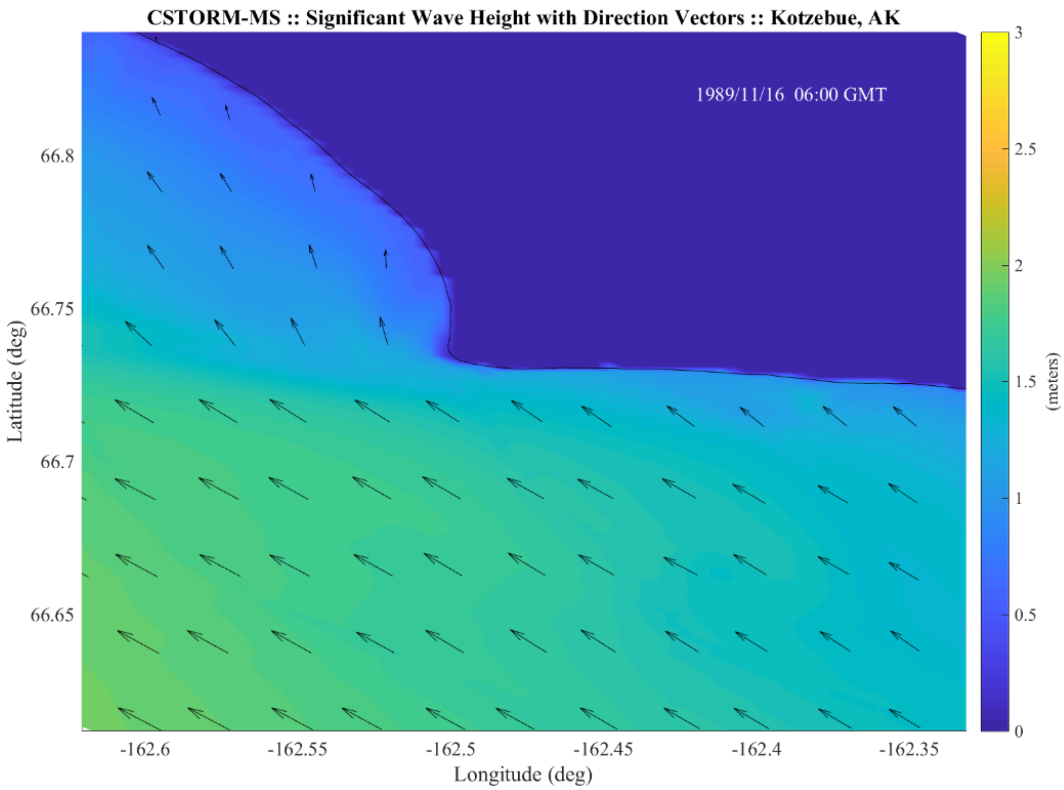

Figure 76 Significant wave height and direction for November 1989 storm

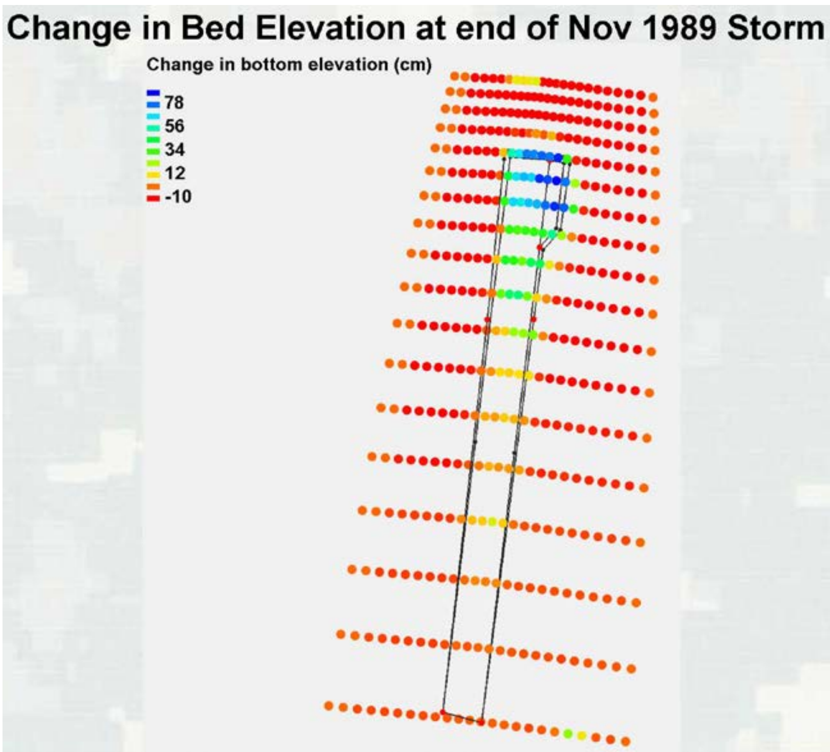

Figure 77 Change in sea bed elevation at the end of November 1989

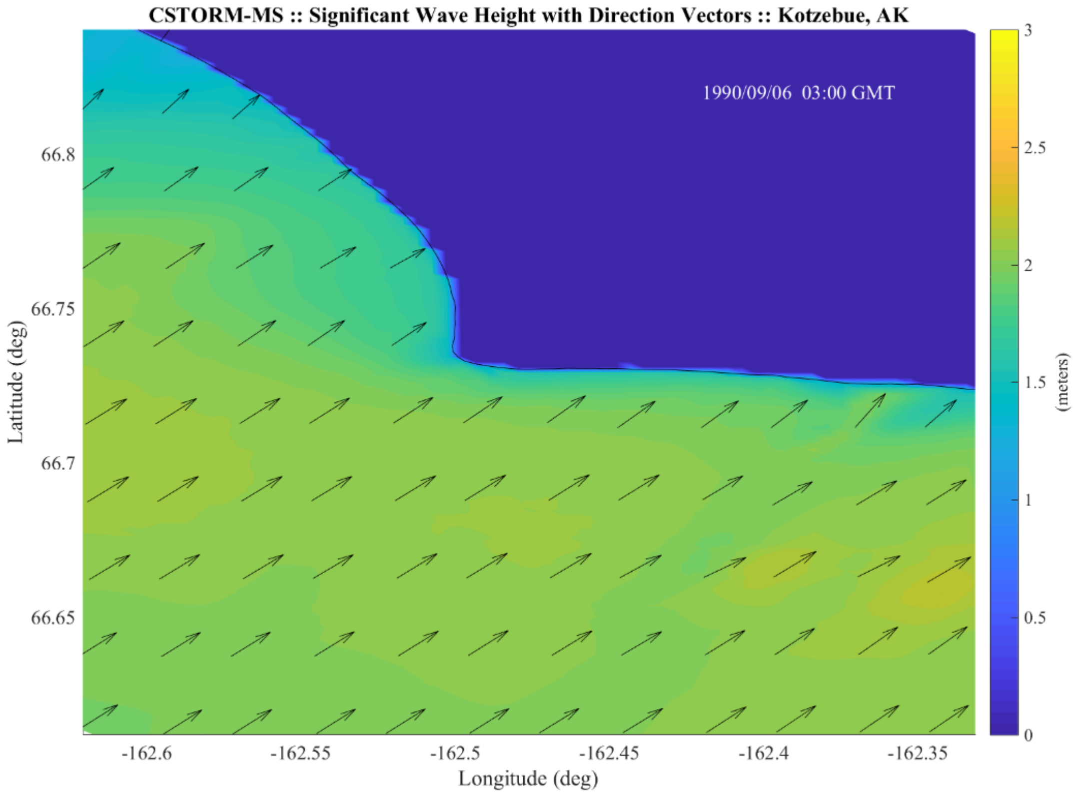

Figure 78 Significant wave height and direction for September 1990 storm

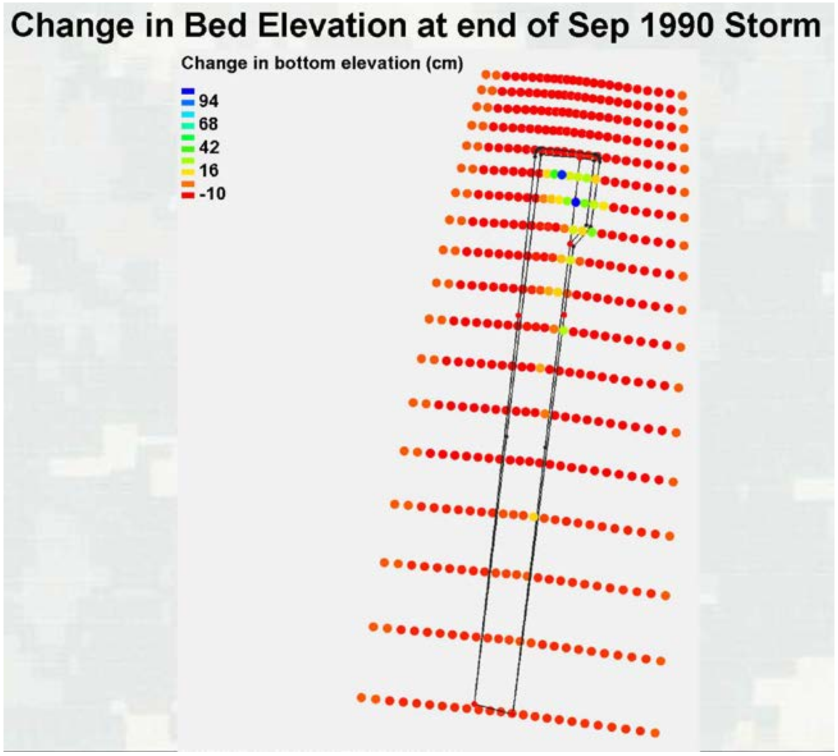

Figure 79 Change in sea bed elevation at the end of September 1990

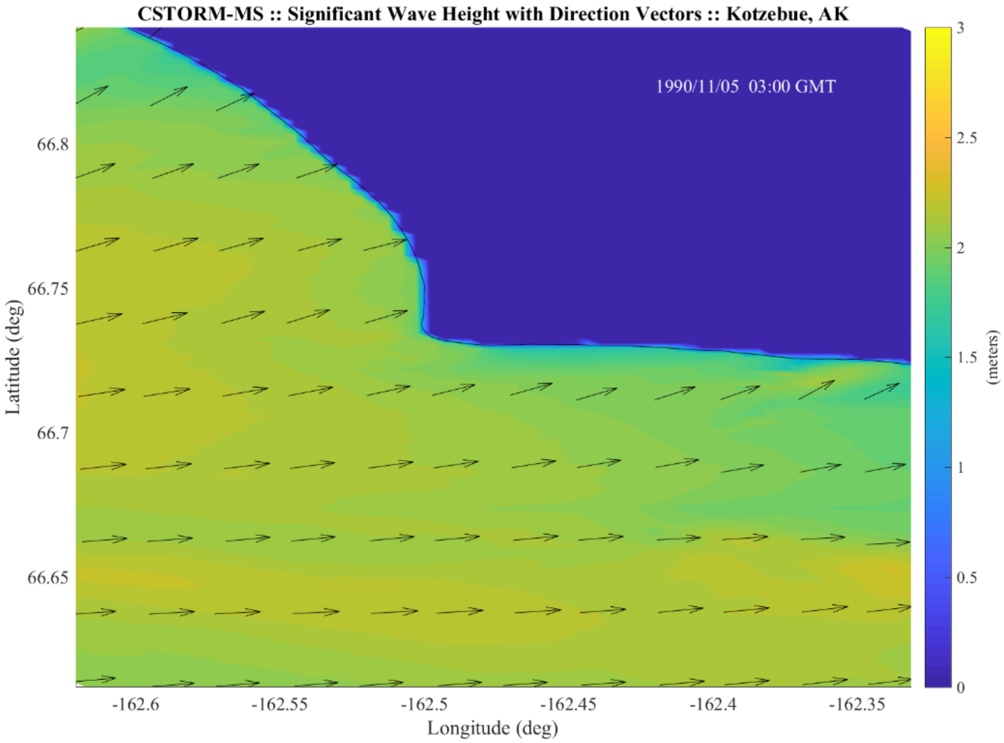

Figure 80 Significant wave height and direction for November 1990 storm

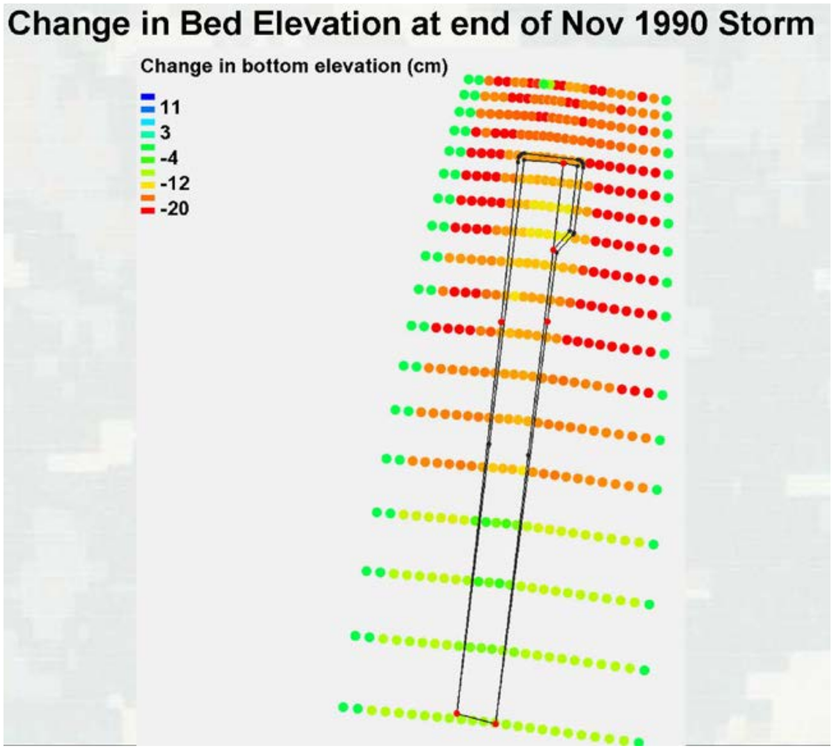

Figure 81 Change in sea bed elevation at the end of November 1990

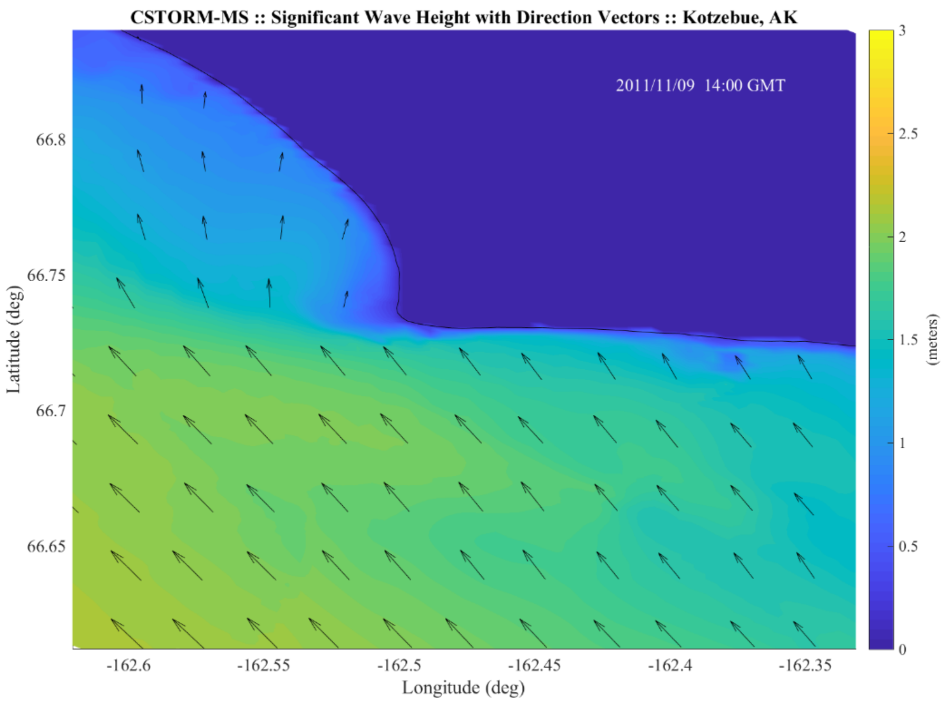

Figure 82 Significant wave height and direction for November 2011 storm

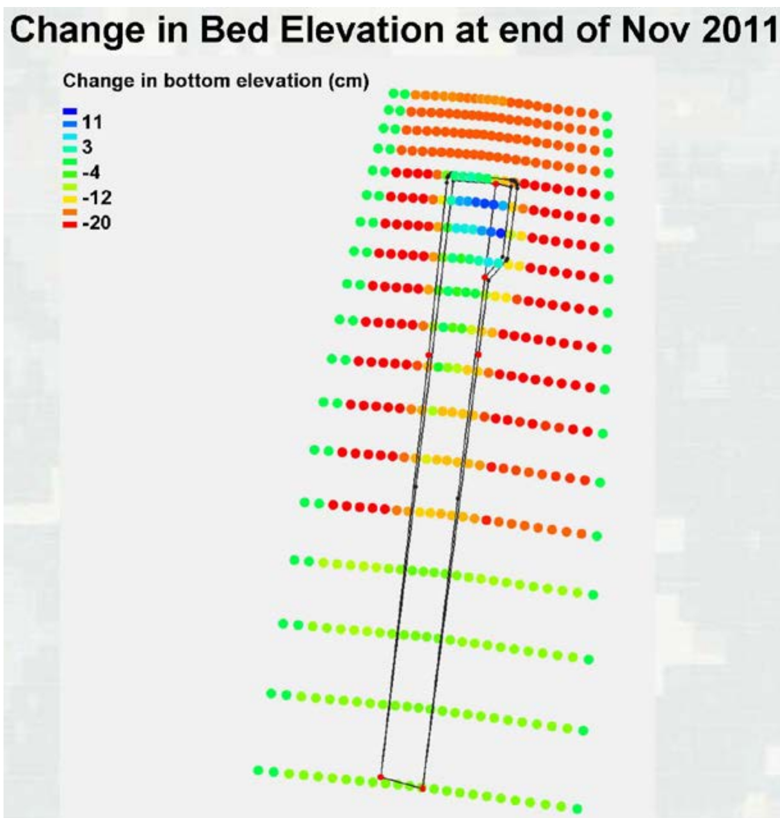

Figure 83 Change in sea bed elevation at the end of November 2011

In order to simulate the channel infilling over time, the sediment conditions at the end of the June-November 2011 simulation were used to set the initial conditions, including modified morphology, for the subsequent six month sediment transport model run. These simulations represent the open water season at the site. The same tidal and meteorological forcing that were used for the 2011 simulation were used for the next June-November simulation.

Because most of the sediment that could be eroded had been eroded and transported away from the project site during the first open water simulation, extremely minimal change in morphology occurred during the second open water simulation. The net change in morphology in the navigation channel at the end of November varied by less than +/- 5 cm indicating that the channel had reached equilibrium.

9.0 NAVIGATION IMPROVEMENTS

Measures considered for improving navigation at Cape Blossom include:

- Dredging a channel to allow offloading closer to shore
- Construction of a breakwater
- Construction of a trestle from shore to a dock in deeper water
- Construction of a rock causeway to a dock in deeper water

The local sponsor indicated that the structure used to access the channel from shore would need to keep beach access open since the beach is used for subsistence activities. With this in mind, it was assumed that the channel access would involve a trestle type structure to keep the beach access open. An example of a similar structure that has been used in the arctic is the loading facility at the Delong Mountain Terminal. This structure consists of cellular trestle supports support the ore conveyor (Figure 84). It was assumed a structure similar to this would support a bridge to the channel. The effect that this would have on sediment transport was evaluated by including five equally spaced 75 foot diameter cellular support structures from the shore to the start of the dredged channel in the sediment transport model.

Figure 84 Cellular support structure at the Delong Mountain Terminal

Dredging a channel to allow offloading closer to shore
This alternative would dredge a channel in towards to the shore to allow a ship to approach the Cape Blossom site loaded. Based on the extent of the channel dredging, the ship/barge could:

- Offload onto a dock connected to shore by a causeway or trestle
- Offload to a smaller draft lighter barge

Construction of a breakwater
This alternative would construct a breakwater that could shelter a vessel and provide a calm environment to transfer cargo to a lighter barge. The ship could anchor within the breakwater area or mooring dolphins could be installed.

Construction of a trestle from shore to deeper water
This alternative would construct gravity structures to support a road that would end at an offloading dock in deeper water. The trestle would start at the shore facility and extend to deeper water. Depending on the extent of the trestle and offloading dock, the vessel could:

- Navigate directly to the offloading dock
- Offload to a smaller draft lighter barge that would navigate directly to the offloading dock

Construction of a rock causeway to a dock in deeper water
This alternative would construct a rock causeway that would end at an offloading dock in deeper water. The causeway would be connected to shore by a trestle structure to enable beach access and then extend to deeper water. Depending on the extent of the causeway and offloading dock, the vessel could:

- Navigate directly to the offloading dock
- Offload to a smaller draft lighter barge that would navigate directly to the offloading dock

The causeway concept was developed to support quantity generation for cost engineering. The design was based on the breakwater design criteria.

10.0 CHANNEL DESIGN

The purpose of dredging the channel is to provide access to an offloading facility located at near the shore. The length of the channel will be determined by a comparison of channel construction and maintenance costs to the construction costs of an alternative method of linking to the shore facility, and the transportation benefits for each different draft loading case.

The channel design followed the standards of Engineering Manual (EM) 1110-2-1613, "Hydraulic Design of Deep-Draft Navigation Projects," and were checked against PIANC guidance.

10.1 Design Vessel Criteria

The first consideration for the channel design is to define the vessels likely to use the prospective channel. The Native Village of Kotzebue has expressed a desire to be able to provide fuel to the outlying villages soon after the ice goes out and the rivers are navigable. Kotzebue is currently serviced by tank barges owned by Kirby Corporation that are chartered to Crowley Maritime Corporation. The Kirby tank barge currently anchors at a 9 fathom buoy and then transfers the fuel to a lighter barge operated by Crowley. A typical tank barge that would be chartered is the design vessel for this project. In addition to the barge, the dimensions of a tug accompanying the barge is also included as the design vessel because its draft requires use of the channel during transit. The dimensions of the design vessel and tug are shown in Table 20.

Table 20 Design Vessel Information

	Design Barge	Design Tug
Length Overall [feet]	380	126
Beam [feet]	96	34
Loaded Draft [feet]	20	17

10.2 Configuration and Use

The channel design is a straight channel that maintains a constant width to accommodate the fully loaded barge until the -23 foot contour. At this contour, the channel widens to accommodate the underkeel clearance of the barge and tug towing alongside side the barge. The channel continues straight with a constant width until it reaches the dock for unloading where it widens into a turning basin for the barge.

10.2.1 Channel Location

The channel for access to the Cape Blossom site is nearly perpendicular to the bathymetry contours and lines up the Alaska Department of Transportation's planned access road (Figure 86). The shoreward end of the channel was located to prevent the channel from being impacted by cross shore sediment transport and to minimize the channels' impact on coastal processes of the foreshore beach.

10.2.2 Channel Width

USACE guidance sets the channel width at 432 feet up to the -23 foot contour. This is based on one way traffic, shallow cross section, average aids to navigation, and currents up to 0.68 knots. The higher current velocity was used due to minimal current data at the site. These design criteria produce beam multiplier of 4.5. At the -32 foot contour, the channel width was widened to provide navigation draft for a tug used to guide the ship. The width calculation was based on the same criteria with the exception that the shallow cross section was now a trench cross section. This criteria produced a beam multiplier of 4.0 and was applied with the combined beam of 96 feet (barge) and 34 feet (tug) resulting in a channel width of 520 feet.

The channel width was checked using Permanent International Association of Navigation Congresses (PIANC) guidance. The PIANC width detailed in Table 21 shows the need for an approximate width of 546 feet which checks well with the channel width determined using USACE guidance.

Table 21 PIANC width factors

Condition	Site Description	Width Factor
Vessel Speed (knots)	slow (5-8)	0.0B
Prevailing Cross Wind (knots)	moderate 15-33	0.6B
Prevailing Cross Current (knots)	strong 1.5-2.0	0.3B
Prevailing Longitudinal Current (knots)	low ≤ 1.5	0.0B
Bean & stern quartering wave height (m)	Hs<1	0.0B
Aids to Navigation	moderate with infrequent poor visibility	0.4B
Bottom Surface	< 1.5T and smooth	0.1B
Depth of Waterway	<1.25T	0.2B
Cargo Hazard Level	Medium	0.0B
Additional Width for Bank Clearance (2x)	Sloping channel edges	0.3B
Basic Ship Maneuvering Lane	Poor Ship Maneuverability	1.8B
Sloping channel edges and shoals	slow (5-8 knots)	0.3B
B = 96 feet + 34 feet = 130	Total	4.2B
Width = 546 feet		

10.2.3 Turning Basin

The channel ends with a turning basin that is 570 feet which is 1.5 times the length of the barge. This allows the barge to be turned fully loaded which will allow for a quick departure from the dock once unloading is complete or in the event that weather conditions change and make it unsafe to remain at the dock.

10.2.4 Channel Depth

Vessels moving in a navigation channel must maintain clearance between their hulls and channel bottom. Navigational design parameters such as squat, safety clearance, vertical motion due to waves, and water density effects were analyzed to determine the required minimum under-keel clearance. Figure 85 illustrates vessel factors that determine the minimum channel depth.

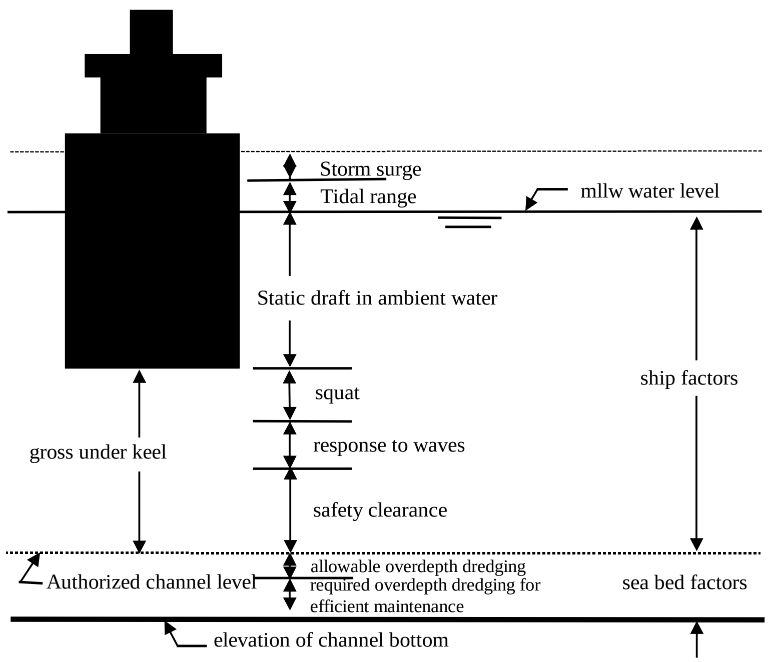

Figure 85 Vessel Factors that Determine Minimal Channel Depth

Draft. The design vessel that is anticipated to call at the Cape Blossom site is a vessel that currently calls on Kotzebue and anchors offshore at a 9 fathom buoy. The fully loaded draft of this barge is 20 feet (Table 22) and the loaded draft of the associated tug is 17 feet.

Squat. Squat is the lowering of the vessel in the water column due to the hydrodynamic pressure gradient created by the fluid velocity around and under the vessel hull when a vessel is underway. The vessel draft increases when sailing as the hydrostatic and kinetic energy is balanced. Squat varies with vessel speed, water depth beneath the keel, and the ratio of the vessel cross-section area to the cross-section area of the channel. Because the vessel is assumed to be moving at a very slow speed, squat was assumed to be 0.5 feet during channel transit.

Response to Waves. Values for vessel response to waves was obtained using EM 1110-2-1613 which cites a Columbia River ship motion study. Critical motions of a ship occur at the bow and stern and are most dependent on the wave height and encounter period, with wave height having the most influence on ship motion. The data collected during the Columbia River study was used to develop a relationship to describe the ship motion assuming a Rayleigh distribution of motion. Assuming channel transit is limited to times when the wave height is 3 feet, the critical ship motion for transit of the channel is 3.5 feet.

Safety Clearance. USACE guidance suggests a minimum net under-keel clearance of 2 feet. The channel bottom is composed of silt, sand, and organics. Based on the description of the material a safety factor of 2 feet was used for this analysis.

Minimum Clearance. The subtotal of squat, response to waves, and safety clearance for the channel provides a design depth of -26 feet MLLW (**Error! Reference source not found.**).

Set Down. Modeling for the Delong Mountain Terminal Study indicated that indicate that severe set down events of up to 11.5 feet lasting for 12 hours are possible. These events are more prevalent in the fall and are generally outside the shipping season window. By keeping the berthing area depth the same as the channel depth, set down events up to 4 feet during the shipping season can be tolerated by a ship at the dock and leave a 2 foot safety clearance.

Dredging equipment and procedures cannot provide a smoothly excavated bottom at a precisely defined elevation. Two feet of allowable over depth dredging was added to the target depth of excavation to guarantee mariners a least-depth equivalent to the sum of ship factors.

Table 22 Channel depth factors

Channel Factor	Depth [ft]
Loaded draft	20
Squat	.5
Ships response to waves	3.5
Safety Clearance	2
Total	26

10.2.5 Sideslopes and Bank Stability

The initial channel dredge cut would have a side slope of 1 vertical to 3 horizontal. The material to be dredged has been characterized as sand, silt, and organics. It is anticipated that this material will eventually lay back on a 1 vertical to 10 horizontal slope. The channel end is located such that the 1 vertical to 10 horizontal slope will not impact the shore.

Over time the channel slope may lay back on slopes that are similar to the local subsurface conditions. Maintenance to stabilize the slope may be necessary if the slope lay back at the end of the channel progresses beyond a 1 vertical to 10 horizontal slope. This scenario is viewed to be so far into the future that maintenance associated with it are not addressed in this analysis.

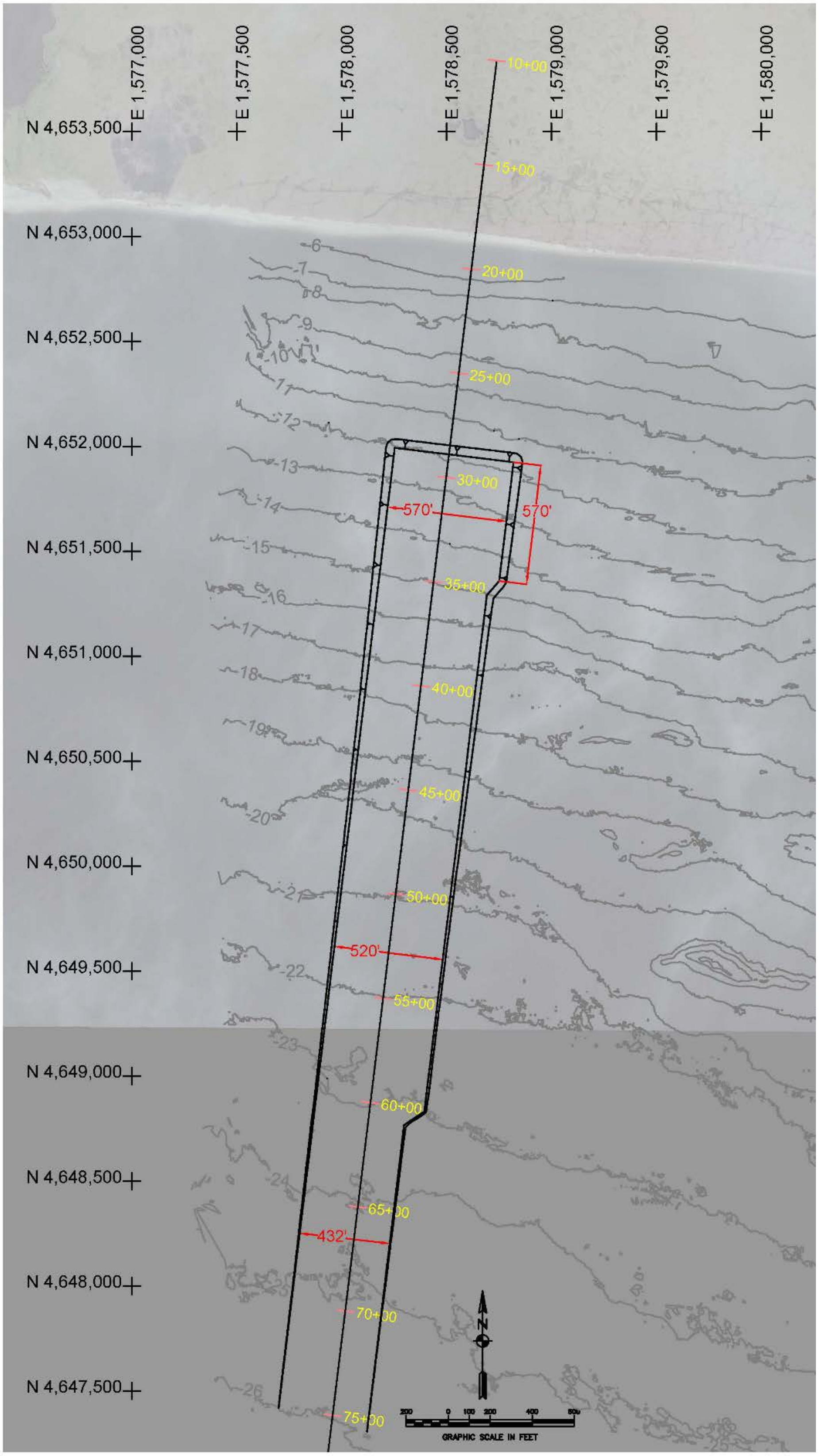

Figure 86 Plan view of navigation channel

10.3 Initial Dredge Quantity

The initial dredging quantity shown below includes 2 feet of allowable overdepth dredging outside the required depth prism to account for inaccuracies in the dredging process in an open ocean environment. Table 23 shows the channel quantities associated with each dredge scenario. The quantities presented include a two-foot over depth allowance for survey and dredging tolerance.

Table 23 Initial Dredge Quantities

Dredge Start Contour [feet]	Dredge Depth -26 feet MLLW plus 2 feet allowable overdepth [feet]	Initial Construction Dredge Quantity [cy]
-12	-26 (required) / -28 (allowed)	707,000
-14	-26 (required) / -28 (allowed)	585,000
-16	-26 (required) / -28 (allowed)	470,000

10.4 Dredge Material Placement

SEDZLJ modeling was performed to evaluate the location for placement of the dredge material from the initial dredge and subsequent maintenance. The initial and subsequent dredge material will be placed in the nearshore environment between -13 feet MLLW and -18 feet MLLW up to elevation -8 feet MLLW. The material will serve as nourishment for the actively eroding nearshore environment. Locations to the east and west of the dredge channel were evaluated to ensure that the placed material does not end up back in the channel.

Two-six month simulations were performed, one with west placement and the other with east placement. Placement of the material 1,320 feet west of the channel resulted in the least amount of sediment infilling as compared to material placement 1,320 feet east of the channel (Figure 87). This is reasonable since the majority of the storms that impact the area are from the southeast.

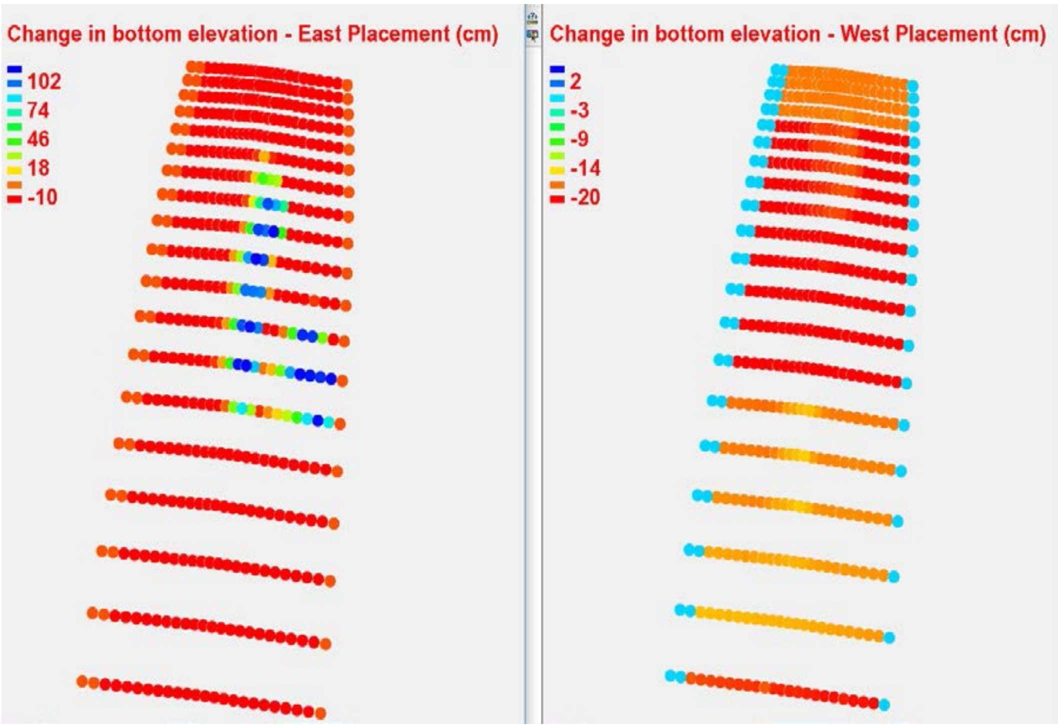

Figure 87 Change in the bottom elevations for both the east and west placement sites.

10.5 Maintenance Dredge Quantity

SEDZLJ modeling was used to evaluate the volume and frequency of maintenance dredging required to keep the channel open. Results indicated that there will be minimal infilling of the channel with the dredge material placed on the west side of the channel (Figure 88). In order to account for some infilling during channel stabilization, maintenance dredging was said to occur in years 5, 15, 25, and 45. The volume of dredging is assumed to be 300,000 cubic yards and it would be placed 1,320 feet west of the channel as discussed in Section 10.4 Dredge Material Placement.

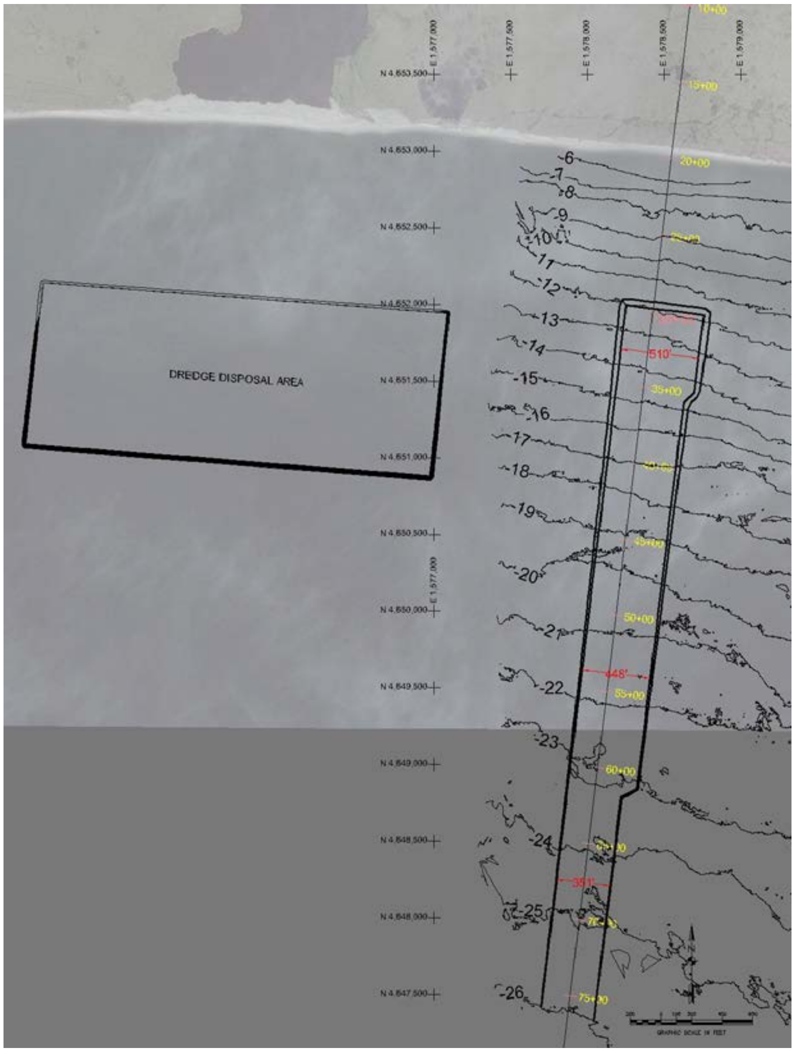

Figure 88 Location of dredge disposal site with respect to the channel

10.6 Navigation Aids

Navigation aids are expected to be similar to the aids that were planned for the deep draft channel that was proposed in the Delong Mountain Terminal (DMT) navigation project. The Coast Guard required two lighted range towers for the proposed channel at the DMT. Any navigation aid other than the Coast Guard required aid would be a local cost and maintenance responsibility.

The Alaska Marine Pilots Association (AMPA) indicated that they preferred buoys spaced every 0.75 miles as navigation aids at the DMT site. The AMPA recommended:

- A lighted bell buoy with Racon located just outside the offshore entrance to the channel.
- A series of lighted buoys along the channel.
- Center and shoulder ranges to provide visual alignment with the channel.
- A permanent current meter.

10.7 Construction Considerations

The channel construction is anticipated to take two years to complete, assuming a contract award in the fall. The type of dredge equipment used to perform the work will not be specified in the contract. It is anticipated that the bidders on the project will be dredgers with a clamshell or a cutterhead. Dredge days at the site will be limited by the wave climate and the lack of shelter to run to under storm conditions. Storms at the site move through the area very rapidly and there is no shelter. The equipment would need to find a place in Kotzebue Sound that is somewhat sheltered and ride out a storm.

To attract a number of bidders, it is recommended that the project be advertised early to interest dredging contractors in bidding on this project. The contract should be awarded in the fall to allow the contractor the winter to prepare the logistics for the upcoming open water season.

The work season length, remote site location, wave climate, lack of local protection from wind and/or wave events are just some of the conditions that a contractor would need to consider when proposing on this contract.

Cape Blossom is a remote location, so a camp would need to be set up to house the crew and support construction operations. It anticipated that the dredges would work two shifts, 10 hours a day, 7 days a week.

The dredging contractor would need to make sure that there is fuel available for him at the site or in Kotzebue. He could bring up his own fuel barge, or he could make arrangements to purchase fuel from Kotzebue. Purchase of fuel from Kotzebue would need to be coordinated early in the year so that arrangements could be made to have additional fuel delivered to Kotzebue.

The placement of the dredge material will need to be examined further to ensure that the beach nourishment goal can be achieved.

If the trestle and dock are constructed prior to the channel being dredged, it is critical that the dock structure be designed to support a channel dredged to -28 feet MLLW at a minimum. Failure to design for the dredged channel depth will prevent the channel from being dredged up to the dock face due to concern that the dock structure would be undermined.

11.0 BREAKWATER/CAUSEWAY DESIGN

An alternative to the dredged channel is the construction of a breakwater. The breakwater would provide a calm transfer climate for the vessel to transfer its load to a lightering barge. The breakwater would be located south of the -26 foot contour to ensure adequate depth to maneuver (Figure 90). The breakwater height is +28 feet MLLW with a seaward slope of 1 vertical to 1.5 horizontal and a crest width of 14 feet (Figure 89). The armor was carried to the bottom of the breakwater to provide a more robust structure to withstand ice push events.

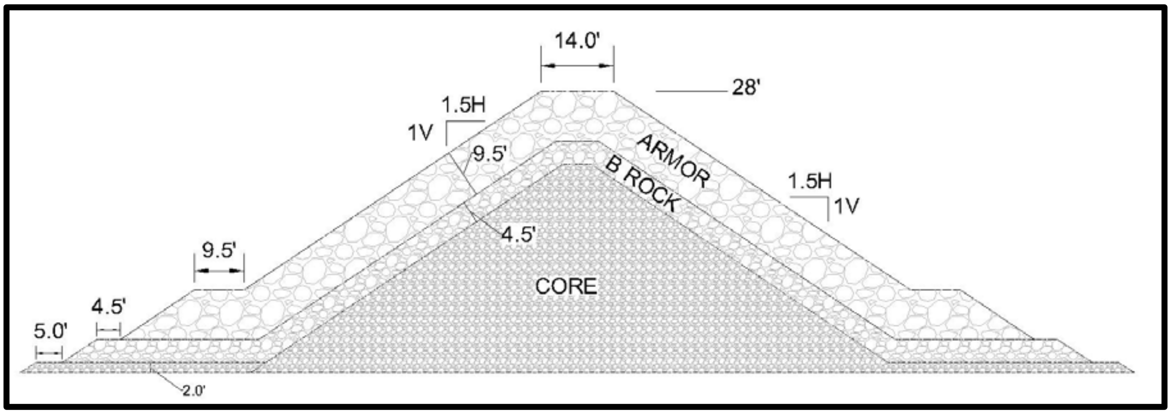

Figure 89 Breakwater cross section

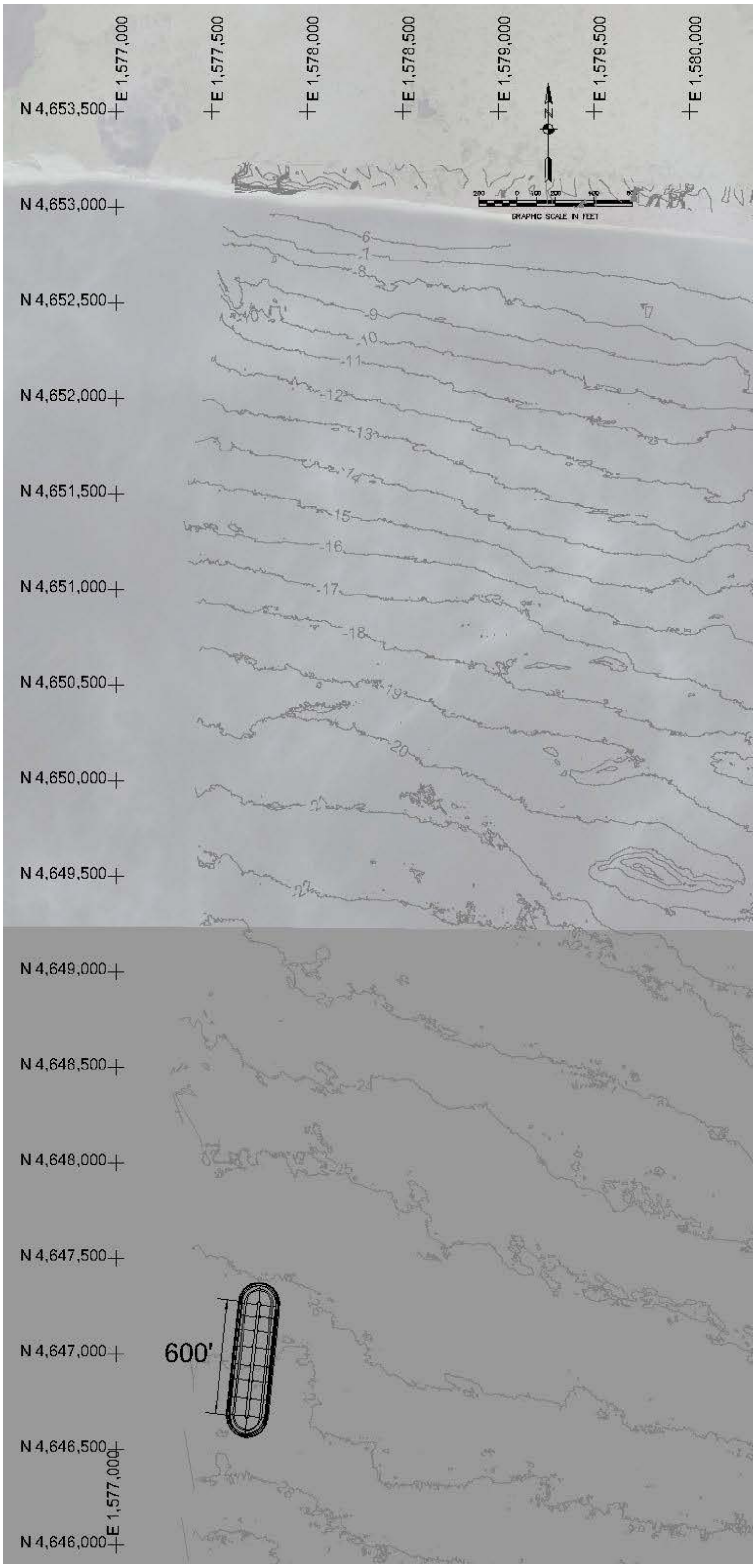

Figure 90 Plan view of off shore breakwater

11.1 Armor Stone

The armor stone sized for the 50-year wave was compared to the armor stone size needed to withstand ice push. The stone sized for wave height was 5.6 tons while the stone sized to withstand ice ride up was 8 tons. The stone sized for ice was based on ice studies performed at the University of Iowa for the Nome causeway design. It showed that 8-ton stone was adequate to protect from ice. The causeway at Nome has performed adequately with no damage since 1986 and has withstood ice ride up.

11.2 Navigation Aids

Navigation aids are expected to be similar to the aids that would have been required for a breakwater that was proposed for Delong Mountain Terminal navigation project. The Coast Guard required a lighted fixed navigation aid on each end of the breakwater. Any navigation aid other than the Coast Guard required aid would be a local cost and maintenance responsibility.

11.3 Construction Considerations

The breakwater construction is anticipated to take three years to complete, assuming a contract award in the fall. The construction contract will be an open invitation for bid. In order to attract a number of bidders, it is recommended that the project be advertised early to interest contractors to bid on this project. The contract should be awarded in the fall to allow the contractor the winter to prepare the logistics for the upcoming open water season.

The work season length, remote site location, wave climate, lack of local protection from wind and/or wave events are just some of the conditions that a contractor will need to consider when proposing on this contract.

The contractor will need to make sure that there is fuel available for him at the site. He could bring up his own fuel barge, or he could make arrangements to purchase fuel at Kotzebue. Purchase of fuel from the site would need to be coordinated early in the year so that arrangements could be made to have additional fuel delivered to the site.

REFERENCES

Alaska Department of Transportation & Public Facilities Northern Region Material Section. (2009). *Geotechnical Data Report Kotzebue to Cape Blossom Road State Project 76884.* Alaska Department of Transportation & Public Facilities.

Bilello, M. A., & Bates, R. E. (1966). *Ice Thickness Observations, North American Arctic and Subarctic, 1962-63, 1963-64; Special Report Pt III.* Hanover: Cold Regions Research & Engineering Laboratory.

Bilello, M. A., & Bates, R. E. (1971). *Ice Thickness Observations, North American Arctic and Subarctic, 1966-67, 1967-68.* Hanover: Cold Regions Research & Engineering Laboratory.

Bilello, M. A., & Bates, R. E. (1972). *Ice Thickness Observations, North American Arctic and Subarctic 1968-1969, 1969-1970; Special Report 43, Pt VI.* Hanover: Cold Regions Research and Engineering Laboratory.

Bilello, M. A., & Bates, R. E. (1991). *Ice Thickness Observations North American Arctic and Subarctic, 1972-73 and 1973-74; Special Report 43 Part VIII.* Hanover: Cold Regions Research & Engineering Laboratory.

Chapman, R. S., Sung-Chan, K., & Mark, D. J. (2009). *Storm-Induced Water Level Prediction Study for the Western Coast of Alaska.* Vicksburg: United States Army Corps of Engineers Engineer Research and Development Center.

Coachman, L. K., & Tripp, R. B. (1970). Currents North of Bering Strait in Winter. *Limnology and Oceanography Volume 15 Issue 4*, 625-632.

Creager, J. S., & McManus, D. A. (1966). Geology of the Southeastern Chukchi Sea. In N. J. Wilimovsky, *Environment of the Cape Thompson Region, Alaska* (pp. 755-786). Oak Ridge : United States Atomic Energy Commission.

Flemming, R., & Heggarty, D. (1966). Oceanography of the Southeastern Chukchi Sea. In N. Wilimovsky, *Environment of the Cape Thompson Region, Alaska* (pp. 697-754). Oak Ridge: United States Atomic Energy Commission.

Jensen, R. E. (2009). *Offshore Wind and Wave Climate.* Not Published.

Kolar, R. W. (1992). *An analysis of the mass conserving properties of the generalized wave continuity equation, Computational Methods in Water Resources IX, Volume 2: Mathematical Modeling in Water Resources.* Southamption, UK: Computational Mechanics Publications, .

Luettich, R. J. (1992). *ADCIRC: an advanced three-dimensional circulation model for shelves coasts and estuaries, report 1: theory and methodology of ADCIRC-2DDI and ADCIRC-3DL.* Vicksburg, MS: U.S. Army Corps of Engineers Waterways Experiment Station.

Massey, T. C. (2011). *ERDC/CHL TR-11-1 STWAVE: Steady-State Spectral Wave Model User's Manual for STWAVE, Version 6.0.* Vicksburg, MS: U.S. Army Corps of Engineers Coastal Hydraulics Laboratory.

Smith, J. M. (2001). *ERDC/CHL SR-01-1 STWAVE: Steady-State Spectral Wave Model User's Manual for STWAVE, Version 3.0.* Vicksburg, MS: U.S. Army Corps of Engineers Coastal Hydraulics Laboratory.

State of Alaska Department of Transportation & Public Facilities Northern RegionMaterial Section. (2009, May 18). *Geotechnical Data Report Kotzebue to*

Cape Blossom Road. State of Alaska Department of Transportation & Public Facilities.

State of Alaska Department of Transportation and Public Facilities Northern Region. (2011). *Material Site Investigation Kotzebue to Cape Blossom Road.* State of Alaska Department of Transportation and Public Facilities.

Tetra Tech and Wright Forssen Associates. (1983). *Feasibility Analysis Kotzebue Deepwater Port/Airport.*

United States Army Corps of Engineers Alaska District. (2005). *Navigation Improvements Draft Interim Feasibility Report, Delong Mountain Terminal.* United States Army Corps of Engineers Alaska District.

Van Woert, M. (2002). U. S. Navy operational sea ice remote sensing. *IGARSS Proceedings, INT_A32_04.* Toronto.